Univerza
v Ljubljani
Fakulteta
za gradbeništvo
in geodezijo

Niko Kristanič

Limit State Design Using Exact Sensitivity Analysis and Shape Optimization

DOCTORAL THESIS

Sinteza konstrukcij z uporabo točne občutljivostne analize in optimizacije oblike v nelinearnem področju

DOKTORSKA DISERTACIJA

Ljubljana, 2008

ERRATA

Page	Line	Error	Correction

BIBLIOGRAPHIC-DOCUMENTALISTIC INFORMATION

UDC: 624.04(043.3)

Author: Niko Kristanič

Supervisor: Assoc. prof. dr. Jože Korelc

Title: Limit State Design Using Exact Sensitivity Analysis and Shape Optimization.

Notes: 148 p., 5 tab., 72 fig., 42 eq.

Keywords: shape optimization, limit load, worst initial imperfection, symbolic approach.

Abstract:

Optimization has become an important tool in engineering activities because it represents a systematic method to improve design with respect to certain criteria. Within the thesis a numeric-symbolic approach to limit load shape optimization is studied which enables the use of an optimization algorithm as an ultimate state design tool. Shape is parameterized symbolically using a general computer algebra system. Therefore the design velocity filed can be computed analytically and an exact sensitivity analysis can be carried out. Accurate sensitivity information is of crucial importance for proper gradient shape optimization.

When analyzing imperfection sensitive structures it turns out that the choice of the shape and size of initial imperfections has a major influence on the response of the structure and its ultimate state. Further on, shape optimization applied on the perfect mathematical model can lead to non-optimal results, e.g. a very light structure but very sensitive to buckling. While imperfections are not known in advance, a method for direct determination of the most unfavorable imperfection of structures by means of ultimate limit states was developed. The method is implemented as an internal and separate optimization algorithm within the global shape optimization process.

Full geometrical and material nonlinearity is considered throughout the global optimization process consistently, resulting in efficient and robust, ultimate limit load structure design algorithm. The numerical examples indicate that the use of a symbolic-numeric system for gradient shape optimization combined with the use of the most unfavorable imperfections can represent a superior alternative to conventional ultimate limit state design.

BIBILIOGRAFSKO-DOKUMENTACIJSKA STRAN IN RAZŠIRJEN IZVLEČEK

UDK: 624.04(043.3)

Avtor: Niko Kristanič

Mentor: izr. prof. dr. Jože Korelc

Naslov: Sinteza konstrukcij z uporabo točne občutljivostne analize in optimizacije oblike v nelinearnem področju.

Obseg in oprema: 148 str., 5 pregl., 72 sl., 42 en.

Ključne besede: oblika konstrukcij, optimizacija oblike, nosilnost konstrukcij, mejna obtežba, najbolj neugodne začetne nepopolnosti, vpliv na stabilnost, simbolni pristop.

Izvleček. Optimizacija postaja vedno bolj pomembno orodje v inženirski praksi saj predstavlja sistematično metodo izboljšanja izdelkov glede na dane kriterije. V okviru disertacije je predstavljen simbolno-numerični pristop k optimizaciji oblike konstrukcij v mejnem stanju nosilnosti. Pristop omogoča uporabo optimizacijskega algoritma kot orodje za projektiranje konstrukcij. Oblika konstrukcije je parametrizirana simbolno s pomočjo sistema za splošno računalniško algebro, ki s pomočjo neposrednega odvajanja omogoča analitičen izračun polja začetnih občutljivosti. Posledično je možno izvesti natančen izračun občutljivosti odziva, kar je ključnega pomena, saj so točne občutljivosti pogoj za uspešno uporabo gradientnih metod optimizacije oblike.

Kadar obravnavamo konstrukcije, občutljive na spremembo začetne geometrije, se izkaže, da ima izbira oblike in velikosti začetnih nepopolnosti velik vpliv na odziv konstrukcije in njeno mejno stanje. Poleg tega uporaba idealne oblike konstrukcije lahko privede do nestabilnosti optimizacijskih algoritmov ali do neoptimalnih rezultatov, na primer izjemno lahkih konstrukcij, ki so močno občutljive na nepopolnosti. Začetne nepopolnosti niso znane v naprej, zato je v okviru disertacije bila razvita metoda za določitev najbolj neugodne začetne nepopolnosti v smislu mejnega stanja konstrukcij. Metoda je implementirana kot ugnezden optimizacijski algoritem v okviru globalne optimizacije oblike.

Skozi celoten proces optimizacije oblike je uporabljen polno nelinearen pristop, ki omogoča učinkovito in robustno sintezo konstrukcij. Prikazani primeri prikazujejo uporabnost metode in nakazujejo, da uporaba simbolno numeričnega okolja za gradientno optimizacijo oblike v povezavi z metodo določitve najbolj neugodnih začetnih nepopolnosti predstavlja napredno alternativo klasičnemu projektiranju konstrukcij.

Zahvala

Delo, ki je bilo opravljeno v okviru disertacije, je bilo delno financirano s strani Ministrstva za visoko šolstvo, znanost in tehnologijo, v okviru programa mladih raziskovalcev.

Iskreno se zahvaljujem svojemu mentorju izr. prof. dr. Jožetu Korelcu za vso pomoč in vodenje skozi znanstveno delo. Prof. dr. Darku Begu se zahvaljujem za strokovno pomoč in koristne nasvete. Zahvala gre tudi vsem sodelavcem, ki so poskrbeli za konstruktivno debato in prijetno vzdušje.

Posebna zahvala je namenjena mojim staršem, ki so me vso dolgo pot podpirali in vzpodbujali ter moji Mateji, ki si mi vselej stala ob strani.

Acknowledgement

I am very grateful for the help received from Krzysztof Wisniewski, Institute of Fundamental Technological Research, Warszawa, Poland who kindly allowed his symbolic description of shell finite elements to be used within the presented research.

Contents

1 INTRODUCTION 1

1.1 Structural limit load design optimization 1
1.2 Background of work and state of the art 4
1.2.1 Limit Load Shape Optimization 4
1.2.2 Sensitivity analysis 6
1.2.3 Imperfections 9
1.3 Motivation and Objectives 13
1.4 Methodology 13
1.5 Thesis Outline 15

2 FINITE ELEMENT MODELING AND SYMBOLIC APPROACH 17

2.1 Automation of FEM 18
2.2 Automatic differentiation 20
2.2.1 Principles of automatic differentiation 20
2.2.2 Automatic differentiation and FEM 21
2.3 Hybrid symbolic-numerical approach 25
2.3.1 Typical example of automatic code generation procedure 28
2.4 Abstract symbolic formulations in computational mechanics 29
2.5 Symbolic-numerical environment *AceFEM* 31

3 DIRECT AND SENSITIVITY LIMIT LOAD ANALYSIS 33

3.1 Definition of ultimate states 33
3.2 Direct Analysis 34
3.3 Sensitivity Analysis 37
3.3.1 The Analytical Design Velocity Field 39
3.3.2 Exact sensitivity analysis 44
3.4 Symbolical formulation of general finite strain plasticity 45
3.5 Finite element models 49
3.6 Example 51

4 INITIAL IMPERFECTIONS 55

4.1 Introduction 55
4.2 Optimization method for the determination of the most unfavorable initial imperfection 56
4.2.1 Representation of imperfections 56

4.2.2 Description of the algorithm 57
4.2.3 Formulation of the optimization problem 60
4.2.4 Direct and sensitivity analysis 62
4.3 Numerical examples (Test Problems and Results) 63
4.3.1 Elasto-plastic cantilever structure 63
4.3.2 Thin-walled T beam 68
4.3.3 Thin-walled I beam 73
4.3.4 Thin-walled Cylinder 76
4.4 Partial conclusions 80

5 LIMIT LOAD DESIGN SHAPE OPTIMIZATION 83

5.1 Introduction 83
5.2 Shape Optimization 84
5.2.1 Evolutionary and Optimality Criteria approaches 84
5.2.2 Mathematical programming 85
5.3 Gradient based Shape Optimization combined with imperfection analysis 88
5.4 Numerical examples 92
5.4.1 2D cantilever shape optimization 92
5.4.2 3D H cross-section thin-walled cantilever structure 95
5.4.3 3D single storey steel building 111

6 FINAL CONCLUSIONS 121

7 POVZETEK 125

REFERENCES 143

INDEX OF FIGURES

FIG. 1: FLOW CHARTS OF CONVENTIONAL STRUCTURAL DESIGN (A) AND OPTIMUM STRUCTURAL DESIGN (B). 2
FIG. 2: SCHEMATIC REPRESENTATION OF THE OVERALL ALGORITHM FOR LIMIT LOAD SHAPE OPTIMIZATION. 14
FIG. 3: MULTI-LANGUAGE AND MULTI-ENVIRONMENT FE CODE GENERATION. 27
FIG. 4: TYPICAL *ACEGEN* INPUT. 29
FIG. 5: TYPICAL AUTOMATICALLY GENERATED SUBROUTINE IN FORTRAN AND C LANGUAGE. 29
FIG. 6: DEFINITION OF ULTIMATE STATES (EN 1993 1-5 2004). 34
FIG. 7: GENERAL FORMULATION OF DIRECT ANALYSIS OF TRANSIENT COUPLED NONLINEAR PROBLEMS. 36
FIG. 8: GENERAL FORMULATION OF SHAPE SENSITIVITY ANALYSIS OF TRANSIENT COUPLED NONLINEAR PROBLEMS. 38
FIG. 9: GEOMETRY OF CANTILEVER WITH MARKED NODE NUMBERS AND SHAPE PARAMETERS. 40
FIG. 10: *ACEFEM* INPUT DATA FOR THE STRUCTURE ILLUSTRATED IN FIG. 9. 40
FIG. 11: *ACEFEM* NODE COORDINATES FOR LINEAR BOUNDARY SHAPE APPROXIMATION. 41
FIG. 12: *ACEFEM* NODE COORDINATES FOR QUADRATIC BOUNDARY SHAPE INTERPOLATION. 41
FIG. 13: DESIGN VELOCITY FIELD BY SYMBOLICAL DERIVATION OF FE NODE COORDINATES FOR THE CASE OF LINEAR INTERPOLATION BETWEEN SHAPE PARAMETERS. 42
FIG. 14: DESIGN VELOCITY FIELD BY SYMBOLICAL DERIVATION OF FE NODE COORDINATES FOR THE CASE OF QUADRATIC INTERPOLATION BETWEEN SHAPE PARAMETERS. 42
FIG. 15: GRAPHICAL REPRESENTATION OF THE *Y* COMPONENT OF THE DESIGN VELOCITY FIELD FOR THE CASE OF LINEAR INTERPOLATION BETWEEN SHAPE PARAMETERS. 43
FIG. 16: GRAPHICAL REPRESENTATION OF THE *Y* COMPONENT OF THE DESIGN VELOCITY FIELD FOR THE CASE OF QUADRATIC INTERPOLATION BETWEEN SHAPE PARAMETERS. 44
FIG. 17: FLOWCHART OF SHAPE SENSITIVITY ANALYSIS BY DUAL SYMBOLIC-NUMERIC FE ENVIRONMENT. 45
FIG. 18: ALGORITHM FOR THE ABSTRACT SYMBOLIC DESCRIPTION OF ELASTO-PLASTIC PROBLEMS. 47
FIG. 19: SUMMARY OF THE FINITE STRAIN PLASTICITY EQUATIONS. 48
FIG. 20: FINITE ELEMENT MODEL FOR THE ONE STORY BUILDING. 52
FIG. 21: EXAMPLE OF A NODAL POINT COORDINATE IN SYMBOLIC FORM. 53
FIG. 22: COMPARISON BETWEEN ANALYTIC AND FD METHOD. 53
FIG. 23: GRAPHICAL SENSITIVITY REPRESENTATION OF THE VERTICAL DISPLACEMENT WITH RESPECT TO THE ROOF ANGLE. 54
FIG. 24: FLOWCHART OF THE METHOD FOR THE DETERMINATION OF THE MOST UNFAVORABLE INITIAL IMPERFECTION. 59
FIG. 25: GEOMETRY AND LOADING (A) AND THE LOGICALLY MOST UNFAVORABLE SHAPE WITHOUT CONSIDERING TECHNOLOGICAL CONSTRAINTS (B) FOR THE CANTILEVER BEAM EXAMPLE. 63
FIG. 26: THE SHAPE BASE FOR THE CANTILEVER BEAM EXAMPLE. 64
FIG. 27: CONVERGENCE TO THE MOST UNFAVORABLE SHAPE BY INCREASING THE NUMBER OF CONSIDERED SHAPES IN THE SHAPE BASE (SCALE FACTOR $F_S = 10$). 66
FIG. 28: GEOMETRY, SUPPORTING AND LOADING CONDITIONS FOR THE THIN-WALLED T BEAM EXAMPLE. 68
FIG. 29: MAXIMAL ALLOWABLE DEVIATION FROM THE PERFECT GEOMETRY USED IN THE EVALUATION. 69
FIG. 30: THE CALCULATED ULTIMATE LOAD OF THE T-BEAM CONSIDERING THE EVALUATED MOST UNFAVORABLE INITIAL IMPERFECTION VARYING THE NUMBER OF BASE SHAPES. 70
FIG. 31: THE LOAD DISPLACEMENT CURVES CONSIDERING VARIOUS IMPERFECTION SHAPE BASES FOR THE T BEAM EXAMPLE. 71
FIG. 32: THE MOST UNFAVORABLE INITIAL IMPERFECTION SHAPE OF THE T CROSS-SECTION THIN-WALLED GIRDER (A) AND THE CORRESPONDING DEFORMED SHAPE AT COLLAPSE (B). 71
FIG. 33: CONVERGENCE OF THE GLOBAL ITERATION PROCESS OF FINDING THE MOST UNFAVORABLE IMPERFECTION SHAPE FOR THE EXAMPLE WITH 52 BASE SHAPES. 72
FIG. 34: EQUILIBRIUM PATHS FOR THE T CROSS-SECTION THIN-WALLED GIRDER. 73
FIG. 35: MAXIMAL ALLOWABLE DEVIATION FROM THE PERFECT GEOMETRY USED IN THE EVALUATION. 74
FIG. 36: ULTIMATE LOAD DEFORMATION CURVES FOR DIFFERENT INITIAL IMPERFECT GEOMETRIES WITH THE SAME AMPLITUDE FOR THE I BEAM EXAMPLE. 75
FIG. 37: INITIAL IMPERFECT GEOMETRIES USED IN ANALYSES ACCORDING TO FIG. 36. 76
FIG. 38: GEOMETRY OF THE AXIALLY AND TRANSVERSELY LOADED CYLINDER. 77

Fig. 39: Most unfavorable initial imperfection for axially and transversely loaded cylinder considering the imperfection amplitude R/165. Scale factor F_S=10. 78
Fig. 40: Load displacement curve considering the most unfavorable initial imperfection. 78
Fig. 41: Deformation state at limit load. 79
Fig. 42: Fold line of the axially and transversely loaded cylinder. 79
Fig. 43: Optimization using symbolic-numeric environment. 89
Fig. 44: Optimization loop using symbolic-numeric environment. 90
Fig. 45: Initial shape (a), Optimal shape (b). 93
Fig. 46: Convergence of the optimization process for two shape parameters. 94
Fig. 47: Structural response of different shapes and the limit load optimal shape. 94
Fig. 48: Initial geometry of H cross-section cantilever. 96
Fig. 49: H cross-section cantilever shape parameters. 97
Fig. 50: The most unfavorable imperfection for the initial (a) and optimal shape (b) (Scale factor=30, Shell thickness A). 99
Fig. 51: Limit load shape optimization process. 101
Fig. 52: Initial and optimum shape of H cross-section cantilever geometry for case A shell thickness. 102
Fig. 53: Mises stress at limit state for optimal H cross-section cantilever shape (undeformed). 103
Fig. 54: Deformation of H cross-section cantilever at limit state (Scale Factor = 1) with Mises stress plotted. 103
Fig. 55: Mises stress for the corresponding load-deformation curve plotted in Fig. 51. 104
Fig. 56: The most unfavorable imperfection for the initial (a) and optimal shape (b) (Scale factor=30, Shell thickness B). 105
Fig. 57: Initial and optimum shape of H cross-section cantilever for case B shell thickness. 106
Fig. 58: Mises stress at limit state for optimal H cross-section cantilever shape (undeformed). 107
Fig. 59: Deformation of H cross-section cantilever at limit state (Scale Factor = 1) with Mises stress plotted. 107
Fig. 60: Mises stress for the corresponding load-deformation curve plotted in Fig. 61. 108
Fig. 61: Load-deformation curve for optimized shape in Case A and Case B. 109
Fig. 62: Initial geometry of single storey steel building. 111
Fig. 63: Loading conditions and shape parameterization for the inner frame. 112
Fig. 64: Loading conditions and shape parameterization for the outer frame. 113
Fig. 65: Optimum shape of the inner frame of the steel structure with the initial geometry in the final optimization run. 114
Fig. 66: Optimum shape of the outer frame of the steel structure with the initial geometry in the final optimization run. 114
Fig. 67: Deformation of the inner frame at limit state (Scale Factor = 10). 115
Fig. 68: Deformation of the outer frame at limit state (Scale Factor = 10). 116
Fig. 69: Mises stress for inner frame for the corresponding load-deformation curve plotted in Fig. 71. 117
Fig. 70: Mises stress for outer frame for the corresponding load-deformation curve plotted in Fig. 71. 118
Fig. 71: Load-deformation curves for the inner and the outer frame with the optimized shape. 119
Fig. 72: Optimized shape of single story steel building. 120

Index of Tables

Table 1: Automatic differentiation exceptions. 25
Table 2: Residual form of equations for mechanical problems. 34
Table 3: Strain energies for the use in the Automatic differentiation exceptions. 50
Table 4: Ultimate load factors for various initial imperfection shapes for the cantilever beam example. 67
Table 5: Optimization parameter values for the optimized structure. 120

1 INTRODUCTION

It is in the nature of mankind and nature itself to strive after the achievement of a goal with the least possible amount of effort. Technical development has always required incessant improvement of solutions. This has been achieved by systematic improvement of initial design, by redesigning, implementing new knowledge and learning from past mistakes. In this manner the initial form of design optimization has been a sort of trial and error process which in the end has given better and better solutions. Although a very time consuming process, the basic idea is adopted by most modern design optimization strategies. Nowadays the technical development is accompanied with a growing competition which demands lower design and production cost, higher quality, less energy consumption, environment friendly and recycling ability design and design of products with the required aesthetic value.

To meet the increasing necessity for competitive products, a scientific approach is needed. The latest knowledge from the field of computational mechanics, sensitivity analysis and optimization has to be used. Within the work presented by the thesis a limit load shape optimization method including worst imperfection evaluation was developed using the latest symbolic-numerical environment technology.

It is difficult to fulfill all the requirements and to claim that one of the evaluated potential optimum designs was the best possible. The decision is left to the design engineer to define the performance criteria and restrictions. In the present work the optimum design is therefore defined as the one that maximizes the chosen performance criteria and satisfies al the constraints given by the engineer.

1.1 Structural limit load design optimization

It is important to recognize the difference between structural analysis and structural design. The analysis problem is concerned with determining the behavior of an existing structural system with a known design, while structural design is a task where the design is varied to meet performance requirements.

Until recently conventional structural design has mostly been used for designing structures. Conventional structural design is a trial and error procedure and depends on the designer's intuition, experience and skill. It can be a difficult challenge for an

engineer to achieve efficiency, cost-effectiveness and an overall integrity of a designed structure. Sometimes this approach can lead to erroneous results and uneconomical structures when dealing with complex structural systems.

The growing industrial competition is forcing engineers to consider different approaches, economical and better design. Design optimization is one of such approaches. The difference between conventional design and design optimization called synthesis is clearly illustrated in Fig. 1.

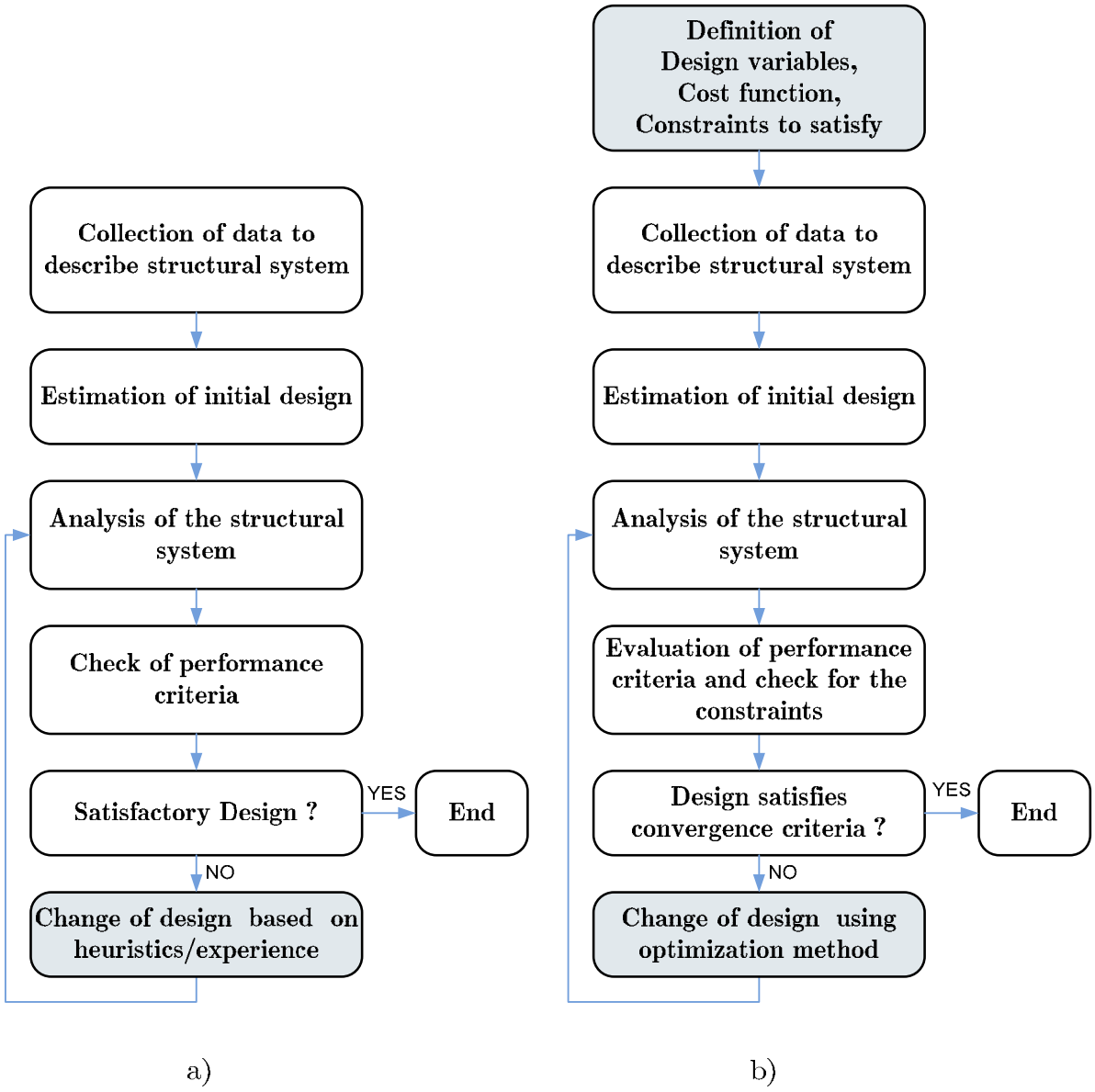

Fig. 1: Flow charts of conventional structural design (a) and optimum structural design (b).
Slika 1: Običajni potek projektiranja (a) in projektiranje s pomočjo optimizacije (b)

Design optimization process forces the designer to define a set of design variables, an objective function to be optimized, and the constraint functions to be taken into account. Despite the extra work the path to better design is certainly shorter than within conventional design. Although the optimization approach seems more formal, it can substantially benefit from the designer's experience and intuition in formulating the problem, choosing proper parameterization and identifying the critical constraints. Thus, the best approach would be an optimum design process aided by the designer's interaction.

Proper mathematical formulation of the design optimization problem is a key to good solutions. The optimization loop within the optimum structural design algorithm (Fig. 1b) can be divided into three characteristic steps:

- Evaluating the performance measure of the structure by using the current design variables (direct analysis).
- Evaluating sensitivity of the design to changes of all design variables, where sensitivities are the gradients of the objective and constraint functions used by the optimization algorithm (design sensitivity analysis).
- Updating the design variables using sensitivity information in a way that improves the objective function (optimization).

Limit load structural optimization design demands a complex interaction of different approaches, used algorithms and methods. When designing structures for the ultimate state, the limit load of the designed structure has to be known and is usually given by technical standards and codes. In the optimization algorithm the limit load presents a constraint that has to be fulfilled.

When dealing with imperfection sensible structures, e.g. thin walled structures, imperfections have to be taken into account. A method for automatic evaluation of the most unfavorable initial imperfection is presented.

In the optimization process the design is changed by varying design variables represented by shape parameters. When using gradient based shape optimization approaches, the hardest problem is to evaluate accurate sensitivities with respect to shape parameters for the gradient information. With the use of a symbolic-numeric system, exact sensitivities can be evaluated by using an analytically calculated velocity field. Arbitrary symbolic shape parameterization can be used with no limitation.

Direct and sensitivity analyses within shape optimization and the evaluation of the most unfavorable initial imperfections are performed to the ultimate limit state of the structure. Within conventional shape optimization methods usually the minimum weight is sought for a certain stress distribution state, the state at first yielding point or buckling load, but no real limit state is considered as it is difficult to define and to evaluate. Within the presented approach the optimal shape is sought for the ultimate limit state of the structure resulting in a robust optimal design which has to satisfy all design criteria.

The combination of a symbolic–numeric system and an algorithm for the automatic determination of most unfavorable initial imperfections gives rise to an effective structural design shape limit load optimization method appropriate to be used as an efficient designing tool.

1.2 Background of work and state of the art

1.2.1 Limit Load Shape Optimization

Historically, structural optimization used to be a global process of progress in structural design, mainly based on experience and experiments. The engineering skills have improved gradually and the results of designs have became more and more optimal. Many results of current basic structural optimization problems solved by contemporary optimization methods are in close relation to the results gained through the historical design development.

The most important point in structural optimization is to define the relation between geometry and the internal flow of forces. Throughout the historical design development this was the focus of experiments and intuitive design. The first analytical works of structural optimization appeared in 17th and 18th century. Important contributors were Galilei (1638; Discorsi e Dimostrazioni Matematiche, intorno a due nuove scienze), Bernoulli (1687; The brachistochrone problem) and Lagrange (1770; Miscellanea Taurinensia). Mainly the first analytical works were interested in particular cases of optimal sections of beams and columns and no general application was developed. In the 19th and 20th century numerical methods constantly developed further.

The key to the modern design was the development of computers, structural analysis methods and mathematical programming. The first to integrate numerical methods into optimization techniques was Schmit (1960) who proposed the concept of structural synthesis. The basic idea of structural synthesis is to integrate finite

element structural analysis into nonlinear mathematical programming methods, which results in an automated optimum design process.

The field of structural synthesis developed further in the next decades. Several other disciplines had to be involved, i.e. structural sensitivity evaluation, CAD preprocessors, and control systems for managing different phases, which interact with each other in the solving process. The first optimization problems considered within structural synthesis were mainly concerned with size optimization of discrete structures.

In size optimization, the geometry of the mathematical model is known (e.g. shape, topology) and the characteristics of the mathematical model elements have to be determined (e.g. cross section, material). An example may be a truss structure modeled with truss finite elements where the cross-sections of the trusses have to be determined so that the overall weight of the structure is the smallest.

In shape optimization, the geometry of the mathematical model itself is the subject under consideration. The crucial difference between sizing and shape optimization is related to how design variables affect the analysis rather than to the physical optimization problem itself. In size optimization the design variables are related to the properties of the finite elements where in shape optimization the design variables are related to the positions of the finite element nodes and therefore directly affect the implementation within structural analysis.

The first attempts of shape optimization were therefore performed on discrete modeled structural systems. Zienkiewicz and Campbell (1973) considered finite element nodes coordinates as design variables which later turned out not to be ideal for solving optimization algorithms. Nevertheless they were the first to set up a shape optimization problem in a general form.

The use of optimization in design began to strengthen in the 1980's together with the intensive development of numerical analysis methods and nonlinear mathematical programming and with expanding computer capabilities. The start of the development of new shape optimization methods gave a clear indication that numerous new problems would arise, which were not known in classical discrete optimization (Haftka, Grandhi 1986).

Nowadays discrete optimization is well developed and already integrated in everyday structural analysis programs. Shape optimization, on the other hand, remains the subject of continuous scientific research (see e.g. Bletzinger, Ramm 2001, Camprubi, et al. 2004, Choi, Kim 2005a, Choi, Kim 2005b, Maute, et al. 1999, Ramm, Mehlhorn

1991, Schwarz, et al. 2001, Uysal, et al. 2007). In continuous shape optimization the design parameterization is not automatically given by the structural model and has to be explicitly defined by the designer in relation to the structural analysis model or to an underlying geometrical model. Within most modern approaches the need of general shape parameterization has evolved in an implicit relation of design variables with respect to the positions of the finite element nodes. As a consequence a complex interaction of the finite element method and sensitivity analysis has to be taken into account. An essential part of the procedure is to evaluate the design velocity field which is defined as the derivative of finite element node coordinates with respect to design variables.

Within the presented work a numeric-symbolic approach to optimization is studied which enables the use of arbitrary symbolic shape parameterization and evaluation of an analytical design velocity field. As a consequence, an exact sensitivity analysis can be carried out. Accurate sensitivity information is of crucial importance for proper gradient shape optimization. The sensitivity analysis and the evaluation of the design velocity field will be further addressed in the next section.

1.2.2 Sensitivity analysis

To overcome the difficulties of evaluating sensitivity within shape optimization, numerous methods have been developed in the past (see review by van Keulen, et al. 2005). The four broad categories of methods in common use for obtaining the derivatives of performance measures with respect to structural parameters are:

a) Overall finite differences
b) Discrete derivatives
c) Continuum derivatives
d) Computational or automatic differentiation

The choice of the method is particularly important in gradient shape optimization where the shape design variables change the discretization of the discretizied problem, e.g. finite element mesh.

All methods except for the finite differences can be implemented using direct or adjoint approach (called also the reverse mode of automatic differentiation explained in Section 2.2). In the direct approach, the derivatives of the entire structural response are evaluated. The sensitivities of performance measures can then be obtained from the chain rule of differentiation. In the adjoint approach an adjoint problem which depends on the performance measure is defined. The sensitivities of

performance measures can then be obtained using the structural and adjoint responses. This approach is of most advantage when the problem consists of many design variables and few performance measures while not all system response sensitivities are required.

Overall finite differences (see e.g. Hörnlein H.R.E.M. 2000, Oral 1996) present the simplest method. The method, also called global finite difference, is based on repeated evaluation of structural analysis code and the use of a finite difference formula to obtain the derivative. Forward, backward and central differences can be used. Higher order difference formulae are very rare. Finite difference derivatives can suffer from truncation errors with large step sizes and also from errors when the step size is too small. The computational time is high due to the repeated code evaluation. Global finite differences become very useful when using commercial structural analysis programs where the analysis code is in a form of a black box with no ability to solve the sensitivity problem.

Continuum derivatives are obtained by differentiating the governing continuum equations. Most commonly these consist of partial differential equations or an integral form, for example, derived from the principle of virtual work. The differentiation leads to a set of continuum sensitivity equations that are then solved numerically. The same discretization as for the original structural response can be used. For shape sensitivities, the two main approaches for continuum derivatives are the material derivative approach (see e.g. Saliba, et al. 2005) and the control volume approach (see e.g. Arora, et al. 1992). The advantage of these methods is the possibility of different meshes for response and sensitivity analysis.

The most widely used methods are the discrete derivatives. While the continuum sensitivity equations are derived by differentiating the governing continuum equations with respect to the design variables and are then subsequently discretized, for discrete derivatives this order is reversed. The advances of these methods are low computational cost and high consistency. They can be separated into analytical and semi-analytical.

The analytical methods use analytical derivatives on the global level as well on the finite element level (see e.g. Maute, et al. 2000). The analytical differentiation process may become tedious. This holds true especially for shape design variables, therefore symbolic computing software can be applied (Korelc 2002, Korelc 2007a, b) which often features the automatic generation of the source code. This code has to be integrated in the used software. Additional procedures must be implemented for each finite element used within the structural analysis. The procedure must account for all

possible design variables, i.e. size, material and shape design variables, as the actual code depends on the type of the design variable. Shape design variables are the most complex ones to implement.

The semi-analytical methods (see e.g. Hörnlein H.R.E.M. 2000, Oral 1996) use finite difference schemes on the finite element level, while the dicretized governing equations on the structure level are differentiated analytically. The main reason for the simplification is the significant implementation effort needed for the evaluation of the finite element sensitivity pseudo-load vector. Therefore approximations in the form of finite differences are frequently accepted for the pseudo-load vector, which reduces the effort. Disadvantages of these methods are common for all finite difference methods, the dependency with respect to the perturbation size, which has a pronounced effect on both consistency and efficiency.

The highest consistency is proved by the methods which use automatic differentiation. Analytical derivation is used on all levels. Even if the finite element program is composed of many complicated subroutines and functions, they are basically a collection of elementary functions. The automatic differentiation method defines the partial derivatives of these elementary functions, and then the derivatives of complicated subroutines and functions are computed using propagation of the partial derivatives and the chain rule of differentiation. Thus, no approximation is introduced.

For the highest efficiency of automatically generated codes it is necessary to fulfill specific requirements in order to produce element source codes that are as efficient as manually written codes (see e.g.Korelc 2002). More reference is given in Chapter 2.

A major step in performing shape design sensitivity analysis is the evaluation of the design velocity field. The purpose of design velocity field is to characterize the changes of the finite element nodal point coordinates with respect to the changes of arbitrary design parameters. While the design derivatives of the finite element quantities (residual, tangent matrix, etc.) can be constructed by automatic procedures (see e.g.Korelc 2002), this is not true for the design velocity field.

Within standard approaches to finite element mesh generation, either with specialized preprocessors or with CAD tools, there exist no explicit relations between the positions of the finite element nodes and the shape design parameter as the choice of the shape parameters is an arbitrary decision of the designer. A number of methods have been proposed in the literature to compute the design velocity field (Choi, Chang 1994).

Most frequently used methods for evaluating the design velocity field are the finite difference methods using mesh generators (a), isoparametric mapping methods (b), boundary displacement and fictitious load methods (c), and methods which combine isoparametric mapping and boundary displacement methods (d). All these methods are based on different numerical approximations.

The most sophisticated methods in use are the design model concept methods basically fitting into the isoparametric approach section (see e.g. Kegl 2000, Samareh 1999). A great review was done by Haftka and Grandhi (Haftka, Grandhi 1986). The basic idea of the design element approach relies on the assumption that the geometrical data of the structure are not a simple set of constants defining directly the finite element mesh. Instead of that, the structural data are extracted from a set of geometrical objects called the design elements. The shape of the design elements is connected to the finite element mesh and varied with a few shape parameters using e.g. Bezier curves or polynomials. Although an analytical design velocity field can be evaluated, these methods are limited in the choice of design shape parameters. In complex structural systems the shape has to be composed of many design elements which limit the general applicability. For example, no shape parameters can be defined for global structure dimensions.

To overcome the difficulties of the design element approach, an arbitrary symbolic parameterization is used in the current work using a symbolic-numeric system (Korelc 2007a, b) further addressed in Chapter 2.

Most methods for evaluating design sensitivity are limited to the use of linear or simple nonlinear material models. The use of complicated nonlinear material models makes the evaluation of design sensitivity very difficult. The attempts to develop methods that address this field are therefore rare.

Nonlinear limit load design sensitivity analysis used in the present work for the use in gradient based limit load shape optimization demands complex interaction between shape parameterization and finite element code. Within the development of integration of commercial finite element analysis programs and new design approaches using optimization, every effort was made (see e.g. Chang, et al. 1995, OptiStruct 2008) although to the author's knowledge an efficient tool for nonlinear limit load design optimization is not available.

1.2.3 Imperfections

Limit load design optimization requires an accurate evaluation of the limit load of a structure. In order to evaluate the limit load correctly, all the relevant phenomena

have to be considered e.g. geometrical and material imperfections, load imperfections, residual stresses and strains, damage, etc. It is now well known that geometrical, structural, material and load imperfections play a crucial role in the load carrying behavior, especially of thin walled structures.

Most structural imperfections (residual stresses, geometrical and welding imperfections, etc.) are not known in advance. To include the imperfections in a structural analysis, they have to be assumed. Technical standards therefore suggest different approaches to include imperfections on an empirical basis. A convenient way to include all relevant imperfections (i.e. geometrical, structural and material imperfections) is to consider equivalent geometrical imperfections. In this way the geometrical imperfections are augmented by the influence of other relevant imperfections to produce the same effect on the load carrying behavior of a structure.

The idea to find imperfections that will cause the structure to fail at the lowest possible load is as old as the ascertainment of the crucial role of imperfections itself. The known discrepancy between theoretical results and experimentally obtained values for ultimate loads of structures can be reduced by properly including imperfections in an analysis. In order to achieve this for a general structure, a series of full geometrical and material nonlinear analyses up to the ultimate limit state need to be performed for a large range of possible imperfections, varying both their shapes and amplitudes. The computational cost involved discourages this kind of direct approach and has been the motivation for the development of computationally less expensive methods.

Numerous approaches for analyzing the effect of imperfections on the response of structures have been proposed. Among them one can basically distinguish between those which are derived from the hypothesis that it is possible to obtain a sufficiently accurate structural response for an imperfect structure from the properties of a perfect structure ("perturbation approach") and those that obtain the structural response by analyzing the imperfect structure itself ("direct approach"). The review of different approaches accompanied with the impact on modern design procedures of engineering structures can be found in (Schmidt 2000).

The origin of the perturbation approach goes to the pioneering work on stability of shells done by (Koiter 1945).The perturbation approach applies to structures showing bifurcation phenomena along their natural equilibrium path and is based on asymptotic descriptions of the initial post critical behavior. Although simple for implementation and numerically efficient, the original Koiters theory does not

account for several effects that can significantly lower the ultimate load of the structure, such as:

a) nonlinear natural equilibrium path,
b) nonlinear material behavior,
c) buckling mode interactions,
d) consideration of realistic technological constraints on the shape and amplitude of the imperfections,
e) large postcritical deflections,
f) large imperfections.

The interaction of several buckling modes can be assessed by the "minimum path theory" of (Ho 1974, Lanzo 2000, Lanzo, Garcea 1996). An overview of some other methods was given by (Godoy 2000). There are numerous difficulties obtaining non-linear post critical behavior. Even with modern methods such as arc-length schemes, branch switching procedures, direct computation of stability points and stabilization techniques, it is sometimes impossible to overcome problems like secondary bifurcations, coincidental or clustered singularities and post critical paths, that cross each other, to get all the possible hypothetic equilibrium paths or at least the minimum one.

Another approach is the "minimum perturbation energy concept", which has recently been applied also to dynamic stability problems (Dinkler, Pontow 2006, Ewert, et al. 2006). The basic idea of the method is to lower the buckling load of a perfect structure by introducing a certain amount of energy into the system, which causes a snap through to the post-buckling path, or to a secondary path in dynamic problems.

Common to all perturbation methods is that they become exceedingly complicated for implementation and numerically inefficient when phenomena such as mode interaction or plasticity are included. This has been an inspiration for the research on the second branch of methods where the structure is analyzed using a full nonlinear analysis that by definition includes phenomena (a), (b), (e) and (f). The buckling or limit load of a theoretically perfect structure is lowered by introducing imperfections directly into the geometry of the structure. There exists a huge amount of uncertainties in the determination of the shape and amplitude of real imperfections because of the nature of the production processes. Therefore it would be natural to use probabilistic approaches where imperfections are introduced as random variables with a certain distribution (Elishakoff 2000, Papadopoulos, Papadrakakis 2005, Schenk, Schueller 2003). However, these methods rely upon very scarce data banks of

measured imperfections and are therefore useful for a certain assortment of applications.

An alternative approach to include imperfections in an analysis is the concept of the "definitely worst" imperfection (Deml, Wunderlich 1997, El Damatty, Nassef 2001, Song, et al. 2004, Wunderlich, Albertin 2000, 2002). Within the "definitely worst" imperfection concept the shape of imperfections is searched that would lead to the lowest ultimate load of the structure. The shape of imperfections is additionally bounded by the given imperfection amplitude. Several variants of the procedure are possible and discussed (Schmidt 2000).

Deml and Wunderlich (Deml, Wunderlich 1997) introduced an elaborate method to obtain the "definitely worst" imperfection. In their case imperfections are treated as additional degrees of freedom. The approach results in an extended system of equations composed of equilibrium equations, equations for direct computation of stability points (Wriggers, Simo 1990), condition equations for the worst imperfections shape and constraint equations that limit the amplitude of the imperfection. The system has to be solved simultaneously for the equilibrium state, the worst imperfection shape and the corresponding ultimate load. The result is the "definitely worst" imperfection within the considered amplitude. Such procedure is rather time consuming and is therefore useful for problems of small order (Wunderlich, Albertin 2000, 2002). Within the approach of Deml and Wunderlich (Deml, Wunderlich 1997) the condition equations for the worst imperfection are based on Koiters asymptotic theory, thus limiting the approach to small imperfections and linear fundamental paths.

The determination of the "definitely worst" imperfection can also be formulated as a nonlinear optimization problem solved by one of the well-known nonlinear optimization methods. This is the most general approach that includes all the relevant phenomena, but is for the same reason also the most computationally expensive one. For example, a genetic optimization algorithm for obtaining the worst imperfection of shell structures was used by (El Damatty, Nassef 2001). Apart from the obvious disadvantage of the optimization approach, i.e. the need for a potentially large number of full nonlinear analyses, there are also advantages. Since the bifurcation-type instability always represents some type of a symmetry breakdown, bifurcations can be avoided if the symmetry is deliberately destroyed by introducing imperfections (Bažant, Cedolin 2003). By limiting the analysis to limit points, one avoids tedious procedures involved in proper determination, classification and sensitivity analysis of bifurcation points. Another certain advantage of the direct

approach is that only stable equilibrium states have to be considered and no hypothetic or unstable states need to be relied upon.

It is doubtful that an approach requiring a large number of fully nonlinear analyses could be used in everyday engineering design in foreseeable future.

In the present work a computationally less expensive optimization method is developed that would still retain the generality of the optimization based "definitely worst" imperfection approach. The method is further addressed in Chapter 4.

1.3 Motivation and Objectives

The integration of optimization methods into engineering design is a complex task. As pointed out in the previous sections, there are numerous difficulties to achieve this for a general nonlinear case. To facilitate the use of synthesis to design engineering structures, an effective optimization method has to be used considering full nonlinearity with the use of automatic definition of proper initial imperfections.

The general objective of this work is to develop a finite element based limit load shape optimization technique which can be used for the ultimate limit design of structures.

The key aspects to be investigated in this work are:

- The use of a symbolic-numeric system for limit load analysis and optimization purposes. Symbolic derivation and automatic code generation of finite elements for direct and sensitivity analysis.
- The evaluation of most unfavorable initial imperfections of a structure by means of ultimate limit states.
- Analytical evaluation of the design velocity field, using arbitrary shape parameterization, for the use in exact sensitivity analysis.
- Development of an efficient gradient based limit load shape optimization method based on all the above components.

1.4 Methodology

Limit load shape optimization is performed with state of the art optimization algorithms using the computer algebra software *Mathematica* (Wolfram 2008) and a symbolic-numeric approach using automatic code generator *AceGen* (Korelc 2007b) and finite element environment *AceFEM* (Korelc 2007a). Finite element method is used to model the structure subjected to optimization. Direct and sensitivity analysis

of structures by using the most unfavorable initial imperfect geometry is performed in *AceFEM*. All the necessary finite element codes are developed using abstract symbolic description with simultaneous optimization of expressions, automatic differentiation technique, theorem proving and automatic generation of finite element code (Korelc 2002) using *AceGen*.

The use of the numeric-symbolic system offers the possibility one to use an analytical approach. Sensitivity calculation with the use of an analytically evaluated design velocity field is of crucial importance for the convergence of the gradient optimization algorithm, especially when dealing with highly geometrical and material nonlinear problems. The overall algorithm is presented in Fig. 2.

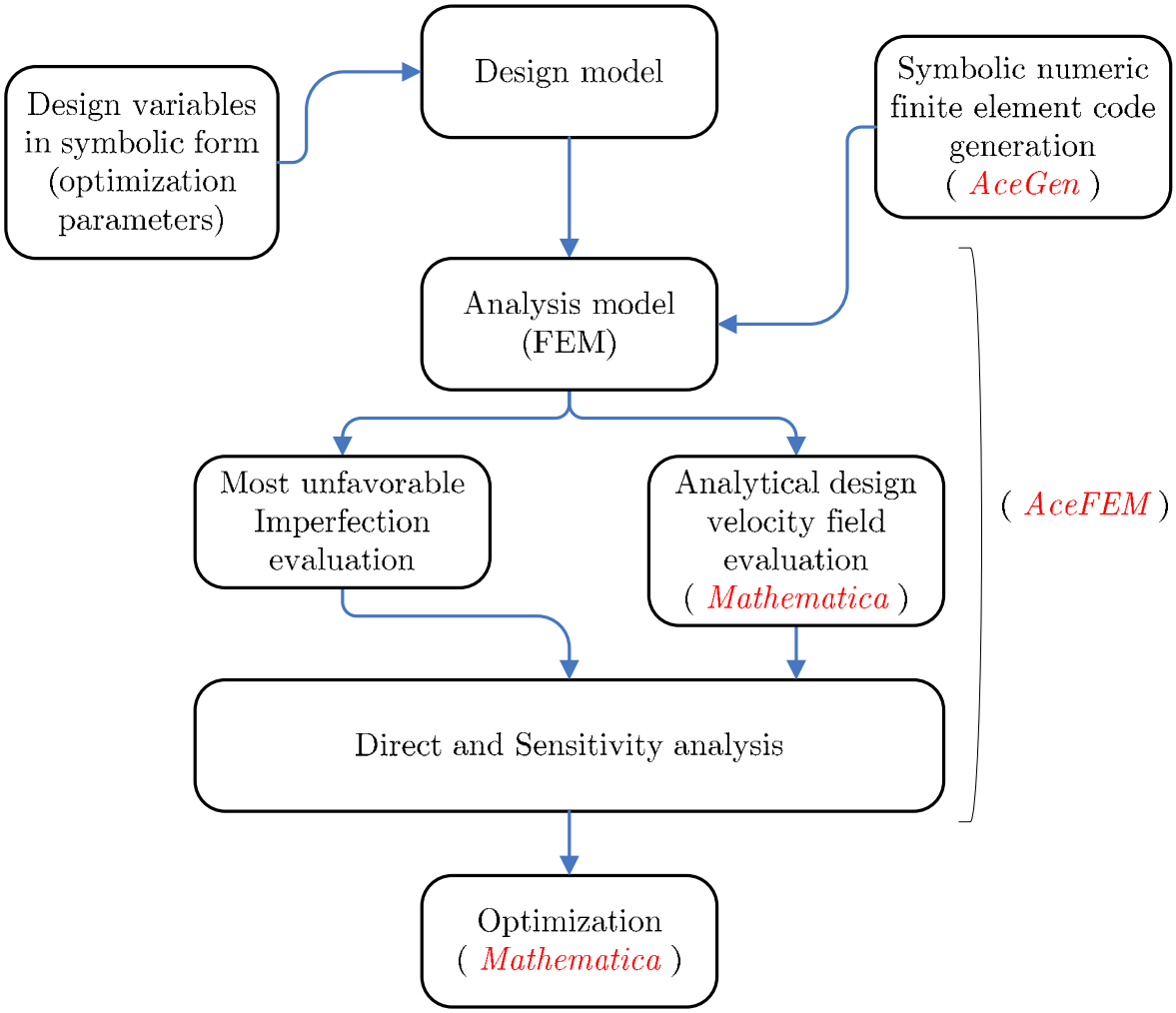

Fig. 2: Schematic representation of the overall algorithm for limit load shape optimization.
Slika 2: Prikaz celotnega postopka optimizacije oblike konstrukcij v mejnem stanju.

1.5 Thesis Outline

The thesis is organized in 4 main chapters.

- Chapter 2 introduces the symbolic description of mechanical problems, the use of advanced automatic differentiation techniques and the hybrid symbolic-numeric environment.
- Chapter 3 is devoted to the structural sensitivity analysis using an analytical design velocity field. The general expressions for the direct and sensitivity analysis which can be used for abstract symbolic description of transient nonlinear coupled systems are given.
- Chapter 4 explains the use of imperfections in a limit load structural analysis. A method for the evaluation of the worst imperfect geometry is presented.
- Chapter 5 incorporates all the relevant techniques presented in previous chapters to perform a limit load shape design optimization. Examples are given for typical civil engineering structures.
- Chapter 6 summarizes the conclusions drawn from present work.

2 FINITE ELEMENT MODELING AND SYMBOLIC APPROACH

The most effective and widely spread method for solving problems in solid mechanics nowadays is the finite element method (FEM). The method originates from the needs to solve complex, structural analysis problems in civil and aeronautical engineering. Today FE methods are far more advanced and can be used for highly nonlinear direct and sensitivity analyses, inverse modeling and optimization of Multi-field, Multi-scale, Multi-body, Multi-phase and Multi-objective problems. Te purpose of the present work is not to introduce fundamental knowledge of Continuum Mechanics and of Finite Element Methods, as many references can be found on these matters. An introduction to Continuum Mechanics is given by (see e.g. Marsden, Hughes 1994) and (Lemaitre, Chaboche 1990). An overture to the Finite Element Method can be found in (Zienkiewicz, Taylor 2000b) and (Crisfield 1996; Crisfield 1997).

With the employment of FEM to increasingly complicated and bounded problems, the implementation of the method has become highly sophisticated. The struggle to automate some of the tasks in the overall processes which starts with the development of theories and ends with a working program is therefore highly appreciated. Some major achievements have been attained in this field of computational mechanics in the last decade. Automation of the finite element method has attracted attention of researches from the fields of mathematics, computer science and computational mechanics, resulting in a variety of approaches and available software tools.

The use of advanced software technologies, especially symbolic and algebraic systems, problem solving environments and automatic differentiation tools influences directly how the mechanical problem and corresponding numerical model are postulated and solved, leading to the automation of the finite element method. In order to formulate nonlinear finite elements symbolically in a general but simple way, a clear mathematical formulation is needed at the highest abstract level possible.

The finite element technology used in the present work is based on a symbolic-numeric approach with a high degree of automation implemented in software

packages *AceGen* and *AceFEM* (Korelc 2007a, b). The basic techniques and methods used within are described in next sections.

2.1 Automation of FEM

Automation of FEM is a complex task because of the various transformations, differentiation, matrix operations, and a large number of degrees of freedom involved in the derivation of characteristic FE quantities, which often leads to exponential growth of expressions in space and time (Korelc 2002). The complete FE simulation can be, from the aspect of the automation level, decomposed into the following steps:

- formulation of strong form of initial boundary-value problem; transformation of the strong form into weak form or variational functionals;
- definition of the domain discretization and approximation of the unknowns and the virtual fields;
- derivation and solution of additional algebraic equations defined at the element level (e.g. plastic evolution equations);
- derivation of algebraic equations that describe the contribution of one element to the global internal force vector and to the global tangential stiffness matrix;
- coding of the derived equations in required compiled language;
- generation of finite element mesh and boundary conditions;
- solution of global problem;
- presentation and analysis of results.

Alternatively, one can also start from the free Helmholtz energy of the problem and derive element equations directly as a gradient of the free energy. This approach is especially appealing for the automation due to the numerical efficiency of the solution when the gradient is obtained by the backward mode of automatic differentiation.

There are almost countless ways of how a particular problem can be solved by the FE method. If the automation of all nine steps is chosen, then only very specific subset of possible formulations can be covered. On the other hand, the standard discretization is of little use for problems involving coarse mesh, locking phenomena and distorted element shapes where highly problem specific formulations have to be used.

The following techniques, which are the result of rapid development in computer science in the last decades, are particularly relevant for the description of a nonlinear finite element model on a high abstract level, while preserving the numerical efficiency:

- Symbolic and algebraic computational systems
- Automatic differentiation tools
- Problem solving environments
- Hybrid approaches

Computer algebra (CA) systems are tools for the manipulation of mathematical expressions in symbolic form. Widely used CA systems such as *Mathematica* or *Maple* have become an integrated computing environment that covers all aspects of computational process, including numerical analysis and graphical presentation of the results.

In the case of complex mechanical models, the direct use of CA systems is not possible due to several reasons. For the numerical implementation, CA systems cannot keep up with the run-time efficiency of programming languages such as FORTRAN and C and by no means with highly problem-oriented and efficient numerical environments used for finite element analysis. However, CA systems can be used for the automatic derivation of appropriate formulae and generation of numerical codes. The FE method is within the general CA systems usually implemented as an additional package or toolbox such as *AceFEM* (Korelc 2007a) for *Mathematica* used in the work covered by this thesis.

The major limitation of symbolic systems, when applied to complex engineering problems, is an uncontrollable growth of expressions and consequently redundant operations and inefficient codes. (see Korelc 1997, Korelc 2002) This is especially problematic when CA systems are used to derive formulae needed in numerical procedures such as finite element method where the numerical efficiency of the derived formulae and the generated code are of utmost priority.

The automation level of FE method can be greatly increased by combining several approaches and tools. A hybrid symbolic numeric system is used within the thesis described in Section 2.3

2.2 Automatic differentiation

Differentiation is an arithmetic operation that plays crucial role in the development of new numerical procedures. The exact analytical derivatives are difficult to derive, which is why the numerical differentiation is often used instead. The automatic differentiation (AD) represents an alternative solution to the numerical differentiation as well as to the symbolic differentiation performed either manually or by a computer algebra system. With the AD technique, one can avoid the problem of expression growth that is associated with the symbolic differentiation performed by the CA system.

2.2.1 Principles of automatic differentiation

If one has a computer code which allows to evaluate a function f and needs to compute the gradient ∇f of f with respect to arbitrary variables, then the automatic differentiation tools, see e.g. Griewank (2000), Bartholomew-Biggs et al. (2000), Bischof et al. (2002), can be applied to generate the appropriate program code. There are two approaches for the automatic differentiation of a computer program, often recalled as the forward and the backward mode of automatic differentiation. The procedure is illustrated on a simple example of function f defined by

$$f = b\,c, \text{with}\, b = \sum_{i=1}^{n} a_i^2 \,\text{and}\, c = Sin(b) \tag{1}$$

where $a_1, a_2, ..., a_n$ are n independent variables. The forward mode accumulates the derivatives of intermediate variables with respect to the independent variables as follows

$$\begin{aligned}
\nabla b &= \left\{ \frac{db}{da_i} \right\} = \{ 2\,x_i \} && i = 1,2,...,n \\
\nabla c &= \left\{ \frac{dc}{dx_i} \right\} = \{ Cos(b)\,\nabla b_i \} && i = 1,2,...,n \\
\nabla f &= \left\{ \frac{df}{da_i} \right\} = \{ \nabla b_i\, c + b\,\nabla c_i \} && i = 1,2,...,n
\end{aligned} \tag{2}$$

In contrast to the forward mode, the backward mode propagates adjoins $\overline{x} = \dfrac{\partial f}{\partial x}$, which are the derivatives of the final values, with respect to intermediate variables:

$$
\begin{aligned}
\overline{f} &= \frac{df}{df} = 1 && 1 \\
\overline{c} &= \frac{df}{dc} = \frac{\partial f}{\partial c}\overline{f} = b\,\overline{f} && 1 \\
\overline{b} &= \frac{df}{db} = \frac{\partial f}{\partial b}\overline{f} + \frac{\partial c}{\partial b}\overline{c} = c\overline{f} + Cos(b)\,\overline{c} && 1 \\
\nabla f &= \{\overline{a}_i\} = \left\{\frac{\partial b}{\partial a_i}\,\overline{b}\right\} = \left\{2\,a_i\,\overline{b}\right\} && i = 1,2,\ldots,n
\end{aligned}
\tag{3}
$$

The numerical efficiency of the differentiation can be measured by numerical work ratio

$$
wratio(f) = \frac{\text{numerical cost}(f(a_1,a_2,a_3,\ldots,a_n),\nabla f = \dfrac{\partial f}{\partial a_i})}{\text{numerical cost}(f(a_1,a_2,a_3,\ldots,a_n))} \tag{4}
$$

The numerical work ratio is defined as the ratio between the numerical cost of the evaluation of function f together with its gradient ∇f and the numerical cost of the evaluation of function f alone. The ratio is proportional to the number of independent variables $O(n)$ in the case of forward mode and constant in the case of backward mode. The upper bound for the ratio in the case of backward mode is $wratio(f) \leq 5$ and is usually around 1.5 if care is taken in handling the quantities that are common to the function and gradient. Although numerically superior, the backward mode requires potential storage of a large amount of intermediate data during the evaluation of the function f that can be as high as the number of numerical operations performed. Additionally, a complete reversal of the program flow is required. This is because the intermediate variables are used in reverse order when related to their computation.

There exist many strategies how the AD procedure can be implemented. The most efficient are source-to-source transformation strategies that transform the source code for computing a function into the source code for computing the derivatives of the function. The AD tools based on source-to-source transformation have been developed for most of the programming languages, e.g. *ADIFOR* for Fortran, *ADOL-C* for C, *MAD* for Matlab and *AceGen* for *Mathematica*.

2.2.2 Automatic differentiation and FEM

The tools for automatic differentiation were primary developed for the evaluation of the gradient of objective function used within the gradient-based optimization procedures or the Hessian of objective function used within the Newton-type

optimization procedures. The objective function is often defined by a large, complex program composed of many subroutines. Thus, one can apply the AD tools directly on the complete FE environment to obtain the required derivatives when the evaluation of the objective function involves FE simulation.

The AD technology can also be used for the evaluation of specific quantities that appear as part of a finite element simulation. It would be difficult and computationally inefficient to apply the AD tools on large FE systems to get e.g. the global stiffness matrix of large-scale problem directly. This is especially problematic when a fully implicit Newton type procedure is used to solve nonlinear, transient and coupled problems involving various types of elements, complicated continuation or arc-length methods and adaptive procedures.

However, one can still use automatic differentiation at the single element level to evaluate element specific quantities in an efficient way, such as:

- strain and stress tensors;
- nonlinear coordinate transformations;
- consistent stiffness matrix;
- residual vector;
- sensitivity pseudo-load vector.

A direct use of automatic differentiation tools for the development of nonlinear finite elements turns out to be complex and not straightforward. Furthermore, the numerical efficiency of the resulting codes is poor. Another solution, followed mostly in hybrid object-oriented systems, is to use problem specific solutions to evaluate local tangent matrix in an optimal way. Another solution, followed in hybrid symbolic-numeric systems, see e.g. (Korelc 2002), is to combine a general computer algebra system and the AD technology.

The implementation of the AD procedure has to fulfill specific requirements in order to get element source codes that are as efficient as manually written codes. Some basic requirements are:

- The AD procedure can be initiated at any time and at any point of the derivation of the formulas and as many times as required (e.g. in the example at the end the AD is used 13 times during the generation of element subroutine). The recursive use of standard AD tools on the same code, if allowed at all, leads to numerically inefficient source code. This requirement limits the use of standard AD tools. An alternative approach is implemented in (Korelc 2007b) where the source-to-source

transformation strategy is replaced by the method that consistently enhances the existing code rather than produces a new one.

- The storage of the intermediate variables is not a limitation when the backward differentiation method is used at the single element level. The finite element formulations involve, at the single element level, a relatively small set of independent and intermediate variables.
- For the reasons of efficiency, the results of all previous uses of AD have to be accounted for when AD is used several times inside the same subroutine.
- The user has to be able to use all the capabilities of the symbolic system on the final and the intermediate results of the AD procedure.
- The AD procedure must offer a mechanism for the descriptions of various mathematical formalisms used within the FE formulation.

The mathematical formalisms that are part of the traditional FE formulation are e.g. partial derivatives $\frac{\partial(\bullet)}{\partial(\bullet)}$, total derivatives $\frac{D(\bullet)}{D(\bullet)}$ or directional derivatives. They can all be represented by the AD procedure, if possible exceptions are treated in a proper way. However, the result of AD procedure may not automatically correspond to any of the above mathematical formalisms. Let us define a "conditional derivative" with the following formalism

$$\nabla f = \left.\frac{\partial f(\mathbf{a},\mathbf{b}(\mathbf{a}))}{\partial(\mathbf{a})}\right|_{\frac{\partial(\mathbf{b})}{\partial(\mathbf{a})}=\mathbf{M}} \tag{5}$$

where function f depends on a set of mutually independent variables $\mathbf{a}$ and a set of mutually independent intermediate variables $\mathbf{b}$. The above formalism has to be taken in an algorithmic way. It represents the automatic differentiation of function f with respect to variables $\mathbf{a}$. During the AD procedure, the total derivatives of intermediate variables $\mathbf{b}$ with respect to independent variables are set to be equal to matrix $\mathbf{M}$. Some situations that typically appear in the formulation of finite elements are presented in Table 1.

In case A there exists an explicit algorithmic dependency of $\mathbf{b}$ with respect to $\mathbf{a}$, hence the derivatives can be obtained in principle automatically, without user intervention, simply by the chain rule. However, there also exists a profound mathematical relationship that enables evaluation of derivatives in a more efficient way. This is often the case when the evaluation of $\mathbf{b}$ involves iterative loops, inverse matrices, etc..

Case B represents the situation when variables $\mathbf{b}$ are independent variables and variables $\mathbf{a}$ implicitly depend on $\mathbf{b}$. This implicit dependency has to be considered for the differentiation. In this case, automatic differentiation would not provide the correct result without the user intervention. A typical example for this situation is a differentiation that involves a transformation of coordinates. Usually the numerical integration procedures as well as interpolation functions require additional reference coordinate. An exception for automatic differentiation of type B is then introduced to properly handle differentiation involving coordinate transformations from initial $\mathbf{X}$ to reference coordinates $\boldsymbol{\xi}$ as follows:

$$\frac{\partial(\bullet)}{\partial \mathbf{X}} \Rightarrow \left.\frac{\partial(\bullet)}{\partial \mathbf{X}}\right|_{\frac{\partial \boldsymbol{\xi}}{\partial \mathbf{X}}=\left[\frac{\partial \mathbf{X}}{\partial \boldsymbol{\xi}}\right]^{-1}} \tag{6}$$

In case C there exists an explicit dependency between variables $\mathbf{b}$ and $\mathbf{a}$ that has to be neglected for differentiation. The status of dependent variable $\mathbf{b}$ is thus temporarily changed. For the duration of the AD procedure, it is changed into an independent variable. The situation frequently appears in the formulation of mechanical problems where instead of the total variation some arbitrary variation of a given quantity has to be evaluated.

The exceptions of cases A, B and C are imposed within automatic differentiation only during the execution of the particular call of the AD procedure. Case D is equal to case A with an AD exception defined globally, thus valid for every call of the AD procedure during the derivation of the problem. When in collision, then exceptions of type A, B and C overrule the D type exception.

Table 1: Automatic differentiation exceptions.
Tabela 1: Izjeme pri avtomatskem odvajanju.

Type	Formalism	Schematic *AceGen* input
A	$\nabla f = \left.\dfrac{\partial f(\mathbf{a},\mathbf{b}(\mathbf{a}))}{\partial(\mathbf{a})}\right\|_{\frac{\partial(\mathbf{b})}{\partial(\mathbf{a})}=\mathbf{M}}$	a ⊨ SMSReal[a$$] b ⊨ SMSFreeze[f_b[a]] δf ⊨ SMSD[f[a, b], a, "Implicit" → {b, a, M}]
B	$\nabla f = \left.\dfrac{\partial f(\mathbf{b})}{\partial(\mathbf{a}(\mathbf{b}))}\right\|_{\frac{\partial(\mathbf{b})}{\partial(\mathbf{a})}=\mathbf{M}}$	b ⊨ SMSReal[b$$] a ⊨ SMSFreeze[f_a[b]] δf ⊨ SMSD[f[b], a, "Implicit" → {b, a, M}]
C	$\nabla f = \left.\dfrac{\partial f(\mathbf{a},\mathbf{b}(\mathbf{a}))}{\partial(\mathbf{a})}\right\|_{\frac{\partial(\mathbf{b})}{\partial(\bullet)}=\mathbf{0}}$	a ⊨ SMSReal[a$$] b ⊨ f_b[a] δf ⊨ SMSD[f[a, b], a, "Constant" → b]
D	$\left.\dfrac{\partial(\bullet)}{\partial(\bullet)}\right\|_{\frac{\partial(\mathbf{b})}{\partial(\mathbf{a})}=\mathbf{M}}$	a ⊨ SMSReal[a$$] b ⊨ SMSFreeze[f_b[a], "Dependency" → {a, M}] ... δf_i ⊨ SMSD[f_i[a, b], a]

2.3 Hybrid symbolic-numerical approach

The real power of the symbolic approach for testing and applying new, unconventional ideas is provided by general-purpose CA systems. However, their use is limited to problems that lead to large systems like finite element simulations. Furthermore, the use of large commercial finite element environments to analyze a variety of problems is an everyday engineering practice. The hybrid symbolic-numerical (HSN) approach is a way to combine both.

Although large FE environments often offer a possibility to incorporate user defined elements and material modes, it is time consuming to develop and test these user defined new pieces of software. Practice shows that at the research stage of the derivation of a new numerical model, different languages and different platforms are the best means for the assessment of specific performances and, of course, failures of the numerical model. The basic tests, which are performed on a single finite element or on a small patch of elements, can be done most efficiently by using general CA system.

Many design flaws, such as element instabilities or poor convergence properties, can be easily identified, if the element quantities are investigated on a symbolic level. Unfortunately a standalone CA system becomes very inefficient once there is a larger number of nonlinear finite elements to process or if iterative numerical procedures have to be executed. In order to assess element performances under real conditions,

the easiest way is to run the necessary test simulations on sequential machines with good debugging capabilities and with the open source FE environment designed for research purposes, e.g. *FEAP*, *AceFEM* or *Diffpack*. At the end, for real industrial simulations involving complex geometries, a large commercial FE environment has to be used.

In order to meet all these demands in an optimal way, an approach is needed that would offer multi-language and multi-environment generation of numerical codes. The automatically generated code is then incorporated into the FE environment that is most suitable for the specific step of the research process. The structure of the hybrid symbolic-numerical system *AceGen* for multi-language and multi-environment code generation introduced by (Korelc 2002) is presented in Fig. 3. Using the classical approach, re-coding of the element in different languages would be time consuming and is rarely done. With the general CA systems, re-coding comes practically free, since the code can be automatically generated for several languages and for several platforms from the same basic symbolic description. An advantage of using a general CA system is also that it provides well known and defined description language for the derivation of FE equations, generation of FE code and possibly also for the complete FE analysis, as opposed to the hybrid object-oriented systems which introduce their own domain-specific language.

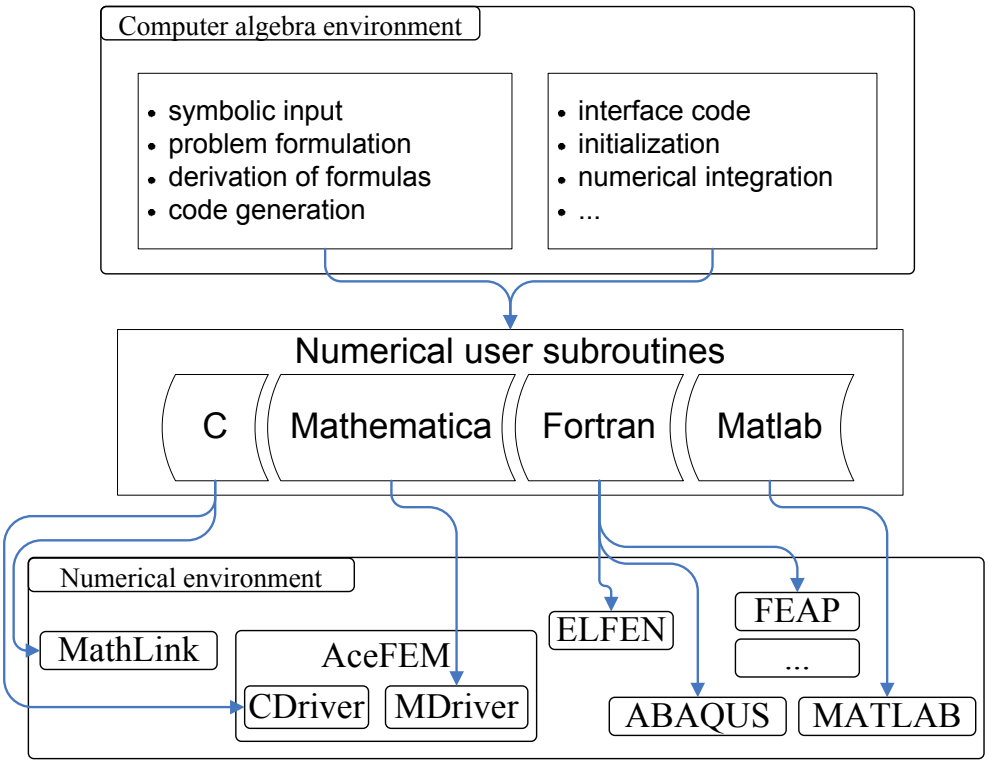

Fig. 3: Multi-language and multi-environment FE code generation.
Slika 3: Več jezično Več okoljsko generiranje kode končnega elementa.

When the symbolic approach is used in a standard way to describe complex engineering problems then the common experience of computer algebra users is an uncontrollable swell of expression, as pointed out before, leading to inefficient or even unusable codes. Not many attempts have been undertaken to design a general FE code generator, where this key issue of the FE code generation would be treated within the automatic procedure.

The classical way of optimizing expressions in CA systems is to search for common sub-expressions after all the formulae have been derived and before the generation of the numerical code. This seems to be insufficient for the general non-linear mechanical problems. An alternative approach for automatic code generation is employed in *AceGen* and called Simultaneous Stochastic Simplification of numerical code, see (Korelc 1997). This approach avoids the problem of expression swell by combining the following techniques: symbolic and algebraic capabilities of general computer algebra system *Mathematica*, automatic differentiation technique and simultaneous optimization of expressions with automatic selection and introduction of appropriate intermediate variables. Formulae are optimized, simplified and replaced

by the auxiliary variables simultaneously with the derivation of the problem. A stochastic evaluation of the formulae is applied for determining the equivalence of algebraic expressions instead of the conventional pattern matching technique. The simultaneous approach is also appropriate for problems where intermediate expressions can be subjected to the uncontrolled swell.

2.3.1 Typical example of automatic code generation procedure

To illustrate the standard *AceGen* procedure, a simple example is considered. A typical numerical sub-program that returns a determinant of the Jacobean matrix of nonlinear transformation from the reference to initial configuration for quadrilateral element topology is derived. The syntax of the *AceGen* script language is the same as the syntax of the *Mathematica* script language with some additional functions. The input for *AceGen* can be divided into six characteristic steps:

- At the beginning of the session the SMSInitialize function initializes the system.
- The SMSModule function defines the input and output parameters of the subroutine "DetJ".
- The SMSReal function assigns the input parameters X$$ and k$$ and e$$ of the subroutine to the standard *Mathematica* symbols. Double $ character indicates that the symbol is an input or output parameter of the generated subroutine.
- During the description of the problem special operators (⊢,⊣,⊨) are used to perform the simultaneous optimization of expressions to create of new intermediate variables. The SMSD function performs an automatic differentiation of one or several expressions with respect to the arbitrary variable or the vector of variables by simultaneously enhancing the already derived code.
- The results of the derivation are assigned to the output parameter J$$ of the subroutine by the SMSExport function.
- At the end of the session the SMSWrite function writes the contents of the vector of the generated formulae to the file in a prescribed language format. The generated subroutine in C and FORTRAN language are presented in Fig. 5.

```
<< AceGen`;
SMSInitialize["DetJ", "Language" -> "C"];
SMSModule["DetJ",
  Real[X$$[2, 4], k$$, e$$, J$$]];
{ξ, η} = SMSReal[{k$$, e$$}];
{Xi, Yi} = SMSReal[Array[X$$, {2, 4}]];
Ni = {(1 - ξ) (1 - η), (1 + ξ) (1 - η),
    (1 + ξ) (1 + η), (1 - ξ) (1 + η)} / 4;
J = SMSD[{Ni.Xi, Ni.Yi}, {ξ, η}];
SMSExport[Det[J], J$$];
SMSWrite[];
```

Fig. 4: Typical *AceGen* input.

Slika 4: Tipični vhodni podatki za *AceGen*.

```
      SUBROUTINE DetJ(v,X,k,e,J)
      IMPLICIT NONE
      include 'sms.h'
      DOUBLE PRECISION v(5001),X(2,4),k,e,J
      v(20)=((-1d0)+k)/4d0
      v(21)=((-1d0)-k)/4d0
      v(22)=(1d0+e)/4d0
      v(19)=((-1d0)+e)/4d0
      J=(v(19)*(X(1,1)-X(1,2))+v(22)*(X(1,3)-X(1,4)))*(v(21)*(X(2,2)
     &-X(2,3))+v(20)*(X(2,1)-X(2,4)))-(v(21)*(X(1,2)-X(1,3))+v(20)*(X
     &(1,1)-X(1,4)))*(v(19)*(X(2,1)-X(2,2))+v(22)*(X(2,3)-X(2,4)))
      END

#include "sms.h"
void DetJ(double v[5001],double X[2][4],double
(*k),double (*e),double (*J)){
v[20]=(-1e0+(*k))/4e0;
v[21]=(-1e0-(*k))/4e0;
v[22]=(1e0+(*e))/4e0;
v[19]=(-1e0+(*e))/4e0;
(*J)=(v[19]*(X[0][0]-X[0][1])+v[22]*(X[0][2]-X[0][3]))*
(v[21]*(X[1][1]-X[1][2])+v[20]*(X[1][0]
 -X[1][3]))-(v[21]*(X[0][1]-X[0][2])+v[20]*
 (X[0][0]-X[0][3]))*(v[19]*(X[1][0]-X[1][1])+v[22]*
 (X[1][2]-X[1][3]));
};
```

Fig. 5: Typical automatically generated subroutine in FORTRAN and C language.

Slika 5: Tipična avtomatsko generirana subrutina za jezika FORTRUN in C.

2.4 Abstract symbolic formulations in computational mechanics

The true benefit of using symbolic tools is not about the development of a theory which is normally done manually on a sheet of paper using a pencil, or if a computer shall be used a simple word processor is adequate for such task. The advantage of the symbolic approach in computational mechanics becomes apparent only when the description of the problem, which means that the basic equations are written down, is appropriate for the symbolic description. Unfortunately, some of the traditional descriptions used in computational mechanics are not appropriate for the symbolic description. The symbolic formulation of the computational mechanics problems often differs from the classical one and thus brings up the need for rethinking and reformulating known and traditional ways. Despite that, there exist strong arguments why at the end symbolic formulations are indeed beneficial, i.e.:

- A symbolic formulation is more compressed and thus gives fewer possibilities for an error.
- Algebraic operations, such as differentiation, are done automatically.
- Automatically generated codes are highly efficient and portable.
- The multi-language and multi-environment capabilities of symbolic systems enable generation of numerical codes for various numerical environments from the same symbolic description.
- An available collection of prepared symbolic inputs for a broad range of finite elements can be easily adjusted for the user specific problem leading to the on-demand numerical code generation.
- The multi-field and multi-physic problems can be easily implemented. For example, the symbolic inputs for mechanical analysis and thermal analysis can be combined into a new symbolic input that would create a finite element for fully coupled and quadratically convergent thermo-mechanical analysis.

For example, the standard formulation (see e.g. Crisfield 1996, 1997, Hughes 2000, Zienkiewicz, Taylor 2000a, Zienkiewicz, Taylor 2000b) of the tangential stiffness matrix $\mathbf{B}^T\mathbf{DB}$ can be easily repeated using the symbolic tools. Having in mind that element tangential stiffness matrix is either the jacobian of the resulting system of discrete algebraic equations or the hessian of the variational functional, then the automatic differentiation should be sufficient for obtaining the tangent matrix. The work of implementing $\mathbf{B}^T\mathbf{DB}$ formulation and the efficiency of the resulting code is inferior to the approach when tangent matrix is derived by the backward AD. The latter approach requires, regardless of the complexity of the topology and the material model, a single line of symbolic input. The standard $\mathbf{B}^T\mathbf{DB}$ formulation would require much more input for the same result.

It should be pointed out that the symbolic differentiation is one of the algebraic operations prone to severe expression growth and it can results even for relatively simple nonlinear elements in hundreds of pages of code. Thus, the use of hybrid system (e.g. *AceGen*) that combines the symbolic tool with the automatic differentiation technique is essential for the high abstract symbolic formulation of FE models. To increase the numerical efficiency of the generated code and to limit the physical size of the generated code, it is essential to minimize the number of calls to automatic differentiation procedure. In backward mode of automatic differentiation the expression $SMSD[a,\mathbf{c}]+SMSD[b,\mathbf{c}]$ can result in a code that is twice as large and twice slower than the code produced by the equivalent expression $SMSD[a+b,\mathbf{c}]$.

In this section, an abstract symbolic formulation is described, which is needed to obtain the contribution of a single element to the internal force vector $\mathbf{\Psi}$ and to the tangential stiffness matrix $\mathbf{K}$. The variational functional approach and the weak form approach are the two basic possibilities open for the derivation of variational formulation of equilibrium equations and their linearizations.

A weak form approach is used for the derivation of a 2D quadrilateral finite element formulation in Section 3.4.

2.5 Symbolic-numerical environment *AceFEM*

Within the work covered by the thesis the *AceFEM* package (Korelc 2007a) is used for direct and sensitivity analysis. *AceFEM* is a general finite element environment designed to solve multi-physics and multi-field problems. It explores advantages of symbolic capabilities of *Mathematica* while maintaining numerical efficiency of commercial finite element environment. The main part of the package includes procedures that are not numerically intensive such as processing of the user input data, mesh generation, control of the solution procedures, graphic post-processing of the results, etc. These procedures are written in *Mathematica* language and executed inside *Mathematica*. The second part includes numerically intensive operations,a such as evaluation and assembly of the finite element quantities (tangent matrix, residual, sensitivity vectors, etc.), solution of the linear system of equations, contact search procedures, etc. The numerical module exists in two versions. The basic version called *CDriver* is an independent executable written in C language and is connected with *Mathematica* via the *MathLink* protocol.

The alternative version called *MDriver* is completely written in Mathematica's symbolic language. It has the advantage of using advanced capabilities of *Mathematica*, such as high precision arithmetic, interval arithmetic, or even symbolic evaluation of FE quantities to analyze various properties of the numerical procedures on relatively small examples.

Both environments operate from Mathematica and they also have the same data structures, functions, command language and input data (for details of the environment see (Korelc 2007a, b)).

Direct and sensitivity analysis using *AceFEM* is further explained in Chapter 3.

3 Direct and Sensitivity limit load analysis

In Chapter 2 the symbolic approach to computational mechanics was introduced and all advances were outlined. In the present Chapter direct and sensitivity limit load analyses is explained which are used later on within the procedure for the evaluation of the most unfavorable imperfections (Chapter 4) as well within the limit load optimization procedure (Chapter 5).

In Chapter 1 an overview was given over the history and the development of different methods of sensitivity analysis. Although sensitivity analysis is used in many areas of science and is by itself a major field of research in structural engineering, the scope of the present work is mostly dedicated to shape optimization. For this reason application to gradient based shape optimization will be studied. Accurate sensitivity analysis with the use of symbolic approach, which is needed for correct gradient shape optimization, will be presented.

3.1 Definition of ultimate states

For the limit load structural analysis, used for the limit load shape optimization, the criteria for the limit load have to be defined. An ultimate state of a structure is generally defined with the limit point of the equilibrium path. In real, imperfect structures, this criterion proves unreliable because of possible exceeding of permissible tolerances of displacements or deformations before reaching the limit point. It is therefore necessary to additionally define the ultimate state of a structure. The ultimate state can be defined as the lowest load factor obtained by the following criteria (see Fig. 6):

a) The maximum load factor on the load-deformation curve (limit load).
b) The bifurcation load factor, before reaching the limit point of the load-deformation curve (does not occur in the presented case).
c) The largest tolerable deformation, where this occurs during loading path before reaching a bifurcation load or limit load.

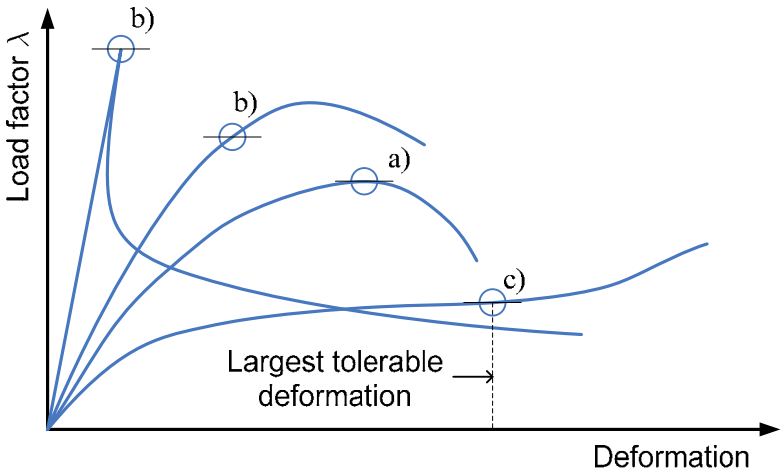

Fig. 6: Definition of ultimate states (EN 1993 1-5 2004).
Slika 6: Definicija računskih mejnih stanj (EN 1993 1-5 2004).

When the first criterion of all criteria defined in Fig. 6 is reached on the load-displacement curve, the equilibrium point is defined as the ultimate load. Throughout the thesis ultimate load analysis is used.

3.2 Direct Analysis

Nonlinear mechanical problems can be in general classified into 4 categories shown in Table 2:

Table 2: Residual form of equations for mechanical problems.
Tabela 2: Ravnotežne enačbe za različne probleme v mehaniki.

Steady-state non-linear systems	$\mathbf{\Psi}(\mathbf{a}) = 0$
Transient non-linear systems	$\mathbf{\Psi}\left(\mathbf{a}, \mathbf{a}^p\right) = 0$
Steady-state coupled non-linear systems	$\mathbf{\Psi}(\mathbf{a}, \mathbf{b}) = 0$ $\mathbf{\Phi}(\mathbf{a}, \mathbf{b}) = 0$
Transient coupled non-linear systems	$\mathbf{\Psi}\left(\mathbf{a}, \mathbf{a}^p, \mathbf{b}, \mathbf{b}^p\right) = 0$ $\mathbf{\Phi}\left(\mathbf{a}, \mathbf{a}^p, \mathbf{b}, \mathbf{b}^p\right) = 0$

In the notation used, $\mathbf{a}$ represents a vector of global generalized displacement parameters (displacements, rotations, enhanced mode parameters, etc.), $\mathbf{b}$ a vector of unknown state variables defined for each integration point (plastic deformations, hardening variables, etc.), $\mathbf{a}^p$ a vector of generalized displacement parameters at the end of previous time step, $\mathbf{b}^p$ a vector of state variables at the end of previous time step, $\boldsymbol{\Psi}$ a set of equilibrium equations, and $\boldsymbol{\Phi}$ a set of local plastic evolution equations.

For an ultimate limit load structural analysis the consideration of geometrical and material nonlinearity is necessary. According to terminology introduced by Michaleris, Tortorelli and Vidal (Michaleris, et al. 1994), the formulation of the system which has to be solved presents a nonlinear transient coupled non-linear system.

A standard "arc-length" type continuation method is used for structural analysis (see e.g. Crisfield 1996, 1997). Therefore, in structural analysis the equilibrium equations are extended with load factor λ as an additional variable and constraint g_c as an additional equation imposed on the increments of generalized displacements.

The complete set of equations which need to be solved for each integration point and for the whole structure can be written as:

$$\bar{\boldsymbol{\Psi}} = \begin{Bmatrix} \boldsymbol{\Psi}\left(\bar{\mathbf{a}}, \bar{\mathbf{a}}^p, \mathbf{b}, \mathbf{b}^p\right) \\ g_c\left(\bar{\mathbf{a}}, \bar{\mathbf{a}}^p\right) \end{Bmatrix} = 0$$

$$\boldsymbol{\Phi}\left(\mathbf{a}, \mathbf{a}^p, \mathbf{b}, \mathbf{b}^p\right) = 0 \tag{7}$$

$$\bar{\mathbf{a}} = \{\mathbf{a}, \lambda\}$$
$$\bar{\mathbf{a}}^p = \left\{\mathbf{a}^p, \lambda^p\right\}$$

The general formulation of the fully implicit quadratically convergent direct analysis is for our case presented in Fig. 7.

Structural level
$\bar{\mathbf{\Psi}}(\bar{\mathbf{a}},\, \mathbf{b}(\mathbf{a})) = 0$ ${}_{\mathbf{\Phi}}\mathbf{K} \cdot \dfrac{\partial \mathbf{b}}{\partial \mathbf{a}} = -\dfrac{\partial \mathbf{\Phi}}{\partial \mathbf{a}} \Rightarrow \dfrac{\partial \mathbf{b}}{\partial \mathbf{a}}$ ${}_{\mathbf{\Psi}}\mathbf{K} = \dfrac{\partial \bar{\mathbf{\Psi}}}{\partial \mathbf{a}}$ ${}_{\mathbf{\Psi}}\mathbf{K}\Delta\bar{\mathbf{a}} + \bar{\mathbf{\Psi}} = 0$ $\bar{\mathbf{a}} := \bar{\mathbf{a}} + \Delta\bar{\mathbf{a}}$
Integration point level
$\mathbf{\Phi}(\mathbf{b}) = 0$ ${}_{\mathbf{\Phi}}\mathbf{K} = \dfrac{\partial \mathbf{\Phi}}{\partial \mathbf{b}}$ ${}_{\mathbf{\Phi}}\mathbf{K}\Delta\mathbf{b} + \mathbf{\Phi} = 0$ $\mathbf{b} := \mathbf{b} + \Delta\mathbf{b}$

Fig. 7: General formulation of direct analysis of transient coupled nonlinear problems.
Slika 7: Splošna formulacija za direktno analizo tranzientnih povezanih nelinearnih problemov.

The actual form of the equations in Fig. 7 is for structural finite elements (trusses, beams, shells etc.) well known and presented elsewhere. In all examples the simplest form of continuation methods, called "displacement controlled at a specific variable"(Crisfield 1996, 1997), was used. In this case the following displacement increment constraint equation g_c is used:

$$g_c = u_m - \gamma\, \bar{u}_m \tag{8}$$

where u_m is the actual and $\bar{u}_m$ the prescribed m-th scalar component of a generalized displacement vector $\mathbf{a}$. Parameter γ is used to parameterize the direct analysis. As soon as one of the criteria for the ultimate load presented in section 3.1 is reached, the analysis is stopped and the ultimate load is determined.

3.3 Sensitivity Analysis

Design sensitivity analysis is used to compute a rate of performance measure change with respect to the system design parameters variation. In structural engineering problems the system performance measure can include any quantity that may be used to characterize system behavior, such as displacements, stress, strain, energy, buckling or limit load, frequency response, weight, etc. The dependence to design parameters such as material property, sizing, shape and configuration parameters is in general implicitly defined by the laws of mechanics. Rarely, in the case of simple problems, there exists an explicit relation (see e.g. Choi, Kim 2005a).

Sensitivities are obtained by derivation. The level of derivation effort required differs drastically in dependence of the nature of the problem and the approach used to evaluate sensitivity. The four general categories of mechanical problems were presented in Table 2.

The derivation of sensitivity terms is significantly more complex for nonlinear systems than linear which will not be addressed here. For transient systems an additional dependency on time has to be considered in the derivations. Further complexity is gained with the choice of design parameters. In the case of sizing or material optimization (e.g. beam cross-section, shell thickness, elastic modulus etc.) the design variables appear explicitly in the variational equations, where in the case of shape optimization the design variables gain an implicit relation to the variational equations. If using FEM for structural analysis, a change in shape design variables implies a change in the finite element model. The dependency of design variables with respect to the coordinates of finite element nodes presents the main difficulty in evaluating sensitivity analysis.

The limit load structural shape optimization leads to a transient coupled nonlinear system of equations where geometrical and material nonlinearities are taken into account. The difficulty of sensitivity expression derivation was an encouragement to use a symbolic-numeric approach which is thoroughly explained in Chapter 2.

The sensitivity analysis based on direct differentiation method (Michaleris, et al. 1994) is used to evaluate the sensitivity of the objective function f with respect to the shape parameters ϕ. Due to the transient nature of the problem, the sensitivity analysis has to be evaluated at the end of each time step and integrated through the whole analysis. The corresponding equations are presented in Fig. 8.

Structural level

$$\bar{\boldsymbol{\Psi}}\left(\bar{\mathbf{a}}\,,\bar{\mathbf{a}}^p,\mathbf{b}\,,\mathbf{b}^p,\phi\,\right)=0$$

$$_{\boldsymbol{\Psi}}\mathbf{K}\frac{D\mathbf{a}}{D\phi}=\frac{\tilde{D}\bar{\boldsymbol{\Psi}}}{\tilde{D}\phi}$$

$$\frac{\tilde{D}\bar{\boldsymbol{\Psi}}}{\tilde{D}\phi}=\left(\begin{array}{l}\dfrac{D\bar{\boldsymbol{\Psi}}}{D\,\mathbf{a}^p}\dfrac{D\,\mathbf{a}^p}{D\phi}+\dfrac{D\bar{\boldsymbol{\Psi}}}{D\,\mathbf{b}^p}\dfrac{D\,\mathbf{b}^p}{D\phi}+\underline{\underline{\dfrac{D\bar{\boldsymbol{\Psi}}}{D\phi}}}-\\ -\dfrac{D\bar{\boldsymbol{\Psi}}}{D\,\mathbf{b}}(\,_{\boldsymbol{\Phi}}\mathbf{K})^{-1}\\ \left(\dfrac{D\boldsymbol{\Phi}}{D\phi}+\dfrac{D\boldsymbol{\Phi}}{D\,\mathbf{a}^p}\dfrac{D\,\mathbf{a}^p}{D\phi}+\dfrac{D\boldsymbol{\Psi}}{D\,\mathbf{a}^p}\dfrac{D\,\mathbf{a}^p}{D\phi}\right)\end{array}\right)$$

Integration point level

$$\boldsymbol{\Phi}\Big(\mathbf{a}\,,\mathbf{a}^p,\mathbf{b}\,,\mathbf{b}^p\Big)=0$$

$$_{\boldsymbol{\Phi}}\mathbf{K}\frac{D\mathbf{b}}{D\phi}=\frac{\tilde{D}\boldsymbol{\Phi}}{\tilde{D}\phi}$$

$$\frac{\tilde{D}\boldsymbol{\Phi}}{\tilde{D}\phi}=\left(\begin{array}{l}\dfrac{D\boldsymbol{\Phi}}{D\,\mathbf{a}}\dfrac{D\,\mathbf{a}}{D\phi}+\\ +\dfrac{D\boldsymbol{\Phi}}{D\,\mathbf{a}^p}\dfrac{D\,\mathbf{a}^p}{D\phi}+\dfrac{D\boldsymbol{\Phi}}{D\,\mathbf{b}^p}\dfrac{D\,\mathbf{b}^p}{D\phi}\end{array}\right)$$

Fig. 8: General formulation of shape sensitivity analysis of transient coupled nonlinear problems.
Slika 8: Splošna formulacija za občutljivostno analizo tranzientnih povezanih nelinearnih problemov.

The evaluation of the underlined term in Fig. 8 requires the derivatives of the finite element node coordinates with respect to shape design parameters (ϕ). The term is usually called "design velocity field" and is required as input for the sensitivity analysis (Korelc, Kristanič 2005).

3.3.1 The Analytical Design Velocity Field

As pointed out before, the most important part of the process of evaluating shape design sensitivity needed in structural gradient based shape optimization is constructing the design velocity field.

The purpose of design velocity field ($\partial \mathbf{X} / \partial \phi$) is to characterize the changes of the finite element nodal point coordinates ($\mathbf{X}$) with respect to the changes of arbitrary design parameters (ϕ). While the design derivatives of the finite element quantities (residual, tangent matrix, etc.) can be constructed by automatic procedures (Korelc, Kristanič 2005), this is not true for the design velocity field. Within standard approaches to finite element mesh generation, either with specialized preprocessors or with CAD tools, there exist no explicit relations between the position of the finite element nodes and the shape design parameter.

The problem of constructing the design velocity field has therefore attracted a lot of attention and various approaches have been proposed (Chang, et al. 1995, Hansen, et al. 2001, Hardee, et al. 1999, Jang, Kim 2005, Kegl 2000). The simplest approach is to evaluate derivatives numerically by the finite difference method. However, the method is prone to large errors for a certain type of shape sensitivity problems. Alternatively, the domain of the problem can be divided in smaller parts, termed the design elements, for which analytical design velocity field can be derived and then evaluated at the positions of the finite element nodes. The approach fails when the design parameter relates to some global measure of the structure for which explicit relations to parameters of the design elements are hard to derive.

The symbolic-numeric approach is used for the evaluation of the design velocity field by general computer algebra system *Mathematica* (Wolfram 2008) and the dual symbolic-numeric FEM environment *AceFEM* (Korelc 2007a). Symbolic systems can deal with arbitrary formulae. Thus, if the particular shape parameter is kept in symbolic form during the model description and mesh generation, then the nodal coordinates of the mesh will be an explicit function of the parameter involved. The design velocity field is then obtained by the direct differentiation of the symbolically parameterized mesh by a single command for symbolic derivation, as can be seen in the next example.

3.3.1.1 Example

A simple cantilever structure modeled by 2D elasto-plastic finite elements is considered where the shape is parametrized with 3 shape parameters as shown in Fig. 9. In Fig. 10 the input data for *AceFEM* are presented.

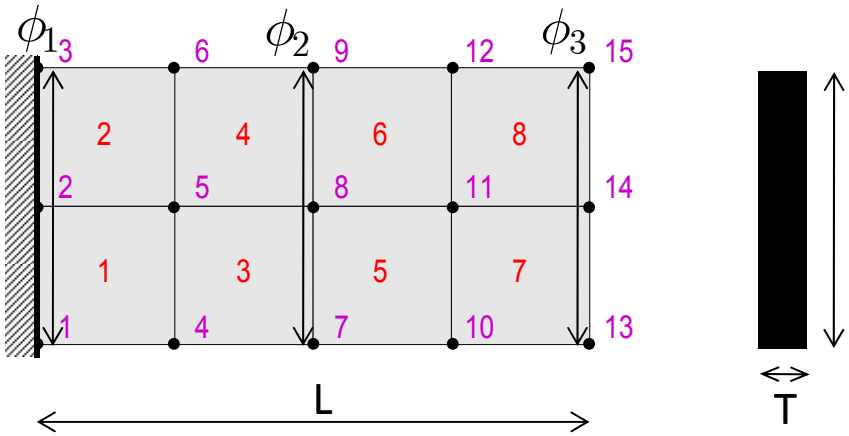

Fig. 9: Geometry of cantilever with marked node numbers and shape parameters.
Slika 9: Geometrija konzolne konstrukcije z označenimi vozlišči in parametri oblike.

```
In[63]:= << AceFEM`;
L = 40; (* Length *)
H = 20; (* Width *)
T = 1; (* Thickness *)
fy = 23.5; (* yield stress *)
Em = 21000;(* elastic modulus *)

intord = 3; (* interpolation order of FE mesh parameterization*)
Nϕ = 3; (*number of geometry parameters through the whole length*)
ϕ = Table[ToExpression["ϕ" <> ToString[i]], {i, Nϕ}] (* Definition of shape parameters *)
SMTInputData["CDriver"];
domains = {{"Domain1", "ElastPlast2DSens", {T, Em, 0.3, fy}}, {"Load", "SurfaceLoadGConst", {0, -1, T}},
   {"PrescDispl", "PrescribedDispl2DY", {1}}};
SMTAddDomain[domains];
SMTAddEssentialBoundary[{"X" == 0 &, 0, 0}];

SMTMesh["Domain1", "Q1", {4, 2}, {Table[{(i - 1) L / (Nϕ - 1), - (H / 2 + H / 2 ϕ[[i]])}, {i, Nϕ}],
   Table[{(i - 1) L / (Nϕ - 1), (H / 2 + H / 2 ϕ[[i]])}, {i, Nϕ}]}, "InterpolationOrder" → intord];

ϕinit = {0, 0, 0}; (* current values of parameters *)
srch = MapThread[Rule, {ϕ // Flatten, ϕinit // Flatten}];
SMTAnalysis["SearchFunction" → (# /. srch &)];
```

Fig. 10: *AceFEM* input data for the structure illustrated in Fig. 9.
Slika 10: *AceFEM* podatki za konstrukcijo iz slike 9 .

The node coordinates can be kept in symbolic form. In the example the three chosen parameters ϕ_1, ϕ_2 and ϕ_3 define the upper and the lower boundary line which is defined by an arbitrary spline function. In Fig. 11 and Fig. 12 the node coordinates in

symbolic form are shown with respect to the use of a linear and quadratic spline function.

Out[88]=

Node Number	X coordinate	Y coordinate
1	0	10. + 1. (10. ϕ1 - 10. ϕ2) + 10. ϕ2 + 1. (-20. - 1. (10. ϕ1 - 10. ϕ2) - 20. ϕ2 + 1. (-10. ϕ1 + 10. ϕ2))
2	0	10. + 1. (10. ϕ1 - 10. ϕ2) + 10. ϕ2 + 0.5 (-20. - 1. (10. ϕ1 - 10. ϕ2) - 20. ϕ2 + 1. (-10. ϕ1 + 10. ϕ2))
3	0	10. + 1. (10. ϕ1 - 10. ϕ2) + 10. ϕ2
4	10.	10. + 0.5 (10. ϕ1 - 10. ϕ2) + 10. ϕ2 + 1. (-20. - 0.5 (10. ϕ1 - 10. ϕ2) - 20. ϕ2 + 0.5 (-10. ϕ1 + 10. ϕ2))
5	10.	10. + 0.5 (10. ϕ1 - 10. ϕ2) + 10. ϕ2 + 0.5 (-20. - 0.5 (10. ϕ1 - 10. ϕ2) - 20. ϕ2 + 0.5 (-10. ϕ1 + 10. ϕ2))
6	10.	10. + 0.5 (10. ϕ1 - 10. ϕ2) + 10. ϕ2
7	20.	10. + 1. (-20. - 20. ϕ2) + 10. ϕ2
8	20.	10. + 0.5 (-20. - 20. ϕ2) + 10. ϕ2
9	20.	10. + 10. ϕ2
10	30.	10. + 0.5 (10. ϕ2 - 10. ϕ3) + 10. ϕ3 + 1. (-20. - 0.5 (10. ϕ2 - 10. ϕ3) - 20. ϕ3 + 0.5 (-10. ϕ2 + 10. ϕ3))
11	30.	10. + 0.5 (10. ϕ2 - 10. ϕ3) + 10. ϕ3 + 0.5 (-20. - 0.5 (10. ϕ2 - 10. ϕ3) - 20. ϕ3 + 0.5 (-10. ϕ2 + 10. ϕ3))
12	30.	10. + 0.5 (10. ϕ2 - 10. ϕ3) + 10. ϕ3
13	40.	10. + 1. (-20. - 20. ϕ3) + 10. ϕ3
14	40.	10. + 0.5 (-20. - 20. ϕ3) + 10. ϕ3
15	40.	10. + 10. ϕ3

Fig. 11: *AceFEM* node coordinates for linear boundary shape approximation.

Slika 11: Koordinate vozlišč z linearno interpolacijo parametrizirane mreže v *AceFEM*.

Out[74]=

Node Number	X coordinate	Y coordinate
1	0	10. + 1. (10. ϕ1 - 10. ϕ2) + 10. ϕ2 + 1. (-20. - 1. (10. ϕ1 - 10. ϕ2) - 20. ϕ2 + 1. (-10. ϕ1 + 10. ϕ2))
2	0	10. + 1. (10. ϕ1 - 10. ϕ2) + 10. ϕ2 + 0.5 (-20. - 1. (10. ϕ1 - 10. ϕ2) - 20. ϕ2 + 1. (-10. ϕ1 + 10. ϕ2))
3	0	10. + 1. (10. ϕ1 - 10. ϕ2) + 10. ϕ2
4	10.	10. + 10. ϕ2 - 0.25 (-2. (10. ϕ1 - 10. ϕ2) + 0.5 (2. (10. ϕ1 - 10. ϕ2) + 1. (-10. ϕ1 + 10. ϕ3))) + 1. (-20. - 20. ϕ2 - 0.25 (-2. (-10. ϕ1 + 10. ϕ2) + 0.5 (2. (-10. ϕ1 + 10. ϕ2) + 1. (10. ϕ1 - 10. ϕ3))) + 0.25 (-2. (10. ϕ1 - 10. ϕ2) + 0.5 (2. (10. ϕ1 - 10. ϕ2) + 1. (-10. ϕ1 + 10. ϕ3))))
5	10.	10. + 10. ϕ2 - 0.25 (-2. (10. ϕ1 - 10. ϕ2) + 0.5 (2. (10. ϕ1 - 10. ϕ2) + 1. (-10. ϕ1 + 10. ϕ3))) + 0.5 (-20. - 20. ϕ2 - 0.25 (-2. (-10. ϕ1 + 10. ϕ2) + 0.5 (2. (-10. ϕ1 + 10. ϕ2) + 1. (10. ϕ1 - 10. ϕ3))) + 0.25 (-2. (10. ϕ1 - 10. ϕ2) + 0.5 (2. (10. ϕ1 - 10. ϕ2) + 1. (-10. ϕ1 + 10. ϕ3))))
6	10.	10. + 10. ϕ2 - 0.25 (-2. (10. ϕ1 - 10. ϕ2) + 0.5 (2. (10. ϕ1 - 10. ϕ2) + 1. (-10. ϕ1 + 10. ϕ3)))
7	20.	10. + 1. (-20. - 20. ϕ2) + 10. ϕ2
8	20.	10. + 0.5 (-20. - 20. ϕ2) + 10. ϕ2
9	20.	10. + 10. ϕ2
10	30.	10. - 0.25 (-0.25 (-2. (10. ϕ1 - 10. ϕ2) + 2. (10. ϕ2 - 10. ϕ3)) - 2. (10. ϕ2 - 10. ϕ3)) + 10. ϕ3 + 1. (-20. + 0.25 (-0.25 (-2. (10. ϕ1 - 10. ϕ2) + 2. (10. ϕ2 - 10. ϕ3)) - 2. (10. ϕ2 - 10. ϕ3)) - 20. ϕ3 - 0.25 (-2. (-10. ϕ2 + 10. ϕ3) - 0.25 (-2. (-10. ϕ1 + 10. ϕ2) + 2. (-10. ϕ2 + 10. ϕ3))))
11	30.	10. - 0.25 (-0.25 (-2. (10. ϕ1 - 10. ϕ2) + 2. (10. ϕ2 - 10. ϕ3)) - 2. (10. ϕ2 - 10. ϕ3)) + 10. ϕ3 + 0.5 (-20. + 0.25 (-0.25 (-2. (10. ϕ1 - 10. ϕ2) + 2. (10. ϕ2 - 10. ϕ3)) - 2. (10. ϕ2 - 10. ϕ3)) - 20. ϕ3 - 0.25 (-2. (-10. ϕ2 + 10. ϕ3) - 0.25 (-2. (-10. ϕ1 + 10. ϕ2) + 2. (-10. ϕ2 + 10. ϕ3))))
12	30.	10. - 0.25 (-0.25 (-2. (10. ϕ1 - 10. ϕ2) + 2. (10. ϕ2 - 10. ϕ3)) - 2. (10. ϕ2 - 10. ϕ3)) + 10. ϕ3
13	40.	10. + 1. (-20. - 20. ϕ3) + 10. ϕ3
14	40.	10. + 0.5 (-20. - 20. ϕ3) + 10. ϕ3
15	40.	10. + 10. ϕ3

Fig. 12: *AceFEM* node coordinates for quadratic boundary shape interpolation.

Slika 12: Koordinate vozlišč s kvadratno interpolacijo parametrizirane mreže v *AceFEM*.

The design velocity field can easily be computed with the use of symbolic derivation function (D[ ]) in *Mathematica,* as shown in Fig. 13 and Fig. 14.

```
In[110]:= Map[D[NodeCoordinates, #] &, {ϕ1, ϕ2, ϕ3}]

Out[110]= {{{0, 0, -10.}, {0, 0, 0.}, {0, 0, 10.}, {0, 0, -3.75}, {0, 0, 0.}, {0, 0, 3.75}, {0, 0, 0},
    {0, 0, 0}, {0, 0, 0}, {0, 0, 1.25}, {0, 0, 0.}, {0, 0, -1.25}, {0, 0, 0}, {0, 0, 0}, {0, 0, 0}},
   {{0, 0, 0.}, {0, 0, 0.}, {0, 0, 0.}, {0, 0, -7.5}, {0, 0, 0.}, {0, 0, 7.5}, {0, 0, -10.},
    {0, 0, 0.}, {0, 0, 10.}, {0, 0, -7.5}, {0, 0, 0.}, {0, 0, 7.5}, {0, 0, 0}, {0, 0, 0}, {0, 0, 0}},
   {{0, 0, 0}, {0, 0, 0}, {0, 0, 0}, {0, 0, 1.25}, {0, 0, 0.}, {0, 0, -1.25}, {0, 0, 0}, {0, 0, 0},
    {0, 0, 0}, {0, 0, -3.75}, {0, 0, 0.}, {0, 0, 3.75}, {0, 0, -10.}, {0, 0, 0.}, {0, 0, 10.}}}
```

Fig. 13: Design velocity field by symbolical derivation of FE node coordinates for the case of linear interpolation between shape parameters.

Slika 13: Polje začetnih občutljivosti izračunano s simboličnim odvajanjem koordinat vozlišč mreže končnih elementov za primer linearne interpolacije mreže med parametri oblike.

```
In[93]:= Map[D[NodeCoordinates, #] &, {ϕ1, ϕ2, ϕ3}]

Out[93]= {{{0, 0, -10.}, {0, 0, 0.}, {0, 0, 10.}, {0, 0, -5.}, {0, 0, 0.}, {0, 0, 5.}, {0, 0, 0},
    {0, 0, 0}, {0, 0, 0}, {0, 0, 0}, {0, 0, 0}, {0, 0, 0}, {0, 0, 0}, {0, 0, 0}, {0, 0, 0}},
   {{0, 0, 0.}, {0, 0, 0.}, {0, 0, 0.}, {0, 0, -5.}, {0, 0, 0.}, {0, 0, 5.}, {0, 0, -10.},
    {0, 0, 0.}, {0, 0, 10.}, {0, 0, -5.}, {0, 0, 0.}, {0, 0, 5.}, {0, 0, 0}, {0, 0, 0}, {0, 0, 0}},
   {{0, 0, 0}, {0, 0, 0}, {0, 0, 0}, {0, 0, 0}, {0, 0, 0}, {0, 0, 0}, {0, 0, 0}, {0, 0, 0},
    {0, 0, 0}, {0, 0, -5.}, {0, 0, 0.}, {0, 0, 5.}, {0, 0, -10.}, {0, 0, 0.}, {0, 0, 10.}}}
```

Fig. 14: Design velocity field by symbolical derivation of FE node coordinates for the case of quadratic interpolation between shape parameters.

Slika 14: Polje začetnih občutljivosti izračunano s simboličnim odvajanjem koordinat vozlišč mreže končnih elementov za primer kvadratne interpolacije mreže med parametri oblike.

The design velocity field can be graphically represented as a scalar function. The x-coordinates do not depend with respect to design variables in the present example as can be seen in Fig. 11 and Fig. 12. The y-coordinate dependence with respect to design variables is plotted in Fig. 15 and Fig. 16 for the case of linear and quadratic spline interpolation between shape parameters respectively.

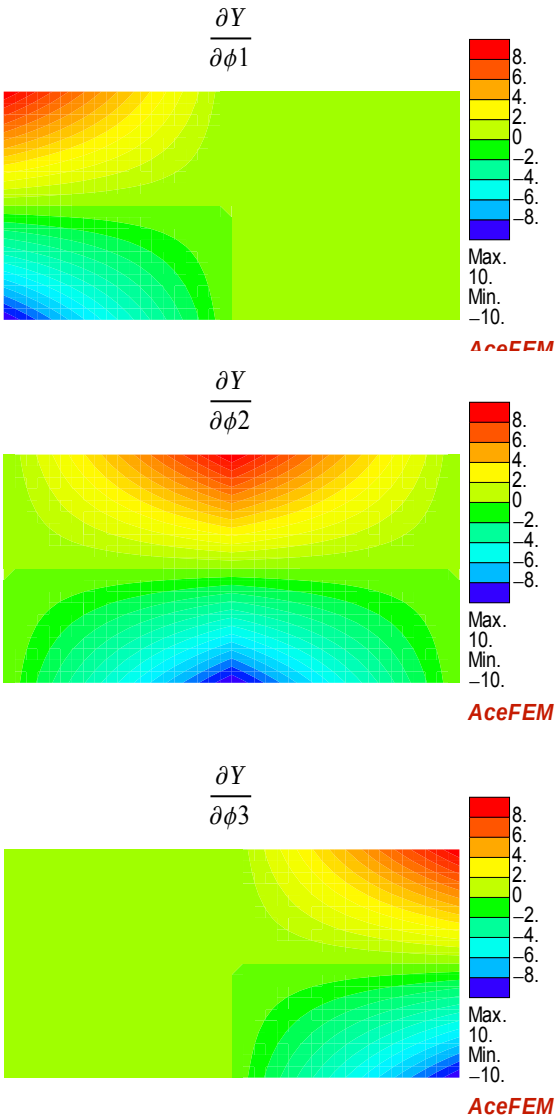

Fig. 15: Graphical representation of the y component of the design velocity field for the case of linear interpolation between shape parameters.

Slika 15: Grafični prikaz y komponente polja začetnih občutljivosti v primeru linearne interpolacije mreže med parametri oblike.

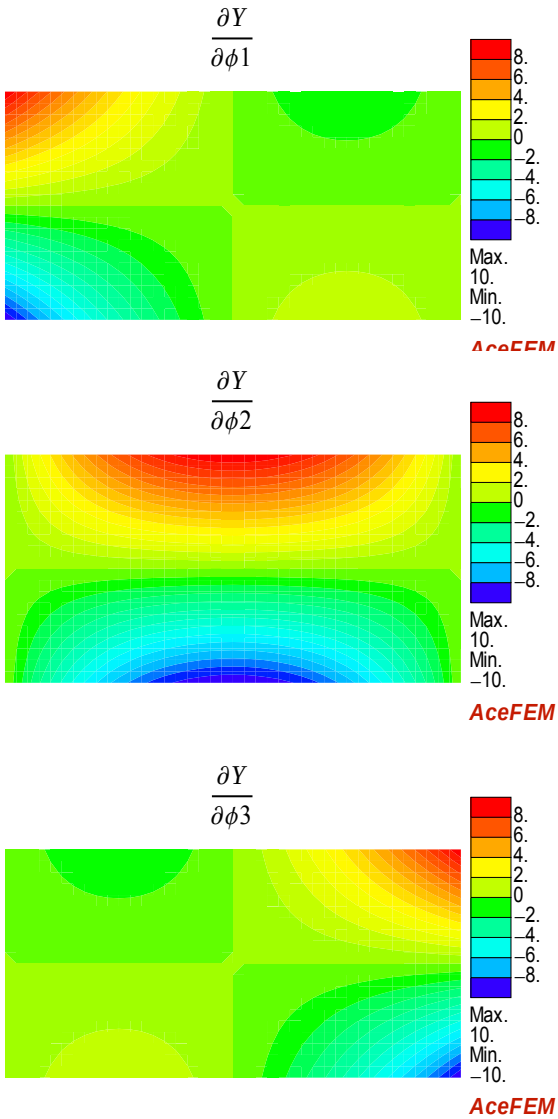

Fig. 16: Graphical representation of the y component of the design velocity field for the case of quadratic interpolation between shape parameters.

Slika 16: Grafični prikaz y komponente polja začetnih občutljivosti v primeru kvadratne interpolacije mreže med parametri oblike.

3.3.2 Exact sensitivity analysis

While the design velocity field can be defined and evaluated symbolically, the numerical analysis done by computer algebra systems cannot keep up with the run-time efficiency of programming languages such as FORTRAN and C. The key idea of the used approach is to use a dual symbolic-numeric finite element environment. Such environment (*AceFEM*) was introduced in Section 2.5. The whole procedure of

the evaluation of analytical sensitivities is presented in Fig. 17 and can be applied on problems with arbitrary complexity.

The sensitivity analysis is done on the basis of automatically derived finite element code explained in Chapter 2. The general expressions for sensitivity analysis are given in Fig. 8.

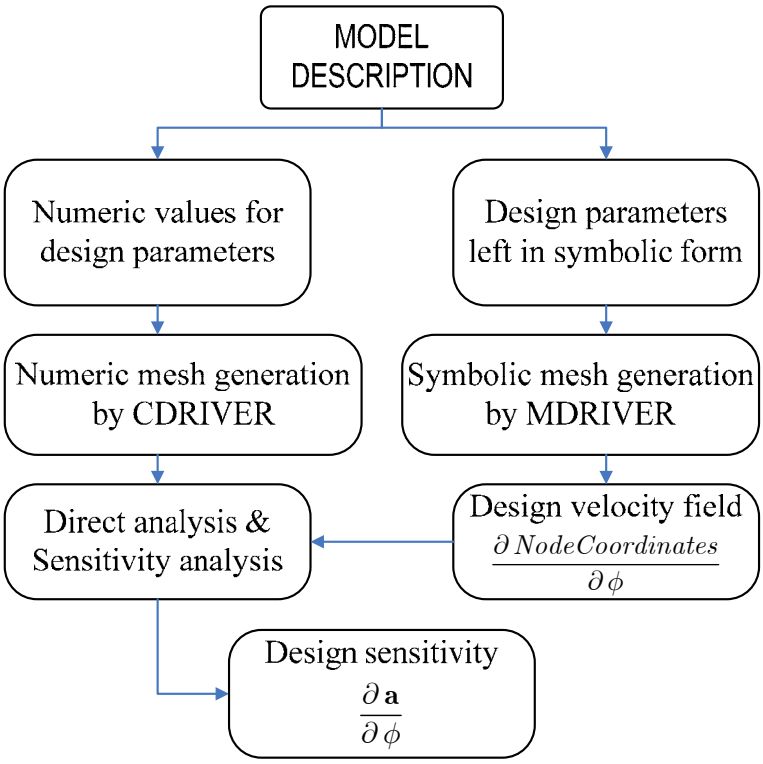

Fig. 17: Flowchart of shape sensitivity analysis by dual symbolic-numeric FE environment.
Slika 17: Potek občutljivostne analize s pomočjo simbolno numeričnega MKE okolja.

3.4 Symbolical formulation of general finite strain plasticity

For the representation of automatic derivation of internal force vector $\mathbf{\Psi}$ and the tangential stiffness matrix $\mathbf{K}$, the 4-node quadrilateral elastic-plastic finite element is derived next.

Let $\mathbf{a}$ be a vector of generalized displacements parameters of the element, $\mathbf{b}$ a vector of unknowns at Gauss point level and $\mathbf{b}^p$ a vector of history values at Gauss point level from the previous time step. The elasto-plastic problem is defined by a hyperelastic strain energy density function W, a yield condition f and a set of algebraic constraints to be fulfilled at Gauss point level $\mathbf{\Phi}(\mathbf{a}, \mathbf{b}, \mathbf{b}^p)$ that have to be solved for unknowns $\mathbf{b}$ when the material point is in plastic state. In general, vector

$\mathbf{b}$ is composed of an appropriate measure of plastic strains (or stresses in the small deformation case), the hardening variables and the consistency parameter λ where $\mathbf{\Phi}$ are composed of the corresponding set of discretized evolution equations that describe the evolution of plastic strains and hardening variables and the consistency condition $f = 0$. The yield condition is evaluated for the trial state by freezing the state variables as follows

$$f^{tr} = f(\mathbf{a}, \mathbf{b}^p) \tag{9}$$

The general algorithm for the abstract symbolic description of elasto-plastic problems is presented in Fig. 18.

$$
\begin{array}{l}
\text{summation over } GAUSS \text{ points} \\
\quad \mathbf{x} := \mathbf{X}(\xi) + \mathbf{u}(\mathbf{a}, \xi) \\
\quad \text{use AD exception of type B for coordinate transformation} \\
\quad \mathbf{F} := \left.\dfrac{\partial \mathbf{x}}{\partial \mathbf{X}}\right|_{\frac{\partial \xi}{\partial \mathbf{X}} = \left[\frac{\partial \mathbf{X}}{\partial \xi}\right]^{-1}} \\
\quad \boldsymbol{\tau}^{trial} := \boldsymbol{\tau}(\mathbf{a}, \mathbf{b}^p) \\
\quad f(\boldsymbol{\tau}^{trial}) \leq 0 \left\{ \mathbf{b} := \mathbf{b}^p \right. \\
\quad f(\boldsymbol{\tau}^{trial}) > 0 \left\{ \begin{array}{l}
\text{local } NEWTON \text{ loop} \\
\tilde{\mathbf{b}} := \mathbf{b}^p \\
\text{repeat} \\
\qquad \mathbf{A} := \dfrac{\partial \boldsymbol{\Phi}(\mathbf{a}, \tilde{\mathbf{b}}, \mathbf{b}^p)}{\partial \tilde{\mathbf{b}}} \\
\qquad \Delta \tilde{\mathbf{b}} := -\mathbf{A}^{-1} \boldsymbol{\Phi}(\mathbf{a}, \tilde{\mathbf{b}}, \mathbf{b}^p) \\
\qquad \tilde{\mathbf{b}} := \tilde{\mathbf{b}} + \Delta \tilde{\mathbf{b}} \\
\text{until } \left\| \Delta \tilde{\mathbf{b}} \right\| < TOL \\
\mathbf{b} := \tilde{\mathbf{b}} \\
\text{define AD exception of type D for } \tilde{\mathbf{b}} \\
\left.\dfrac{\partial(\cdot)}{\partial(\cdot)}\right|_{\frac{\partial \mathbf{b}}{\partial \mathbf{a}} = -\mathbf{A}^{-1} \frac{\partial \boldsymbol{\Phi}(\mathbf{a}, \mathbf{b}, \mathbf{b}^p)}{\partial \mathbf{a}}}
\end{array} \right. \\
\quad \text{use AD exception of type C} \\
\quad \boldsymbol{\Psi} := \left.\dfrac{\partial W(\mathbf{a}, \mathbf{b})}{\partial \mathbf{a}}\right|_{\frac{\partial \mathbf{b}}{\partial (\bullet)} = 0} \\
\quad \mathbf{K} := \dfrac{\partial \boldsymbol{\Psi}}{\partial \mathbf{a}} \\
\text{end loop}
\end{array}
\tag{10}
$$

Fig. 18: Algorithm for the abstract symbolic description of elasto-plastic problems.
Slika 18: Algoritem za abstrakten simbolni zapis elasto-plastičnega problema.

Here $\tilde{\mathbf{b}}$ denotes a vector of the local unknowns at Gauss point level within the iterative loop. $\mathbf{A}$ is a matrix that follows from the linearization of the nonlinear equation set $\boldsymbol{\Phi}$. The "basic equation of the symbolic plasticity" is written as:

$$
\boldsymbol{\Psi} = \int_{\Omega_e} \left.\frac{\partial W}{\partial \mathbf{a}}\right|_{\frac{\partial \mathbf{b}}{\partial (\bullet)} = 0} d\Omega \tag{11}
$$

An efficient and accurate numerical solution of the corresponding coupled non-linear system of algebraic equations requires a quadratically convergent numerical procedure. For this the linearization of (11) is needed, which leads to the tangent stiffness matrix. This matrix can be derived for a finite element by directly applying the automatic differentiation procedure leading to

$$\mathbf{K} = \frac{\partial \mathbf{\Psi}}{\partial \mathbf{a}} \tag{12}$$

Tangent stiffness matrix derived in this way is already "consistent" with the algorithm used for plasticity. Hence no additional procedures to derive a consistent tangent modulus are required.

The parts necessary for the abstract symbolic description are briefly summarized in Fig. 19.

$$\begin{aligned}
\mathbf{F}_e &= \mathbf{F}\mathbf{F}_{pl}^{-1} \\
\mathbf{C}_e &= \mathbf{F}_e^T \mathbf{F}_e \\
J^2 &= Det(\mathbf{C}_e) \\
W &= \frac{\mu}{2}(tr(\mathbf{C}_e) - 3 - \ln(J^2)) + \frac{\lambda}{4}(J^2 - 1 - \ln(J^2)) \\
\boldsymbol{\tau} &= 2\mathbf{F}_e \frac{\partial W}{\partial \mathbf{C}} \mathbf{F}_e^T \\
s &= \boldsymbol{\tau} - \frac{tr(\boldsymbol{\tau})}{3}\mathbf{I} \\
\alpha &= \sqrt{2\,/\,3}\lambda \\
f &= \sqrt{s \cdot s} - \sqrt{2\,/\,3}(Y0 + H\alpha) \\
\mathbf{\Phi} &= \begin{Bmatrix} \mathbf{F}_e - exp(-(\lambda_{pl} - \lambda_{pl}^p)\frac{\partial f}{\partial \boldsymbol{\tau}})\mathbf{F}\,\mathbf{F}_{pl}^{p-1} = 0 \\ f = 0 \end{Bmatrix} \\
\mathbf{b} &= \left\{\mathbf{F}_{pl}^{-1}, \lambda_{pl}\right\} \\
\mathbf{b}^p &= \left\{\mathbf{F}_{pl}^{p-1}, \lambda_{pl}^p\right\}
\end{aligned}$$

Fig. 19: Summary of the finite strain plasticity equations.
Slika 19: Povzetek enačb plastičnosti.

where $\mathbf{C}_e$ is right Cauchy-Green tensor and $\mathbf{F}_e$ is the deformation gradient. μ and λ are the first and the second Lame's material constants and λ_{pl} is the plastic

multiplier. $\mathbf{b}$ and $\mathbf{b}^p$ are the vectors of state variables at the current step and at the end of previous time step, respectively.

3.5 Finite element models

In the work covered by the thesis 5 types of finite elements were used:

- 2D and 3D Point Load finite element
- 2D and 3D Line Load finite element
- 3D Truss finite element
- Quadrilateral, 4-node, elastic-plastic finite element
- 6-parameter, elastic-plastic, shell finite elements

All finite elements were derived and coded with the help of AceGen (Korelc 2007b). The equations used in the general algorithm for the abstract symbolic description shown in Fig. 18 for the used elements are summarized in Table 3. The load finite elements are used only to apply load on the numerical model.

Table 3: Strain energies for the use in the Automatic differentiation exceptions.
Tabela 3: Izjeme pri avtomatskem odvajanju.

Element	Equilibrium Equations on FE level
Point Load 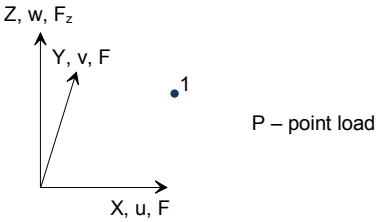	$\mathbf{\Psi}= \mathrm{P}.\dfrac{\partial u}{\partial \mathbf{a}}$
Line Load 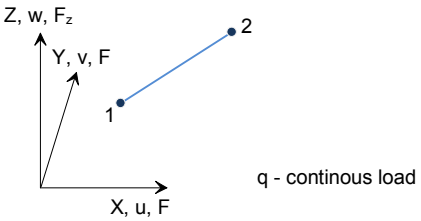	$\mathbf{\Psi}= \int_L q.\dfrac{\partial u}{\partial \mathbf{a}} dL$
Truss 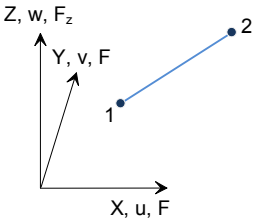	$W = \int_L \frac{1}{2} A\, L_0\, Em\, \varepsilon^2 dL \;\; ; \;\; \mathbf{\Psi}= \int_{\Omega_e} \dfrac{\partial W}{\partial \mathbf{a}} d\Omega$
2d quadrilateral 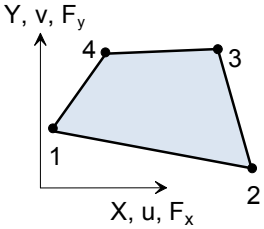	See Section 3.4
3d shell 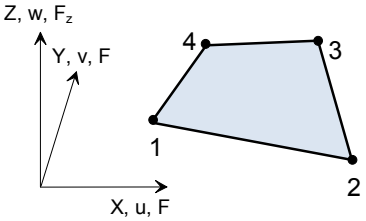	See references (Wisniewski, Turska 2000, 2001).

3.6 Example

An example of sensitivity analysis of a single-storey steel building is presented. The finite element model of the structure is shown in Fig. 20.

The model consists of the following parts:

- The main structure consists of four portal frames modeled by the four node shell elements based on finite rotations, 6 parameter shell theory combined with ANS and two enhanced modes for improved performance (Wisniewski, Turska 2000, 2001)
- The purlins and braced system are modeled by large displacement truss elements.
- Special "load" elements were generated to apply wind and snow loads.

The analytical shape sensitivity pseudo-load vector is derived for all elements by direct differentiation method and with the use of symbolic code generation explained in Chapter 2.

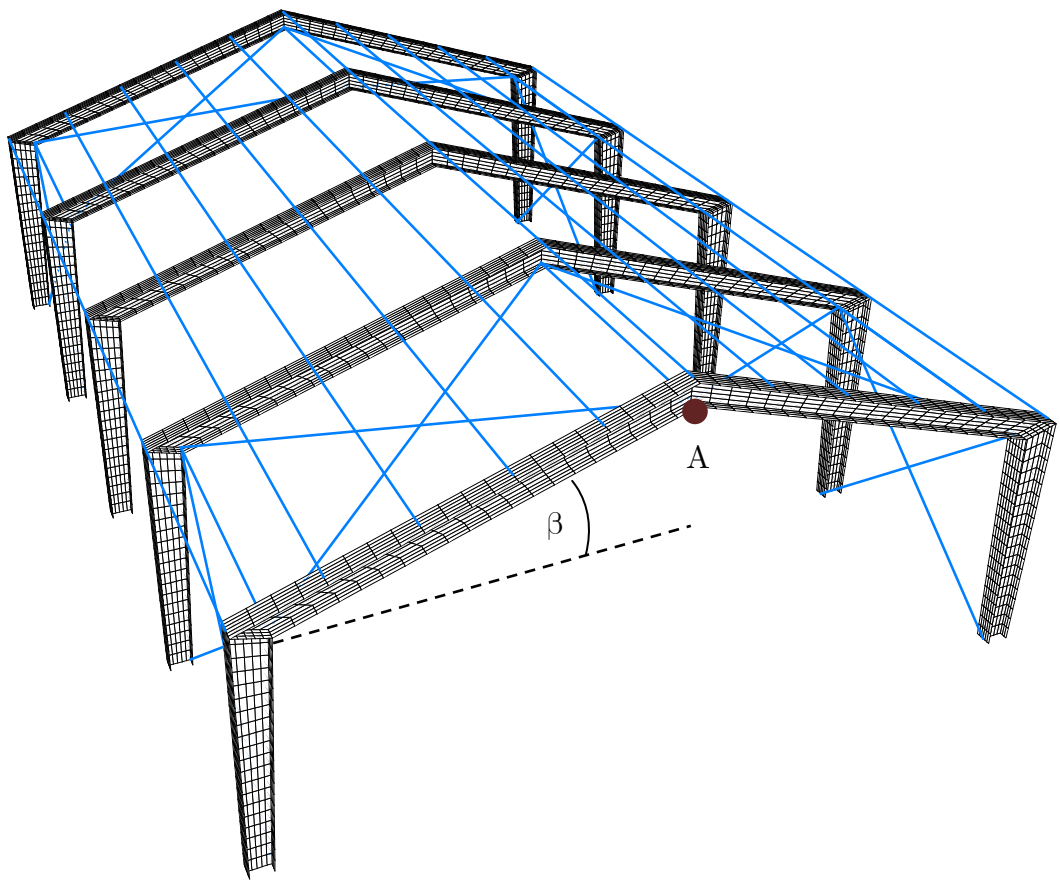

Fig. 20: Finite element model for the one story building.
Slika 20: Model konstrukcije enoetažne hale.

In the example the angle of the roof (β) is used for the design shape parameter. Fig. 21 presents the typical symbolic form of the nodal coordinate generated by the *MDriver*. Differentiation of the symbolically parameterized mesh with respect to β results in a design velocity field that is used within the sensitivity analysis (Michaleris, et al. 1994). The sensitivity of the vertical displacement is presented in Fig. 23. The results of analytical sensitivity analysis are then compared with the results obtained by the finite difference method in Fig. 22. The finite differences are computed considering a relative perturbation size of $9.5 \cdot 10^{-8}$, for which an optimal perturbation size study has to be done. With the evaluated optimal perturbation size finite differences coincide with the analytical method with an average relative error of $4 \cdot 10^{-5}$.

$$
\begin{aligned}
&4950. + 4600.\,\mathrm{Tan}[\beta] + \\
&0.3\left(50. - 4600.\,\mathrm{Tan}[\beta] - \frac{2.76\times 10^{6}}{9950. + 4600.\,\mathrm{Tan}[\beta]} + 0.666667\left(-50. + 4600.\,\mathrm{Tan}[\beta] + \frac{2.76\times 10^{6}}{9950. + 4600.\,\mathrm{Tan}[\beta]}\right)\right) + \\
&0.8\left(-400. + 0.3\,(-50. - 4600.\,\mathrm{Tan}[\beta] + 0.666667\,(50. + 4600.\,\mathrm{Tan}[\beta])) - \right. \\
&\quad \left. 0.3\left(50. - 4600.\,\mathrm{Tan}[\beta] - \frac{2.76\times 10^{6}}{9950. + 4600.\,\mathrm{Tan}[\beta]} + 0.666667\left(-50. + 4600.\,\mathrm{Tan}[\beta] + \frac{2.76\times 10^{6}}{9950. + 4600.\,\mathrm{Tan}[\beta]}\right)\right)\right)
\end{aligned}
$$

Fig. 21: Example of a nodal point coordinate in symbolic form.

Slika 21: Primer koordinat vozlišča mreže končnih elementov v simbolni obliki.

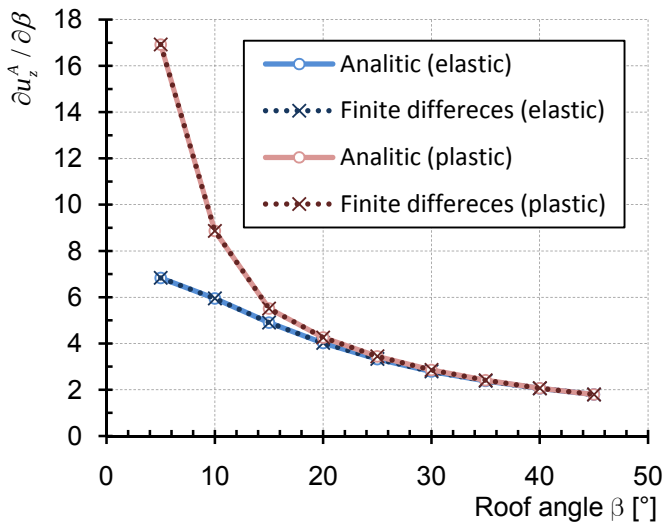

Fig. 22: Comparison between analytic and FD method.

Slika 22: Primerjava analitične občutljivosti in občutljivosti po metodi končnih diferenc.

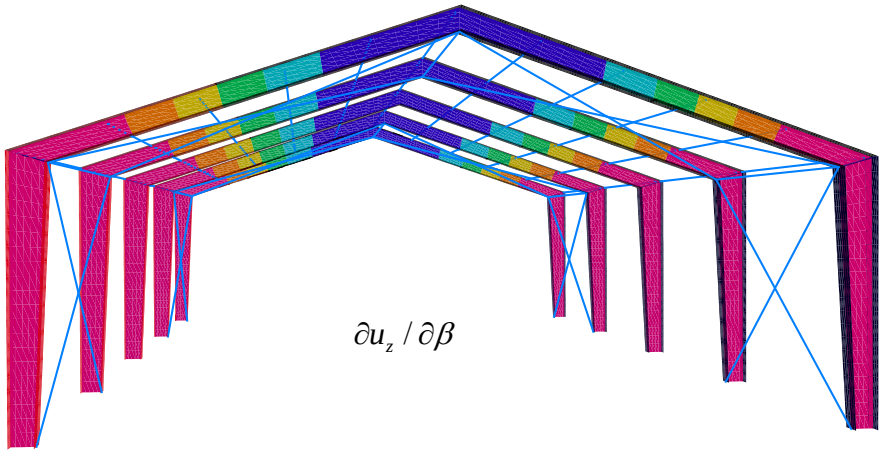

Fig. 23: Graphical sensitivity representation of the vertical displacement with respect to the roof angle.

Slika 23: Grafični način prikaza občutljivosti vertikalnega pomika glede na naklon strehe.

4 Initial imperfections

4.1 Introduction

Limit load design optimization requires the use of imperfect geometry of a structure in order to evaluate the correct limit load. While the imperfections are not known in advance, a method has to be used which is capable of proper involvement of imperfection effects. It is now well known that geometrical, structural, material and load imperfections play a crucial role in the load carrying behavior, especially of thin walled structures.

The determination of the "definitely worst" imperfection can be formulated as a nonlinear optimization problem solved by one of the well-known nonlinear optimization methods as explained in Section 1.2.3. It is doubtful that an approach that requires a large number of fully nonlinear analyses could be used in everyday engineering design in foreseeable future.

In the present work a computationally less expensive optimization method is developed that would still retain the generality of the optimization based "definitely worst" imperfection approach.

Geometrical, structural and material imperfections are considered by means of equivalent geometrical imperfections. The basic idea of the approach is to replace the nonlinear optimization problem with an iterative procedure that would involve only linear optimization problems. Within the iteration the objective function for the minimum ultimate load is constructed by the means of a fully nonlinear direct and first order sensitivity analysis. Constraints on the shape and the amplitude of the imperfections have to be taken into account. When carefully constructed, they remain linear, thus enabling the use of efficient and readily available linear programming algorithms for the solution of the corresponding optimization problem.

In the case where only the amplitude of the imperfections is constrained, numerical studies show that the procedure tends to lead to significantly lower ultimate loads than experimentally observed, as the result is associated with imperfection shapes that are not necessarily technologically feasible. Therefore it is essential to take into account realistic technological constraints on the shape and the amplitude of the imperfections. In the present approach the imperfections are represented by a linear

combination of base shapes with the base constructed from the sufficient number of buckling modes augmented by the eigenvectors of the structure subjected to "technological" boundary conditions and characteristic deformation modes. The construction of the shape base requires the solution of several generalized eigenvector problems and is done only once. The computational cost of each iteration is equivalent to one full nonlinear analysis up to the ultimate load accompanied by the nonlinear sensitivity analysis with respect to all base shapes and the solution of the linear optimization problem. Thus the total computational cost remains within the range that is acceptable for design procedures.

4.2 Optimization method for the determination of the most unfavorable initial imperfection

4.2.1 Representation of imperfections

The applied initial imperfection shape with specified amplitudes has to represent a change in the geometry of a structure in the most unfavorable way so that the ultimate load of the imperfect structure is the smallest possible. The imperfections are represented as a linear combination of the chosen base shapes within amplitude e_0 prescribed by the principle of equivalent geometrical imperfections. Equivalent geometrical imperfections include geometrical and structural imperfections. Geometrical imperfections represent a general deviation from the perfect geometry. Geometrical imperfections can be augmented to include structural imperfections that are not included into the finite element model directly. Structural imperfections arise from the manufacturing method, for example residual stresses produced by welding.

The geometry of an imperfect structure $\mathbf{X}$ is defined by:

$$\mathbf{X} = \mathbf{X}_p + \sum_{j=1}^{N} \alpha_j \mathbf{\Gamma}_j \,, \tag{13}$$

where $\mathbf{X}_p$ is the initial perfect geometry, α_j are the unknown shape parameters and $\mathbf{\Gamma}_j$ are the base shapes. The unknown shape parameters α_j are obtained as a solution of the optimization problem. The base shapes can be chosen arbitrary, but they have to be linearly independent in order to have a well defined minimum of the corresponding optimization problem. The overall numerical efficiency of the procedure strongly depends on the number of base shapes (N). The obvious choice, well explored by other authors (see e.g.Song, et al. 2004), are buckling modes ($\mathbf{\Gamma}^A$) of the structure obtained by initial buckling analysis. Alternative and cheaper to

evaluate are the eigenvectors ($\mathbf{\Gamma}^B$) of the initial elastic tangent matrix $\mathbf{K}_0$. The kinematic boundary conditions for imperfections can be different than kinematic boundary conditions of the structure. This can be observed in rigid support connections where the member is usually considered clamped and it is not possible to describe the support imperfections with the eigenvectors of the original structure. For this purpose the base can be extended by eigenvectors ($\mathbf{\Gamma}^C$) of the elastic tangent matrix $\bar{\mathbf{K}}_0$ of the same structure but with different kinematic boundary conditions. In this way the technological imperfections can be added. Some authors have observed (Schneider 2006, Schneider, Brede 2005, Schneider, et al. 2005) that sometimes the most unfavorable imperfection resembles deformation shapes rather than buckling modes. In order to reduce the total number of the necessary considered base shapes, an additional set of deformation shapes ($\mathbf{\Gamma}^D$) of the structure in elastic and plastic range can be added. And finally, the set of shapes which are empirically known to represent the worst imperfections for certain type of structures ($\mathbf{\Gamma}^E$) can be added. The total base $\mathbf{\Gamma}$ is then in general composed of:

$$\mathbf{\Gamma} = \mathbf{\Gamma}^A \cup \mathbf{\Gamma}^B \cup \mathbf{\Gamma}^C \cup \mathbf{\Gamma}^D \cup \mathbf{\Gamma}^E \tag{14}$$

The optimized imperfection shape (most unfavorable initial imperfection shape) depends on the number of shapes included in the shape base and the density of the finite element mesh. For reasonable results it is necessary to increase them proportionally. With the increase of the considered shapes, the result converges to a final shape. For practical reasons it is necessary to include at least that much different shapes to allow including all local and global collapse mechanisms. The shape of the most unfavorable initial imperfection changes with different loading patterns, supporting conditions, changes in geometry or the amplitude of initial imperfections. In this sense, the shape of the most unfavorable initial imperfection in means of ultimate load of a structure has to be evaluated for every individual structure separately and can not be generalized.

4.2.2 Description of the algorithm

In the presented approach a fully geometrically and materially nonlinear analysis is used. When dealing with thin-walled structures with moderate thickness, it is necessary to take geometrical and material nonlinearity into account. Since the algorithm starts from the beginning with the imperfect structure, bifurcation points usually do not occur prior reaching the limit point in a load-deformation curve. By limiting the analysis to limit points one avoids tedious procedures involved in proper determination, classification and sensitivity analysis of bifurcation points. Only stable

equilibrium states have to be considered and no hypothetic states need to be taken in account.

Within this method the most unfavorable initial imperfection shape is sought, defined by the shape base $\mathbf{\Gamma}$ and the shape parameters $\boldsymbol{\alpha}$ at which the ultimate load will be the lowest. Unknown shape parameters $\boldsymbol{\alpha}$ are evaluated iteratively by an optimization process. The iterative procedure for the k-th step can be written as:

$$\begin{aligned} \mathbf{X}_k &= \mathbf{X}_{k-1} + \Delta\mathbf{X}_k \\ \Delta\mathbf{X}_k &= \sum_{i=1}^{N} \Delta\alpha_i^k \, \mathbf{\Gamma}_i \\ \alpha_i^k &= \alpha_i^{k-1} + \Delta\alpha_i^k \\ \bar{\mathbf{X}}_k &= \sum_{i=1}^{N} \alpha_i^k \, \mathbf{\Gamma}_i \end{aligned} , \tag{15}$$

where $\mathbf{X}_k$ is the imperfect geometry, $\Delta\alpha_i^k$ the increment of the imperfection parameters, $\Delta\mathbf{X}_k$ the increment of the imperfection and $\bar{\mathbf{X}}_k$ the total imperfection. The increment of the imperfection parameters in the k-th iteration $\Delta\alpha_i^k$ is obtained as a solution of the corresponding optimization problem described in Section 4.2.2. The flowchart of the method is illustrated in Fig. 24. The algorithm starts with the first base shape Γ_1, normalized by the amplitude e_0, as the initial guess $\mathbf{X}_0$ for the geometry of the imperfect structure:

$$\begin{aligned} &\alpha_i^0 = 0; \; \Delta\alpha_i^0 = \begin{cases} \dfrac{e_0}{\max \Gamma_i} & i = 1 \\ 0 & i \neq 1 \end{cases} \\ &\mathbf{X}_0 = \mathbf{X}_p + \Delta\alpha_1^0 \, \Gamma_1 \end{aligned} \tag{16}$$

and then improves the solution by solving a sequence of optimization problems until the convergence condition $\left\| \Delta\alpha_i^k \right\| < tolerance$ is reached. Within each step of the iterative procedure a fully nonlinear direct and sensitivity analysis of the structure with imperfect geometry $\mathbf{X}_k$ is performed followed by the formulation and solution of the optimization problem.

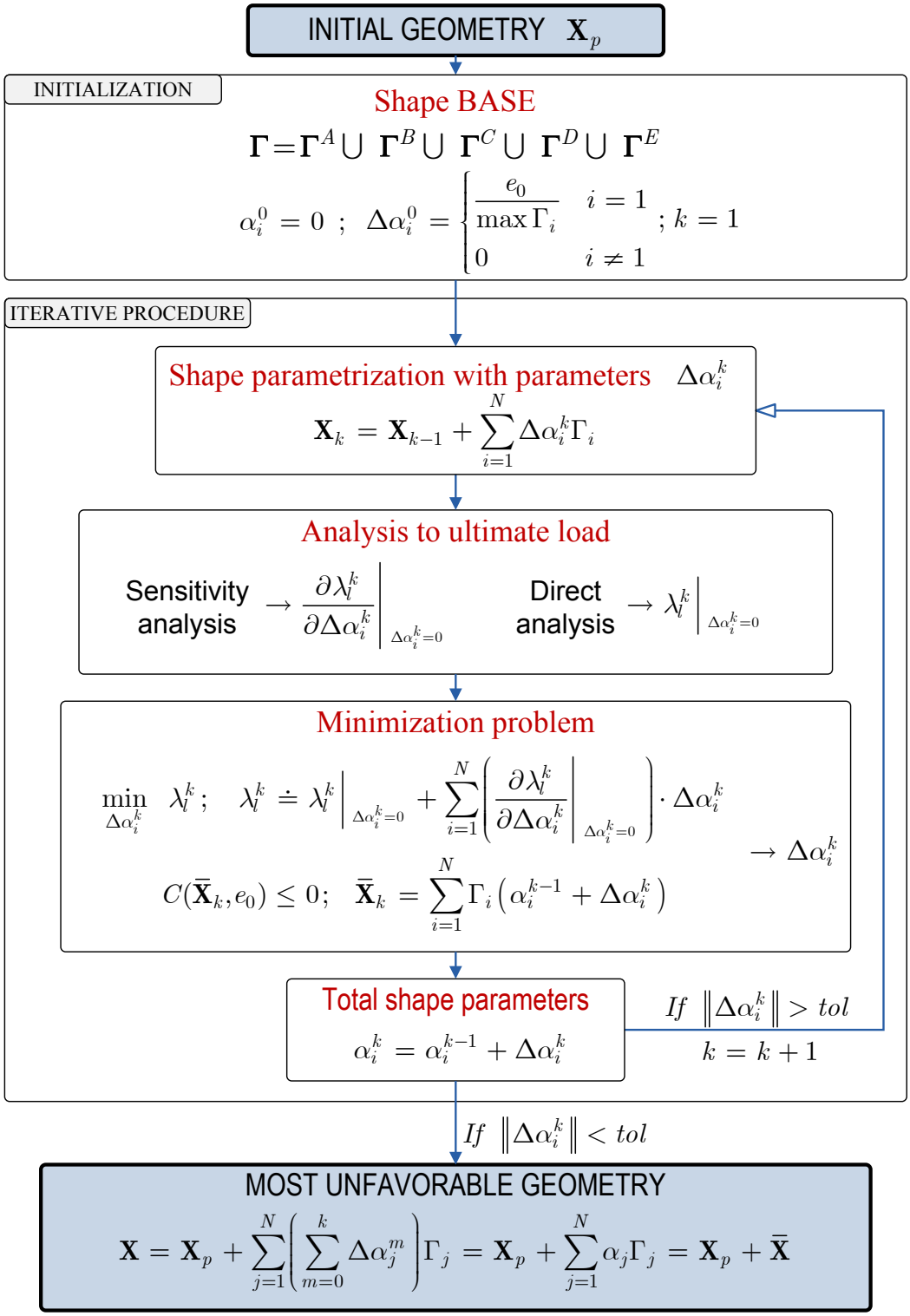

Fig. 24: Flowchart of the method for the determination of the most unfavorable initial imperfection.
Slika 24: Potek metode določitve najbolj neugodne začetne nepopolnosti.

The presented approach gives the advantage of use of arbitrary state of the art optimization algorithms, as the optimization part is completely separated from the direct and sensitivity analysis. An alternative approach would be performing a fully coupled nonlinear optimization where the most unfavorable imperfection shape parameters would be determined simultaneously within the direct and sensitivity analysis. Such an evaluation is to authors experience not feasible for larger structural systems at this time.

4.2.3 Formulation of the optimization problem

The ultimate load factor of the imperfect structure in k-th iteration λ_l^k represents the minimizing function, where the maximal amplitude of the total imperfection $\overline{\mathbf{X}}_k$ has to be equal to or smaller than the amplitude of the prescribed equivalent geometrical imperfections e_0:

$$\begin{gathered} \min_{\Delta\alpha_i^k} \lambda_l^k \\ C(\overline{\mathbf{X}}_k, e_0) \leq 0 \end{gathered} \tag{17}$$

where $C(\overline{\mathbf{X}}_k, e_0)$ is a constraint function.

The decoupling of the direct analysis and optimization is achieved by expansion of the ultimate state load factor λ_l^k to a Taylor series around the ultimate state load factor of the current imperfect geometry. The ultimate load factor is then written as:

$$\lambda_l^k \doteq \lambda_l^k \Big|_{\Delta\alpha_i^k=0} + \sum_{i=1}^{N} \left(\frac{\partial \lambda_l^k}{\partial \Delta\alpha_i^k} \Big|_{\Delta\alpha_i^k=0} \right) \cdot \Delta\alpha_i^k \ , \tag{18}$$

where $\lambda_l^k \Big|_{\Delta\alpha_i^k=0}$ is the evaluated ultimate load factor of the structure and $\frac{\partial \lambda_l^k}{\partial \Delta\alpha_i^k} \Big|_{\Delta\alpha_i^k=0}$ the sensitivity of the ultimate load factor with respect to optimization parameters $\Delta\alpha_i^k$ in the current step. The minimizing function λ_l^k in this instance is a linear function. The constraining function, on the other hand, can be a highly nonlinear function or a simple set of linear constraints, depending on way it is defined. The employment of constraints (17) arises from the demand of the technical standards (see e.g. EN 1090/2 2007) which specify requirements for execution of structures or manufactured components of structures. The location of the point of

maximal amplitude is unpredictable, which makes it very difficult to choose the appropriate restraining function.

For small order problems (i.e. up to 5000 nodes) where nonlinear optimization algorithms can be used, a simple norm of the total imperfection (Deml, Wunderlich 1997) gives satisfactory results. The norm that proved to be reliable for small order problems is the L^{2p} vector norm with the exponent 2p. With the increase of the constant p the norm limits to the maximal value of components of the total imperfection vector $\overline{\mathbf{X}}_k$:

$$\lim_{2p\to\infty} \left\| \overline{\mathbf{X}}_k \right\|_{2p} = \max \left| \overline{\mathbf{X}}_k \right|;$$
$$\left\| \overline{\mathbf{X}}_k \right\|_{2p} = \left(\sum_{j=1}^{N} \left(\overline{\mathrm{X}}_j^k \right)^{2p} \right)^{\frac{1}{2p}}, \tag{19}$$

The minimization problem (17) with inequality constraints can be solved by an advanced penalty method or an extended Lagrange multiplier type method.

For large problems the necessity of a high exponent p of the L^{2p} norm in order to achieve the necessary accuracy makes the huge constraint function highly nonlinear and the minimization problem difficult to solve. In this case it is necessary to define a set of linear constraints for the maximal amplitude of the total imperfection vector:

$$\left| \overline{X}_k^m \right| \le e_0^m \quad ...m \in \left[n_1, n_2, ..., n_{cp} \right], \tag{20}$$

where n_i is the index of the i-th constrained component of the total imperfection vector, n_{cp} is the total number of constrained components and e_0^m is the amplitude value of the m-th constraint. In this way different constraint amplitudes can be applied for parts of a structure, which is of high significance when dealing with complicated structural systems where every part of the structure has its own prescribed amplitude of equivalent geometrical imperfection. While the minimizing function (18) and the set of constraints (20) are all linear, linear programming with an advanced interior point algorithm can be applied for the fast determination of a global minimum.

4.2.4 Direct and sensitivity analysis

With the use of direct and sensitivity analysis of the imperfect structure under a real load the ultimate load factor λ_l^k and its derivatives $\dfrac{\partial \lambda_l^k}{\partial \Delta\alpha_i^k}$ with respect to unknown base shape parameters $\Delta\alpha_i^k$ are evaluated.

The structure is analyzed in accordance with the standard "arc-length" type continuation method (see e.g.Crisfield 1996, 1997). Therefore, in direct and sensitivity analysis the equilibrium equations are extended with load factor λ as an additional variable and constraint g_c as an additional equation imposed on the increments of generalized displacements. The general expressions are given in Section 3.2 and Section 3.3. The limit load sensitivity analysis of the imperfect structure is in fact equivalent to the standard shape sensitivity analysis and is done using the same procedures described in Sections 3.2 and 3.3. The only open question is the design velocity field.

Because of the way the imperfection shape is parameterized, the design velocity field is easily obtainable, since the base shape Γ_i itself represents the design velocity field:

$$\frac{D\bar{\mathbf{\Psi}}}{D\Delta\alpha_i^k} = \frac{\partial \bar{\mathbf{\Psi}}}{\partial \mathbf{X}} \frac{\partial \mathbf{X}}{\partial \Delta\alpha_i^k} \tag{21}$$

$$\frac{\partial \mathbf{X}}{\partial \Delta\alpha_i^k} = \frac{\partial \left(\mathbf{X}_p + \sum_{j=1}^{N} \left(\sum_{m=0}^{k} \Delta\alpha_j^m \right) \Gamma_j \right)}{\partial \Delta\alpha_i^k} = \delta_{ij} \cdot \Gamma_j = \Gamma_i \tag{22}$$

where Γ_i is the shape base, $\dfrac{D\bar{\mathbf{\Psi}}}{D\Delta\alpha_i^k}$ is the sensitivity with respect to shape parameters and $\dfrac{\partial \mathbf{X}}{\partial \Delta\alpha_i^k}$ the design velocity field used within the standard shape sensitivity analysis.

4.3 Numerical examples (Test Problems and Results)

To illustrate the proposed method, a simple example of a cantilever structure is presented. Further on, more complex structures are analyzed to represent the applicability of the proposed method to large scale models.

4.3.1 Elasto-plastic cantilever structure

The most unfavorable imperfection for a 2D cantilever structure is sought. The structure is modeled by plane stress, finite strain, ideal elasto-plastic, 4-node quadrilateral finite elements (Korelc 2002). On the free end, a horizontal force in axial direction is applied (Fig. 25 (a)). The height of the cantilever is 2 cm and the width is 1 cm. The elastic modulus has been taken as 210000 MPa and the yield stress as 235 MPa. The Poisson ratio was taken as 0.3.

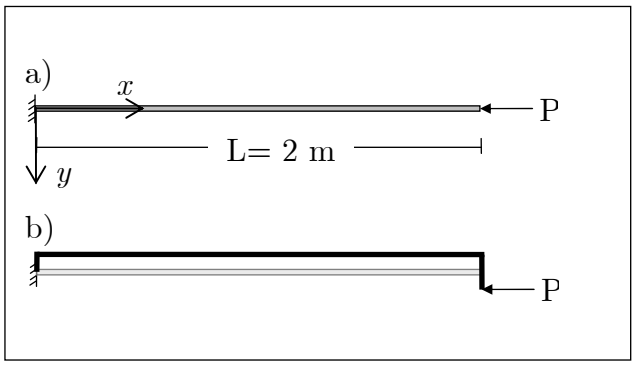

Fig. 25: Geometry and loading (a) and the logically most unfavorable shape without considering technological constraints (b) for the cantilever beam example.

Slika 25: Geometrija in obtežbe (a) ter logična optimalna oblika brez upoštevanja tehnoloških pogojev (b).

According to the method described in Section 4.2, the shape base is defined first. The considered base consists of 20 buckling modes ($\mathbf{\Gamma}^A$), 20 alternative boundary condition shapes ($\mathbf{\Gamma}^C$), and the shape of the plastic deformed structure ($\mathbf{\Gamma}^D$) (see Fig. 26). The alternative boundary condition shapes are evaluated as eigenvectors of the linear elastic tangent matrix of a substitute system, which can give description of the "technological" imperfections in the vicinity of the support. In order to achieve that, the degrees of freedom have to be released to allow rotation of the structure in the originally fixed support.

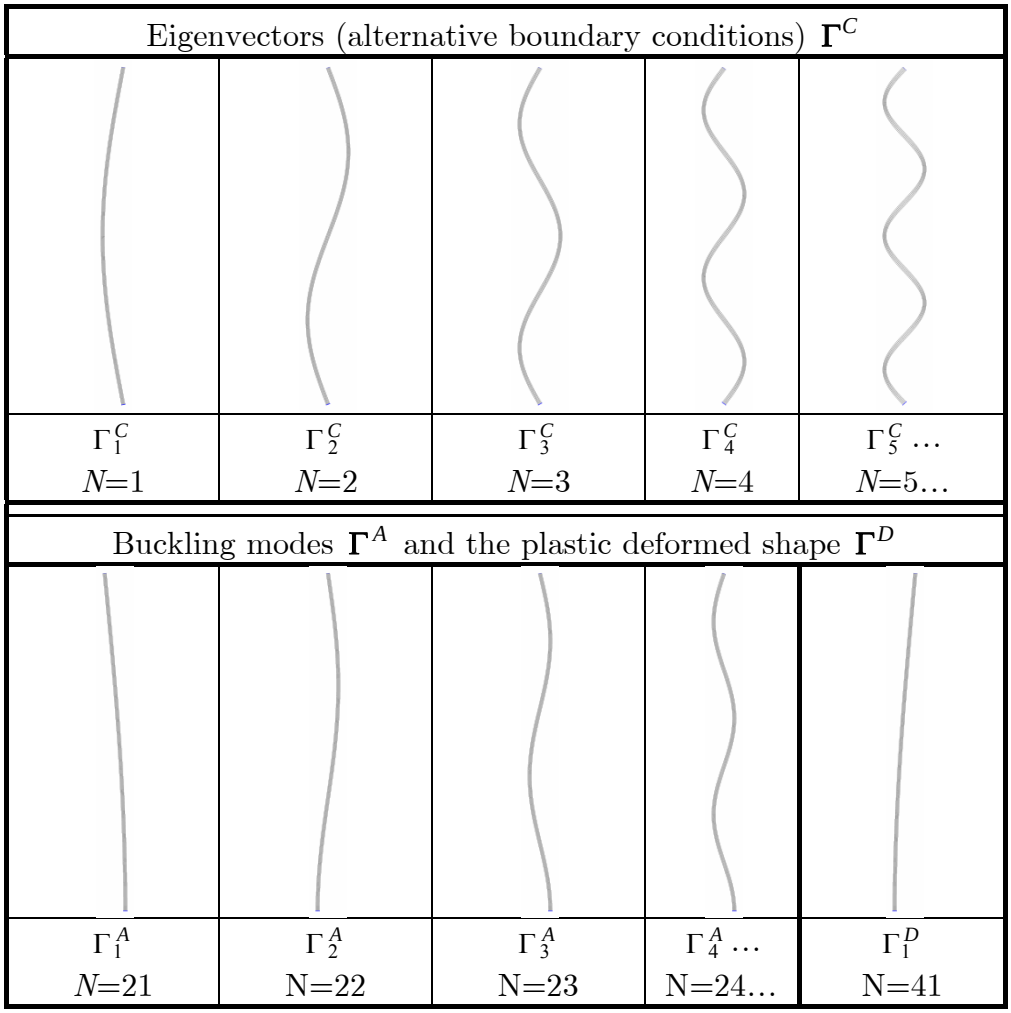

Fig. 26: The shape base for the cantilever beam example.

Slika 26: Baza oblik za primer konzole.

The plastic deformed shape and the buckling modes are calculated in consideration of the perfect initial geometry of the structure. The final shape base $\mathbf{\Gamma}$ consists of 41 base shapes. In the optimization part of the process it is necessary to satisfy the constraint conditions (17) which arise from the demand of the maximal amplitude of the equivalent geometrical imperfections. In this example an equivalent geometrical imperfection of L/250 is prescribed, where L is the length of the cantilever.

In general it is not necessary to constrain all nodes of the model. The constraint equations in form of (20) taken in account were only connected to the center line and longitudinal boundary lines of the cantilever beam. As a result, 401 constraint equations connected to the center line considering the maximal initial imperfection amplitude of $e_0^y = \mathrm{L}/250$ in y direction and 802 constraint equations from the

boundary lines considering the maximal initial imperfection amplitude of $e_0^x = e_0^y / 100$ in x direction were obtained. The constraints considering the imperfection amplitude in x direction were necessary to exclude unfeasible results due to the 2D finite element model used. The resulting minimizing function and all constraint equations are linear. The standard linear programming procedure with an interior point algorithm built in *Mathematica* was applied to solve the resulting linear optimization problem within each iteration of the global iterative procedure described in Section 4.2.

The logical most unfavorable initial shape which causes the structure to fail at minimum load would be the one illustrated in Fig. 25(b). Such kind of imperfection shape is not technologically feasible because of the sharp edges in it. The feasibility issue can be eliminated by the employment of additional constraints in the calculation of the most unfavorable initial imperfection. In the present simple example it was not necessary to employ them explicitly as the shapes considered in the shape base had such geometries that no sharp edges could be produced. The maximal curvature was therefore implicitly controlled by the considered base shapes. In Fig. 27 the calculated most unfavorable initial imperfection shapes and the corresponding ultimate load factors are shown for different number of considered shapes in the shape base.

Number of considered shapes	The most unfavorable initial imperfection geometry	λ_u
5		0.200
17		0.197
29	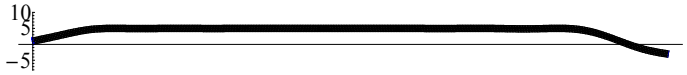	0.196
41		0.194

Fig. 27: Convergence to the most unfavorable shape by increasing the number of considered shapes in the shape base (scale factor $f_s = 10$).

Slika 27: Konvergenca najbolj neugodne oblike z večanjem števila upoštevanih oblik (faktor povečave $f_s = 10$)

The shape and the amplitude of the equivalent geometric imperfections should be in general chosen in such a way that it has the same effect on the load bearing capacity of the structure as all relevant imperfections together.

The shapes and amplitudes for geometric imperfections can be chosen in accordance with the manufacture tolerances (e.g. EN 1090/2 2007) although it is possible that taking the amplitude of the considered initial imperfections equal to the manufacture tolerances can lead to a too low characteristic resistance. This can be even more pronounced where several different imperfections interact (Johansson, et al. 2007). There is little information about equivalent geometrical imperfections for a general structure found in existing technical standards.

In the present example a comparison has been made for the ultimate load factor of the structure, considering different manually defined combinations of base shapes and the calculated most unfavorable initial shape. In Table 4 there are ultimate load factors (λ_u) shown for the cantilever structure with different initial imperfections considered according to the specified combination methods. The contribution of the chosen shapes from the shape base to the final result is represented by values of parameters α_i. The smallest calculated ultimate load factor resulting from the use of various combinations of imperfection shapes is 0.219 for the combination method $\tilde{\Gamma} = \Gamma_i + \Gamma_j$ where the most unfavorable combination of two base shapes is

considered. Other combination methods produce higher ultimate load factors. The ultimate load factor of the structure obtained by the proposed method, taking the calculated most unfavorable initial imperfect shape into account, is 0.194, which results in a 11% smaller ultimate load with respect to other combination methods. If the number of considered base shapes was increased, the corresponding most unfavorable imperfection shape would lead to an even lower ultimate load factor. To prevent the curvatures of the imperfection shape to exceed common values, the number of considered base shapes 41 was chosen in this example.

Table 4: Ultimate load factors for various initial imperfection shapes for the cantilever beam example.
Tabela 4: Mejni obtežni faktorji za različne kombinacije obtežb za primer konzole.

Perfect geometry		$\lambda_u = 0.366$
Initial geometry according to recommended combinations of shapes:		
Shape combination method	Combination at minimal λ_u	λ_u
$\tilde{\Gamma} = \Gamma_i$	$i = 41$	0.268
$\tilde{\Gamma} = \Gamma_i + \Gamma_j$	$i = 1, \quad j = 41$	0.219
$\tilde{\Gamma} = \Gamma_i + 0.7\sum_{\substack{j=1 \\ j \neq i}}^{N} \Gamma_j$	$i = 41$	0.342
$\tilde{\Gamma} = \Gamma_i + \Gamma_j + 0.7 \sum_{\substack{k=1 \\ k \neq i,j}}^{N} \Gamma_k$	$i = 1, \quad j = 41$	0.343
$\Gamma = \frac{\tilde{\Gamma}}{\max\lvert\tilde{\Gamma}\rvert} e_0$		
Most unfavorable initial imperfection by proposed method:		
$-2997\,\Gamma_1 + 106.6\,\Gamma_2 + 898\,\Gamma_3 + 33.5\,\Gamma_4 + 62.4\,\Gamma_5 - 4.4\,\Gamma_6 - 17.4\,\Gamma_7 + 3.3\,\Gamma_8 + 4.3\,\Gamma_9 + 1.23\,\Gamma_{10} - 3.47\,\Gamma_{11} + 0.41\,\Gamma_{12} - 5.25\,\Gamma_{13} + 1.30\,\Gamma_{14} + 2.07\,\Gamma_{15} - 0.04\,\Gamma_{16} + 2.06\,\Gamma_{17} - 1.28\,\Gamma_{18} + 0.28\,\Gamma_{19} + 0.04\,\Gamma_{20} - 2310\,\Gamma_{21} - 3722\,\Gamma_{22} + 1858\,\Gamma_{23} - 762\,\Gamma_{24} + 0.71\,\Gamma_{25} + 105\,\Gamma_{26} + 10.0\,\Gamma_{27} - 44.5\,\Gamma_{28} - 18.9\,\Gamma_{29} + 4.2\,\Gamma_{30} + 11.8\,\Gamma_{31} - 2.4\,\Gamma_{32} - 7.7\,\Gamma_{33} - 5.9\,\Gamma_{34} - 3.5\,\Gamma_{35} - 1.8\,\Gamma_{36} + 1.3\,\Gamma_{37} + 4.6\,\Gamma_{38} - 0.3\,\Gamma_{39} - 0.4\,\Gamma_{40} + 0\,\Gamma_{41}$		$\boldsymbol{\lambda_u = 0.194}$

4.3.2 Thin-walled T beam

Structures composed of thin–walled components in general prove a high degree of imperfection sensitivity. The thin-walled girders in this section were modeled by elasto-plastic four node shell elements based on finite rotations, 6 parameter shell theory combined with assumed natural strain formulation and two enhanced strain modes for improved performance (Wisniewski, Turska 2000, 2001).

The example refers to the ultimate load calculation of a simply supported thin-walled beam with a T cross-section, loaded with a concentrate force at the mid-length. The geometrical details and loads are presented in Fig. 28. The example was taken from (Lanzo, Garcea 1996)

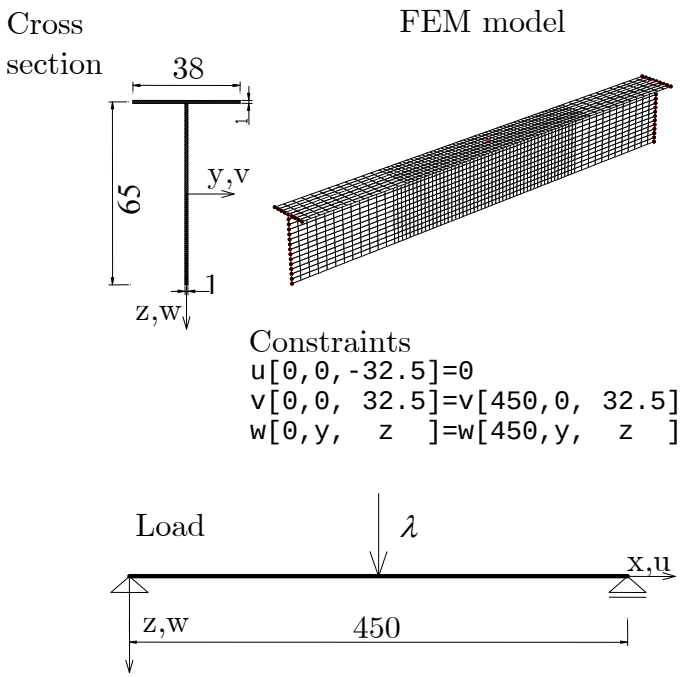

Fig. 28: Geometry, supporting and loading conditions for the thin-walled T beam example.

Slika 28: Geometrija, podpore in obtežba tankostenskega T nosilca.

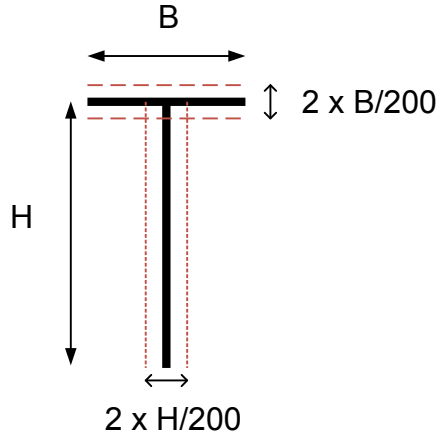

Fig. 29: Maximal allowable deviation from the perfect geometry used in the evaluation.
Slika 29: Največje dopustno odstopanje od popolne oblike pri izračunu.

Different constraint conditions (20) were used for the flange and the web of the girder. The maximal amplitude of the equivalent geometrical imperfection for the web was taken as H/200, where H is the height of the web and the amplitude for the flange was taken as B/200, where B is the width of the flange. Within the optimization problem (17) it was therefore necessary to define 3150 constraint equations for the maximal initial imperfection amplitude perpendicular to the web and 2025 constraint equations for the maximal imperfection amplitude perpendicular to the flange. In this case, only the y-direction web components and the z-direction flange components of the total imperfection vector $\overline{\mathbf{X}}_k$ are constrained.

First the structure is analyzed considering the shape base Γ consisting of buckling modes. In Fig. 30 the calculated limit load of the T-beam with increasing number of base shapes is shown. The results show clear convergence of the calculated limit load.

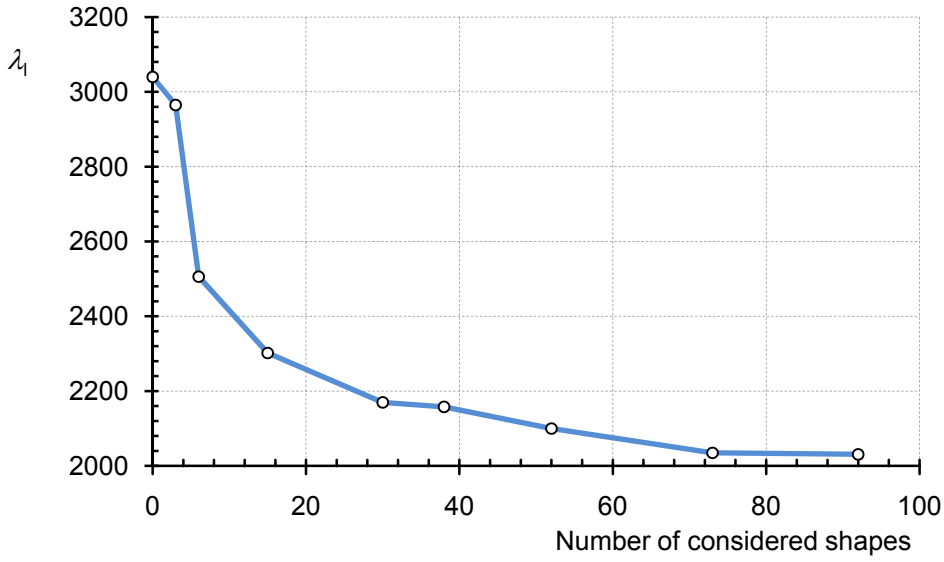

Fig. 30: The calculated ultimate load of the T-beam considering the evaluated most unfavorable initial imperfection varying the number of base shapes.

Slika 30: Mejna obtežba T nosilca pri upoštevanju izračunane najbolj neugodne nepopolnosti pri različnem številu oblik v bazi.

Furthermore the structure is analyzed by two different shape bases in order to assess the influence of the chosen shape base on the numerical efficiency of the proposed procedures. The first shape base (sbA) consists of 50 buckling modes ($\mathbf{\Gamma}^A$) and two deformation shapes ($\mathbf{\Gamma}^D$) and the second (sbB) of 50 eigenvectors of the elastic tangent matrix $\mathbf{K}_0$ ($\mathbf{\Gamma}^B$) and two deformation shapes ($\mathbf{\Gamma}^D$). In Fig. 31 the ultimate load-deformation curves for the two cases are plotted. The difference in results between the two cases is small and decreases with increasing the number of considered shapes. In the present example the shape base composed of eigenvectors of the elastic tangent matrix (sbB) turned out to be more appropriate than the shape base composed of buckling modes (sbA), since a lower ultimate load was computed with the same number of considered base shapes. The shape base (sbB) is used for further analysis. The most unfavorable initial imperfection evaluated by the presented approach for the shape base (sbB) and the corresponding deformed state at collapse are presented in Fig. 32.

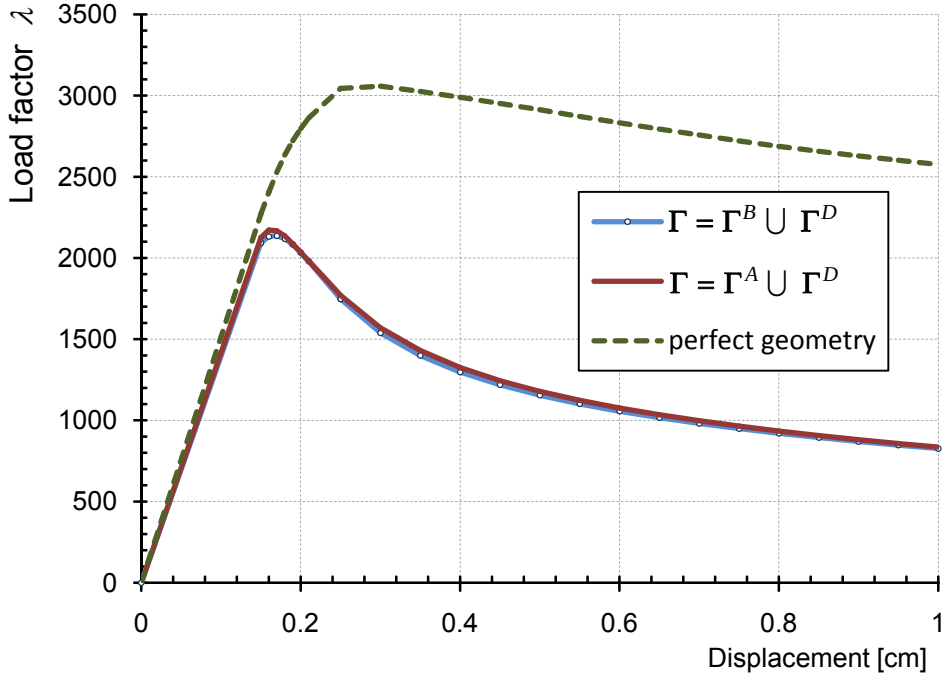

Fig. 31: The load displacement curves considering various imperfection shape bases for the T beam example.

Slika 31: Graf sila-pomik za T nosilec z upoštevanjem različnih baz oblik.

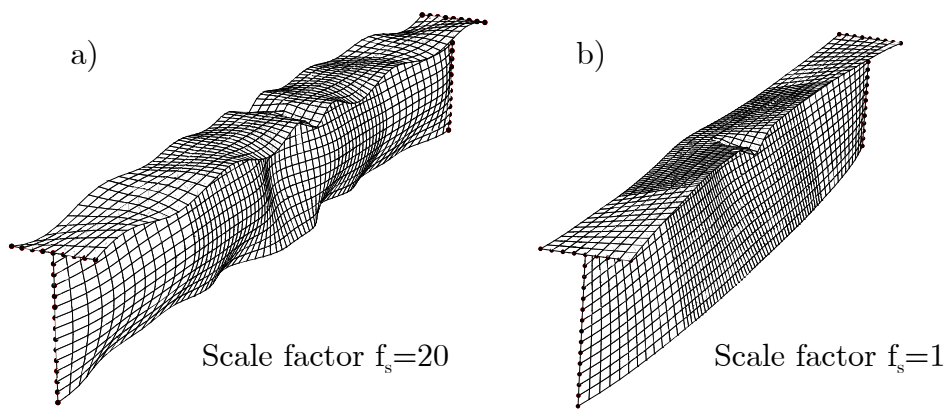

Fig. 32: The most unfavorable initial imperfection shape of the T cross-section thin-walled girder (a) and the corresponding deformed shape at collapse (b).

Slika 32: Najbolj neugodna začetna nepopolnost za primer T nosilca (a) in pripadajoče stanje pri limitni obtežbi(b).

Fig. 33 presents the convergence of the global iterative procedure for the considered shape base (sbB). The result of the first iteration, where the first eigenvector is taken for the initial imperfection, gives a good approximate to the final result. Only 9

iterations were necessary to achieve convergence within tolerances and to determine the most unfavorable initial imperfection.

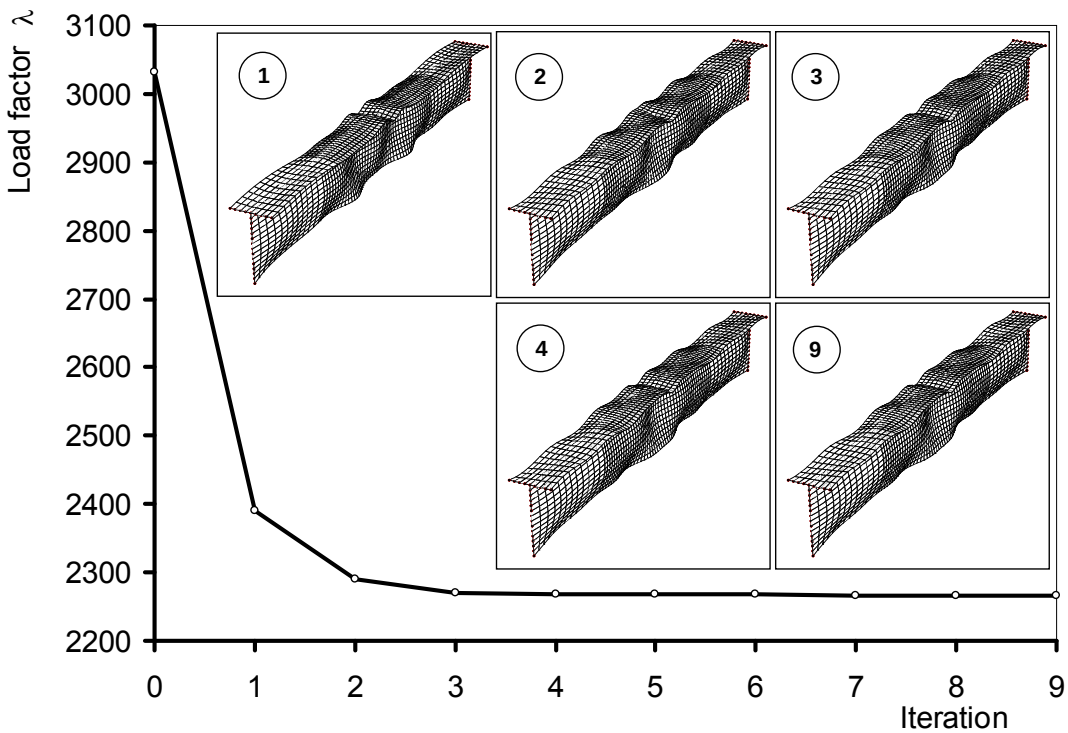

Fig. 33: Convergence of the global iteration process of finding the most unfavorable imperfection shape for the example with 52 base shapes.

Slika 33: Konvergenca globalnega iteracijskega procesa iskanja najbolj neugodne oblike z upoštevanjem 52 baznih oblik..

In Fig. 34 equilibrium paths calculated for various values of amplitudes of equivalent geometrical imperfections are plotted. The e_{0w} is the maximal amplitude of the equivalent geometrical imperfections perpendicular to the surface of the web with height H and the e_{0f} is the maximal amplitude of the equivalent geometrical imperfections perpendicular to the surface the flange with width B. The calculated ultimate load depends to a large extent on the amplitude of the used initial imperfection. The choice of the amplitude is therefore very important and a crucial part for determining the most unfavorable initial shape. For the purpose of comparison the equilibrium path calculated on a basis of the Koiters asymptotical approach to nonlinear instability for the same example was taken from (Lanzo, Garcea 1996).

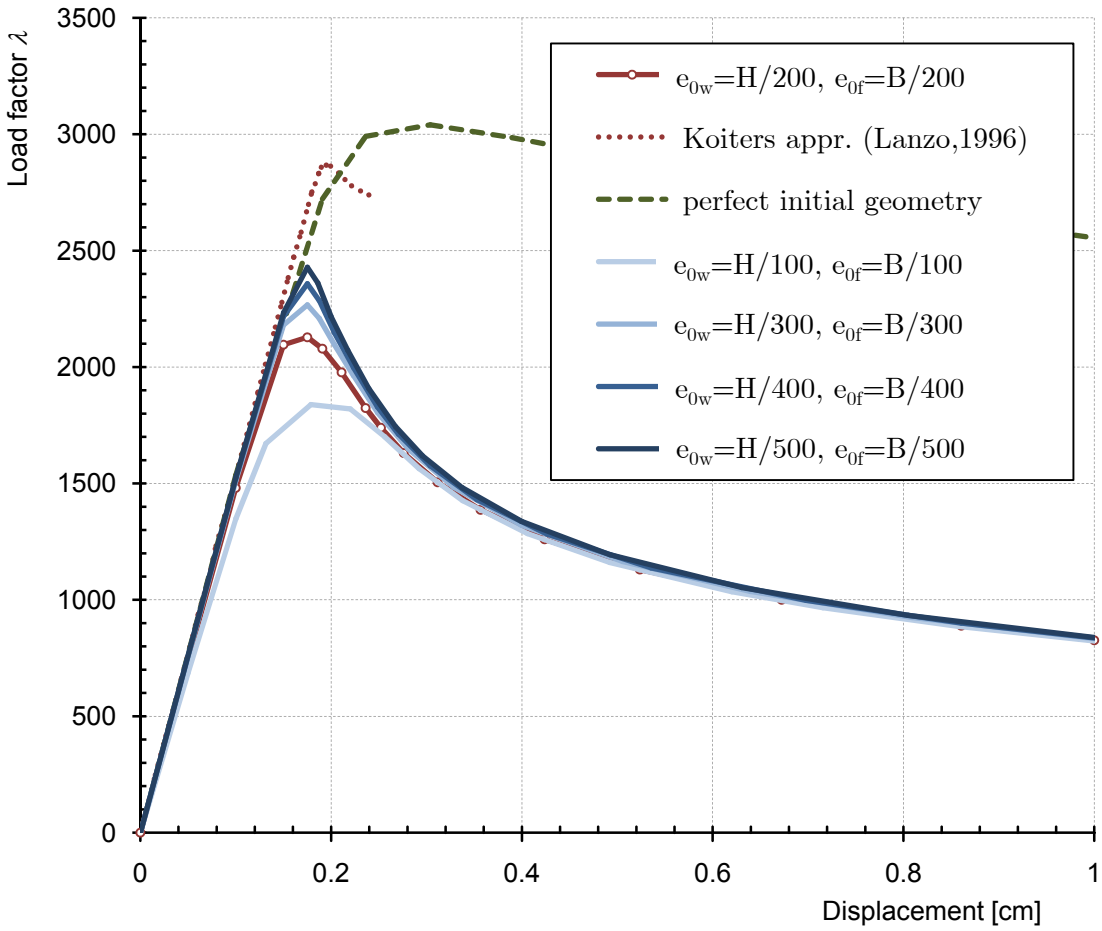

Fig. 34: Equilibrium paths for the T cross-section thin-walled girder.
Slika 34: Ravnotežne poti za primer T nosilca.

4.3.3 Thin-walled I beam

In the third example, the most unfavorable imperfection for a standard 8m long HEA400 structural steel I beam is computed. The beam is fully rigidly supported at the ends. The elastic modulus has been taken as 21000 kN/cm^2 and the yield stress as 23.5 kN/cm^2. The Poisson ratio was taken as 0.3. The structure is modeled by the same finite elements as in previous section.

A vertical line load is applied along the upper flange center line. The considered shape base $\mathbf{\Gamma}$ consists of 58 eigenvectors of the elastic tangent matrix $\mathbf{K}_0$ and 2 deformation shapes corresponding to the elastic deformed state and the plastic limit state. The optimization problem includes 3111 constraint equations. All components of the total imperfection vector $\bar{\mathbf{X}}_k$ are constrained with the amplitude $e_0 = H/200$, where the height of the cross-section $H = 39\,\text{cm}$ (see Fig. 35).

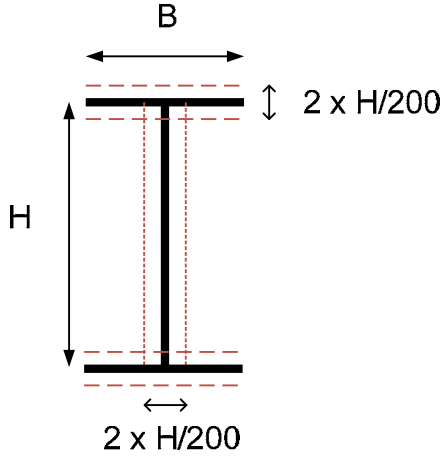

Fig. 35: Maximal allowable deviation from the perfect geometry used in the evaluation.
Slika 35: Največje dopustno odstopanje od popolne oblike pri analizi.

In Fig. 36 equilibrium paths are plotted for various combinations of imperfection shapes taken from $\mathbf{\Gamma}$. Shapes and combinations of shapes considered are:

a) initial imperfection in the shape of elastic deformed shape,

b) initial imperfection in the shape of the plastic deformed shape,

c) combination of two shapes $\Gamma_i + \Gamma_j$,

d) combination of all shapes in form $\Gamma_i + \Gamma_j + 0.7 \sum_{k=1;k\neq i,j}^{N} \Gamma_k$,

e) computed most unfavorable initial imperfection shape for shape base $\mathbf{\Gamma}$.

In the case (c) as in the case (d) the minimum limit load calculated was achieved for $i = 34$ and $j = 37$. All considered initial imperfection shapes were normalized by the value of the equivalent geometrical imperfection amplitude e_0 for the purpose of comparison.

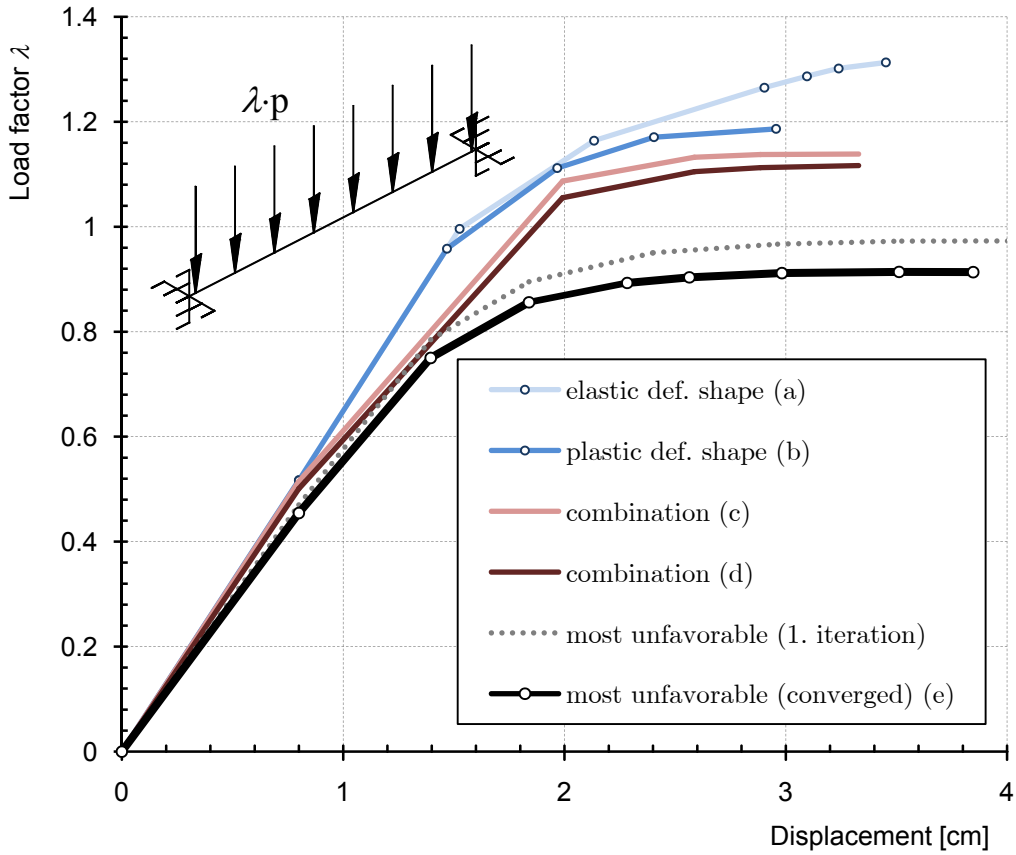

Fig. 36: Ultimate load deformation curves for different initial imperfect geometries with the same amplitude for the I beam example.

Slika 36: Mejne krivulje za različne oblike začetnih nepopolnosti z enako amplitudo za primer I nosilca.

The corresponding imperfect geometries are plotted in Fig. 37. For case (e) two load curves are plotted belonging to the first iteration of the global iterative procedure and the final converged state. The various recommended combinations of shapes (a-d) result in significantly higher limit load when compared to the ultimate load obtained by the new approach.

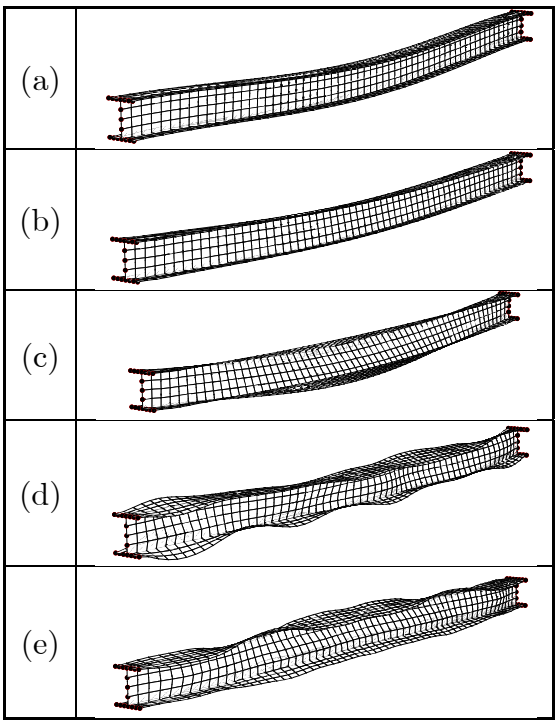

Fig. 37: Initial imperfect geometries used in analyses according to Fig. 36.
Slika 37: Prikaz začetnih nepopolnosti.

4.3.4 Thin-walled Cylinder

Among all thin-walled structures axisymetric structures (e.g. spheres and cylinders) prove to have the highest imperfection sensitivity. Several papers deal with the problem of finding the initial imperfection connected to the lowest ultimate load of cylindrical structures (Schmidt 2000, Schneider 2006, Schneider, Brede 2005, Schneider, et al. 2005, Schranz, et al. 2006, Song, et al. 2004). In the early stages of imperfection studies on cylinders, the analogy to column and plate buckling was considered appropriate and therefore the imperfection affine to the lowest eigenmode was taken as the worst initial imperfection. Recent studies dealing with the direct determination of the worst initial imperfections suggest that single dimple imperfections may be worse than eigenmode-affine patterns covering the whole structure (Wunderlich, Albertin 2000, 2002).

In the present example an axially compressed cylinder is studied Fig. 38. The cylinder is fully rigidly supported at z=0 and free at z=H.

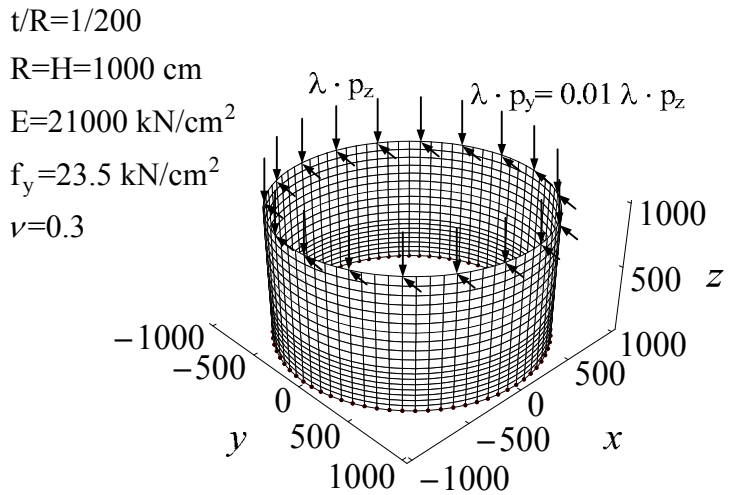

Fig. 38: Geometry of the axially and transversely loaded cylinder.
Slika 38: Geometrija osno in prečno obremenjenega cilindra.

After the convergence study, the shape base was chosen that consists of 68 shapes including 59 eigenvectors ($\mathbf{\Gamma}^B$) of the elastic tangent matrix $\mathbf{K}_0$, 7 buckling modes ($\mathbf{\Gamma}^A$) and 2 deformation shapes ($\mathbf{\Gamma}^D$) corresponding to the elastic deformed state and the plastic ultimate state. Technical standards (EN 1993 1-6 2006) prescribe the maximal amplitudes for the equivalent geometrical imperfections for cylindrical structures. In the present example the maximal amplitude of the equivalent geometrical imperfections perpendicular to the cylinder wall was taken as $e_0 = 1.22\,\mathrm{t}$ as for class A fabrication tolerance quality.

In order for the constraints to remain linear and to preserve the possibility of using linear optimization methods the projection of the imperfection vector $\overline{\mathbf{X}}^n = \left\{ \overline{X}_x^n, \overline{X}_y^n, \overline{X}_z^n \right\}$ in the n-th node in the radial direction was chosen to be bounded. The resulting optimization problem includes 2888 linear constrained equations of the form $\left| \overline{\mathbf{X}}^n . \mathbf{r}^n \right| \le e_0$, where $\mathbf{r}^n$ stands for a unit vector in radial direction. Additionally, the z component of the nodal imperfection was constrained by 2888 linear constrained equations of the form $\left| \overline{X}_z^n \right| < \frac{e_0}{10} = 0.12\,\mathrm{t}$. In this way each node of the perfect mesh can move to its imperfect location by $1.22\,\mathrm{t}$ in radial direction of the x-y plane and by $0.12\,\mathrm{t}$ in z direction. The optimization problem was solved using linear programming with an advanced interior point algorithm. Imposing constrain equations directly in radial direction would result in a nonlinear optimization problem that would be difficult to solve.

In Fig. 39 the most unfavorable initial imperfection calculated considering 68 base shapes for the cylindrical structure is presented. The load-displacement curve for the point at coordinates (0,-R,H) is plotted in Fig. 40. The corresponding deformation state at limit load is illustrated in Fig. 41. Further on, a fold line for the calculated most unfavorable imperfection shape was computed and is presented in Fig. 42.

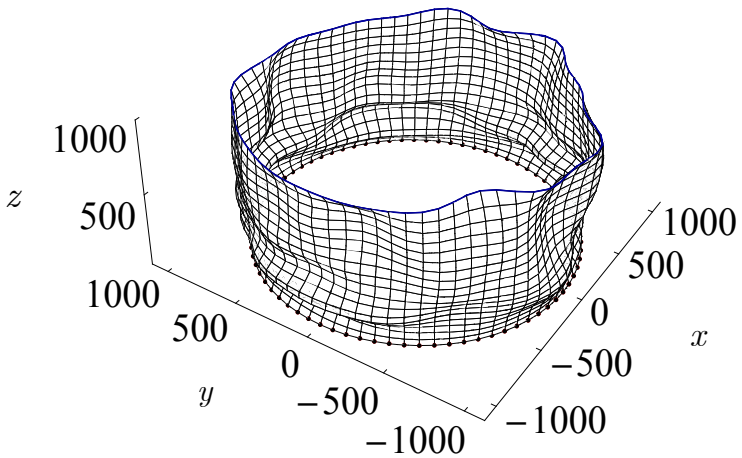

Fig. 39: Most unfavorable initial imperfection for axially and transversely loaded cylinder considering the imperfection amplitude R/165. Scale factor f_s=10.

Slika 39: Najbolj neugodna začetna nepopolnost pri amplitudi nepopolnosti R/165.

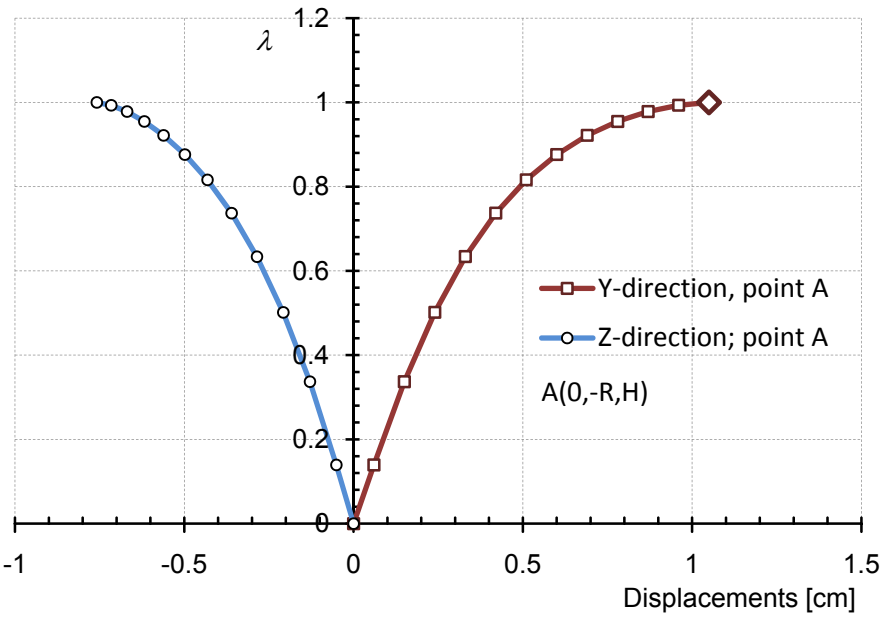

Fig. 40: Load displacement curve considering the most unfavorable initial imperfection.

Slika 40: Krivulja sila-pomik z upoštevanjem izračunane najbolj neugodne začetne nepopolnosti.

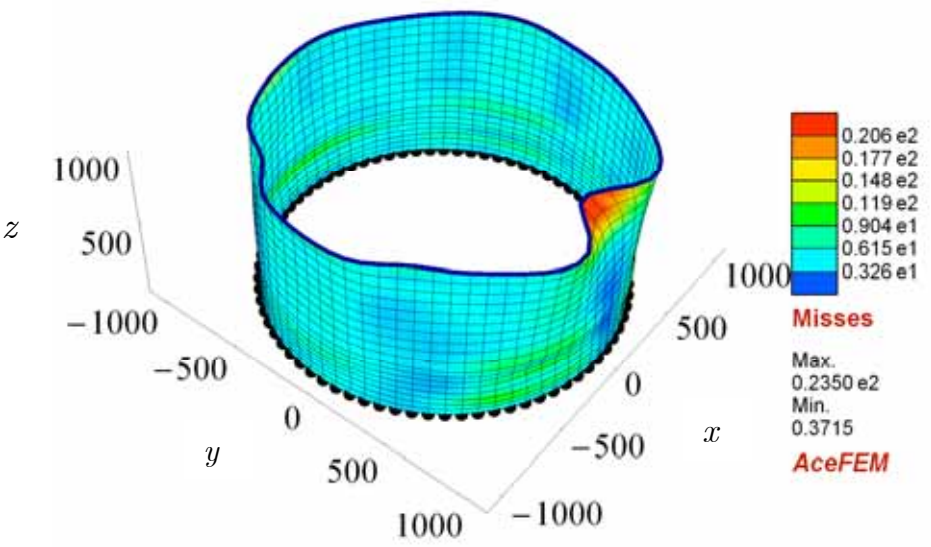

Fig. 41: Deformation state at limit load.

Slika 41: Deformacijsko stanje v mejnem stanju.

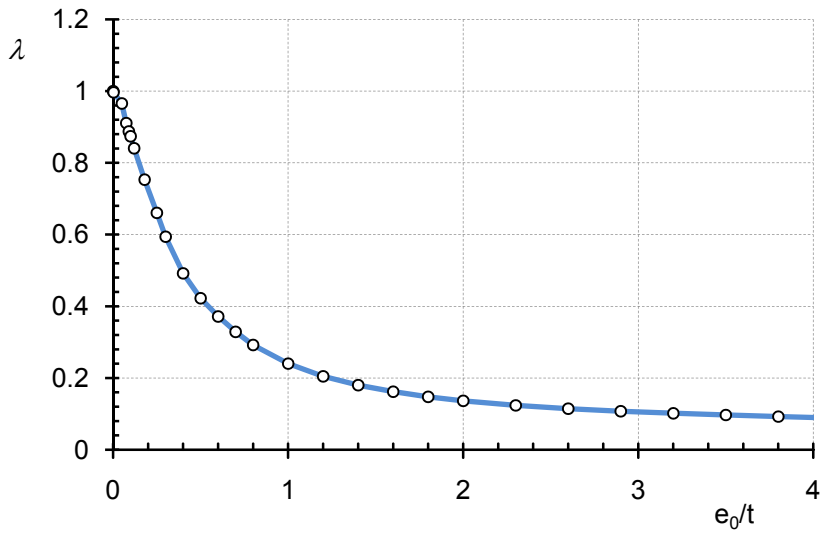

Fig. 42: Fold line of the axially and transversely loaded cylinder.

Slika 42: Nosilnost v odvisnosti od amplitude začetne nepopolnosti osno in prečno obremenjenega cilindra.

4.4 Partial conclusions

An effective method for evaluating the most unfavorable imperfection is presented. Despite intensive research of theoretical, experimental and numerical aspects of stability limit of imperfection-sensible structures, there is still no consensus on how the ultimate state should be evaluated, owing to numerous difficulties which arise. According to the results of the presented approach, it is difficult to characterize certain structures with certain types of imperfections. Every change in thickness, geometry or loading conditions can lead to a drastic change of the worst imperfection shape.

In complex structures where intuitive determination of initial most unfavorable imperfections is not possible or where there is a lack of known empirically obtained worst imperfections, the use of a method for determining the worst initial shape is essential. Within the presented approach it is shown that with the use of geometrical and material nonlinear direct and sensitivity analysis of imperfect structure combined with optimization it is possible to directly evaluate the imperfection shape of a structure, at which the ultimate load of the structure is the smallest. Additionally, the method is not limited to the linear natural equilibrium path and small imperfections and allows introduction of various constraints on the shape of the initial imperfection.

The direct determination of the worst imperfection shape results in a highly nonlinear global optimization problem. Unfortunately, no truly effective optimization algorithm exists for the global optimization of problems where the numerical cost of the minimizing function allows only a small number of repetitions. Thus, depending on an initial guess for the worst imperfection shape, the obtained worst imperfection shape can correspond to the local minimum of the limit load rather than a global minimum. A natural choice for the initial guess is the imperfection affine to the lowest buckling mode.

In the present approach, the imperfections are represented by a linear combination of base shapes with the base constructed from the subset of buckling modes augmented by the eigenvectors of the structure subjected to “technological” boundary conditions and characteristic deformation modes. The decision to include the base shapes that are not consistent with the kinematic boundary conditions of the problems should be based on technological considerations. With the increasing number of base shapes, the discretization error of the description of the worst imperfection shape approaches the discretization error of the underlying finite element mesh. This ensures the

convergence of the method with mesh refinement and increasing number of base shapes to at least a local worst imperfection shape.

Because of the high unpredictability of the imperfection forms, the technical standards for designing thin-walled structures recommend to use empirical methods to define initial imperfections used for nonlinear analyses. The ultimate loads of structures evaluated in accordance with the method presented turned out to be smaller than the ultimate loads considering various combinations of imperfections prescribed by the technical standards or calculated with approaches based on Koiters asymptotic theory or parametric studies. It can be concluded that these methods may lead to too optimistic results. On the other hand, the probability of the real structure imperfections to take the exactly most unfavorable form is very low. However, the information about the structures lowest limit load due to initial imperfections is of high importance when analyzing structures. Usually imperfection analyses with a great number of repetitions are done to determine which combinations are unfavorable. Despite the effort it is still very hard to determine how the limit load is lowered by the gathered imperfection shapes in comparison with the most unfavorable ones. In this sense it is possible to establish that the consideration of imperfections in a geometrically and materially nonlinear analysis is a task where a holistic method for finding the worst imperfection is indispensable.

The importance of the ability to evaluate the most unfavorable equivalent geometrical imperfections as presented in the thesis is further stressed out in the next chapter where it is used to optimize the shape of the structure in such a way that it has a minimum volume considering all optimization constraints and in the same time it is optimized to be at least sensible to initial imperfections. This represents a convenient way to properly optimize the shape of imperfection sensible structures.

5 Limit load design Shape Optimization

In the present chapter a limit load shape optimization method will be presented using an analytical sensitivity analysis introduced in Chapter 3 with consideration of the most unfavorable initial imperfections presented in Chapter 4.

5.1 Introduction

The purpose of structural design problems is to find the best design among all possible candidates. For this reason, the design engineer has to specify both the candidates and the best design. To satisfy the problem constraints, the candidates have to exist in a feasible region, where all candidates are acceptable. The most appropriate design is usually the one that minimizes or maximizes different objective functions, such as for example weight, cost, deformation energy, frequency response, manufacturing or other technical requirements. In engineering design the mechanical laws are applied to determine the structural response while the loads, geometry and boundary conditions are given. When it comes to optimization design, the process has to be reversed and the load, material, topology or shape, etc. have to be determined for the required structural response.

Basically, structural optimization can be divided into material optimization (MO), shape optimization (SO) and topology optimization (TO), depending on what is varied in the optimization process. This includes configuration and size optimization for discreet modeled structures. For the best results different approaches can be combined. An effective way is to combine topology optimization (determination of material distribution) and shape optimization (determination of the boundary shape). While TO is mostly used to define the general geometrical layout, SO can be used to additionally define the boundaries, as TO is mostly applied on a very coarse discretization mesh (see e.g. Chang, Tang 2001, Schwarz, et al. 2001, Tang, Chang 2001). Additionally, it is possible to apply SO by subsequently adding holes with parameterized boundaries into the initial geometry. In this way it is possible to optimally distribute the material with exact boundaries essentially performing TO. Even though this approach is rather of subjective nature, it is very effective in practical design. The current work deals mostly with SO based on the supposition that the basic geometric layout is known or prescribed, either by manufacturing limitations, cost, aesthetic or serviceability demands.

5.2 Shape Optimization

Structural optimization approaches to shape optimization can be classified into three categories:

- Evolutionary approach
- Optimality criteria
- Mathematical programming

The basic purpose of an optimization algorithm is to minimize the objective function and to find a feasible result at minimum computational cost. Regardless the approach used, optimization is done by some sort of iteration process. Application in structural engineering FEM modeling by considering geometrically and materially nonlinear structural response including most unfavorable initial imperfections requires a fair amount of computational time in the case of larger structural systems, even for a single iteration. The approach used for nonlinear structural design optimization therefore has to include a strategy allowing minimum number of iterations used for the determination of the optimum result.

Numerous approaches have been used for nonlinear structural optimization. The use of the more sophisticated "smart" mathematical programming approaches requires computation of sensitivities needed for the mathematical treatment of the optimization problem. For the success of the optimization algorithm the sensitivities have to be evaluated exactly as described in Chapter 3. While this is a computationally demanding task, many other methods belonging to all three categories of optimization approaches have been developed in order to avoid the evaluation of sensitivity information.

5.2.1 Evolutionary and Optimality Criteria approaches

The category of evolutionary approaches covers many different heuristic approaches which take their inspiration from nature, such as Genetic Algorithms and Evolution Strategies. Modern approaches in this field include Swarm Optimization such as Particle Swarm Optimization and Ant colony optimization. Based on Darwin's evolutional theory and the principle of the survival of the fittest all these approaches have one thing in common: the stochastic search of the optimum result is improved by strategies comparable to optimal processes discovered in nature. These methods and other stochastic methods, like Simulated Annealing, will find a good solution with high probability, but very little can be said about the mathematical properties of the solution. It is not guaranteed to even be a local optimum. Although far better

than calculating all the possible candidates and finding the optimum solution among all possible results, the number of iterations needed exceeds the reasonable amount of iterations for nonlinear structural optimization of full size engineering structures. One of the advances of evolutionary approaches is the relatively simple implementation of parallel computing, as several independent analyses have to be run in a single iteration. For small order problems, such as sizing or small order shape and topology optimization, successful evolutionary approaches have been used (see e.g. Cappello, Mancuso 2003, Che, Tang 2008, Garcia, Gonzalez 2004, Li, et al. 1999, Li, et al. 2005, Rong, et al. 2007, Ryu, Lee 2007).

The second major category of structural optimization is covered by the Optimality Criteria (OC) approaches, e.g. Fully Stressed Design or Karush-Kuhn-Tucker OC method. The idea is to formulate an optimality criterion which has to be fulfilled by a feasible solution. The optimal solution is considered to be found, when the optimality criterion is fulfilled. When designing an OC-algorithm, an optimality criterion and a redesign formula for the update of variables has to be defined. These methods are not generally applicable and are mathematically unreliable, although they allow very fast convergence for suited problems. Some successful application to specific structural optimization problems can be found in references (Meske, et al. 2006, Steven, et al. 2002).

It can be concluded that geometrically and materially nonlinear structural limit load shape optimization of real world structures requires a mathematical programming method which is capable to determine the optimum result in the least possible number of iterations. Accurate sensitivity information to shape parameters is of crucial importance for achieving convergence within the lowest possible computational cost.

5.2.2 Mathematical programming

An optimization problem solved with principles of mathematics is called a mathematical program. Mathematical programming covers a large, growing spectrum of algorithms and methods for optimization purposes. Structural optimization problems have three main difficulties in common which makes them hard to solve. Typical structural optimization problems are nonlinear, constrained and the relevant constraints are not known in advance. In principle every nonlinear optimization algorithm tries to converge to the optimal solution iteratively with some sort of prediction where to move next and how far. While heuristic approaches, such as genetic, evolutionary, simulated annealing, particle swarm or a simple stohastic minimum search of trial solutions do, not use prediction information, the strength of

sophisticated mathematical programming approaches is the use of direction prediction. The only drawback is the unfavorable possibility of finding a local minimum only when there is lack of a good starting point. Some hybrid approaches can overcome this difficulty by combining heuristics with mathematical programming with a good possibility to find the global optimum. On the other hand, these approaches again induce the need of greater number of iterations and more computations of direct and sensitivity analysis and consequently more computational time requirement. The many available algorithms differ according to the way how the prediction is used and how it is calculated. Basically, they can be distinguished according to the problem they solve and according to the types of data do they use. The problems can be divided in constrained and unconstrained problems and the data they use can be either the function values only (direct methods), or additionally first order information (gradient methods), or additionally second order information (Newton type methods).

Most of the strategies for constrained problems use the methods for solving unconstrained problems by subdividing the constrained problems into more unconstrained sub problems. Therefore, also methods for solving unconstrained problems are frequently used in structural optimization. Optimization is a fast growing field of scientific research. Numerous strategies and methods have been developed. For a greater preview the following references can be used (Arora 2004, Bonnans, et al. 2006, Choi, Kim 2005a, Choi, Kim 2005b, Nocedal, Wright 2006). In the following section a brief preview will be given regarding possible approaches to structural shape optimization. Specific algorithms used in numerical examples will be addressed within each example.

5.2.2.1 Strategies for solving constrained optimization problems

A basic constrained optimization problem can be defined as:

$$\begin{aligned} &\text{minimize} && f(\phi, \overline{\mathbf{a}}(\phi), \mathbf{b}(\mathbf{a}(\phi))) \\ &\text{such that} && g_i(\phi, \overline{\mathbf{a}}(\phi), \mathbf{b}(\mathbf{a}(\phi))) = 0; && i = 1,..n \\ & && h_j(\phi, \overline{\mathbf{a}}(\phi), \mathbf{b}(\mathbf{a}(\phi))) \leq 0; && j = 1,..m \end{aligned} \tag{23}$$

where f is the objective function to be minimized, ϕ are the design variables, $\overline{\mathbf{a}} = \{\mathbf{a}, \lambda\}$, $\mathbf{a}$ the generalized displacements, λ the limit load factor, $\mathbf{b}$ the state variables, g_i are the equality constraints and h_j the inequality constraints.

Mathematical programming strategies for constrained structural optimization can be divided with respect to the way of how the variables are defined. If N is the number

of unknowns (parameters) and M is the number of constraints, the strategies can be divided according to the space they are working in:

- Primal methods N – dimensional
- Dual methods N,M – dimensional
- Penalty and barrier methods N – dimensional
- Lagrange methods $N+M$ – dimensional

Primal methods are the simplest and work directly in the N-dimensional space of the optimization variables ϕ. No use of Lagrange multipliers or of the KTT necessary conditions is reacquired here. Direct search methods, evolutionary strategies and genetic algorithms belong to this group. They are preferably useful to handle discrete variables. Successful primal methods which make use of gradient information are known as general reduced gradient methods or methods of feasible directions.

Penalty and Barrier function methods are working also in the N-dimensional space of the optimization variables. Here, the constrained problem is transformed into an unconstrained here by using penalty and barrier functions. The approach is in principle simple and quite robust. An old methodology is known as sequential unconstrained minimization technique, which generates a series of unconstrained sub-problems to finally get a solution near the optimum. However, the exact optimum can not be reached. For this reason the method became unpopular. Recently the basic idea of using barrier functions has been incorporated into successful interior point methods which generate iterates that stay away from the boundary of the feasible region defined by the inequality constraints. As the solution of the nonlinear program is approached, the barrier effects are weakened to permit an increasingly accurate estimate of the solution. Interior-point methods have proved to be as successful for nonlinear optimization as for linear programming, and together with active-set SQP methods they are currently considered the most powerful algorithms for large-scale nonlinear programming. Some of the key ideas, such as primal-dual steps, are carried over directly from the linear programming case.

Dual methods are working primarily in the dual M-dimensional space of Lagrange multipliers l. The primal optimization variables are determined by back substitution. Dual methods split the original optimization problem into two partial problems which have to be solved sequentially. One is unconstrained and formulated in terms of design variables ϕ, the other is formulated in terms of Lagrange multipliers l and is only constrained by simple bounds for the case of inequality constraints. It is unbounded in the case of equality constraints. Methods for unconstrained

optimization can be successfully applied because of the simple structure of the sub-problems.

Lagrange methods are working in the full (N+M) dimensional space of primal and dual variables. They make use of the Kuhn-Tucker necessary conditions directly by solving a sequence of linearized sub-problems with a quadratic objective and linear constraints. Because of the quadratic objective function these methods are called Sequential Quadratic Programming methods (SQP). SQP methods are considered to be one of the most effective methods for nonlinearly constrained optimization. They can be used both in line search and trust-region frameworks, and are appropriate for small or large problems. These methods show their strength when solving problems with significant nonlinearities in the constraints. However, they appear not to be robust enough for very large problems.

5.3 Gradient based Shape Optimization combined with imperfection analysis

The use of symbolic-numeric environment for solving a structural gradient based shape optimization problem enables one to take the great advantage of the powerful combination of symbolic capabilities and numeric efficiency provided by the environment (Korelc 2002, Korelc 2007a, b).

The procedure of shape optimization within the symbolic-numeric environment is illustrated in Fig. 43. The mechanical problem description is written on a high abstract level in symbolic form (see Section 2.4). By using automatic formulae differentiation, simultaneous optimization of expressions and theorem proving with the help of *AceGen* (Korelc 2007b), an efficient finite element code is obtained for symbolic and numeric evaluation. For symbolic finite element computations a special finite element environment is required. *AceFEM* (Korelc 2007a) is used. According to the procedures described in Chapters 3.3.1 and 3.3.2 an analytical design velocity field is computed with the help of the part of the *AceFEM* system with symbolical evaluation capability *MDriver*. The analytical design velocity field is then used for analytical sensitivity evaluation with the numeric part of *AceFEM* (*CDriver*). The derivatives of the objective function and constraints with respect to design parameters are then passed to the gradient optimization algorithm implemented in the general algebra system *Mathematica* (Wolfram 2008). As pointed out before, accurate gradient information on the basis of analytical design velocity field used in sensitivity analysis is of crucial importance for the convergence of the optimization algorithm when dealing with geometrical an material nonlinearity.

AceGen and *AceFEM* operate within the general algebra system *Mathematica* (Wolfram 2008), which is very convenient as there is no need of using a special interface for coupling with other environment optimization software. *Mathematica* offers a great variety of state of the art optimization algorithms which can be used directly with *AceFEM*'s direct and sensitivity analysis.

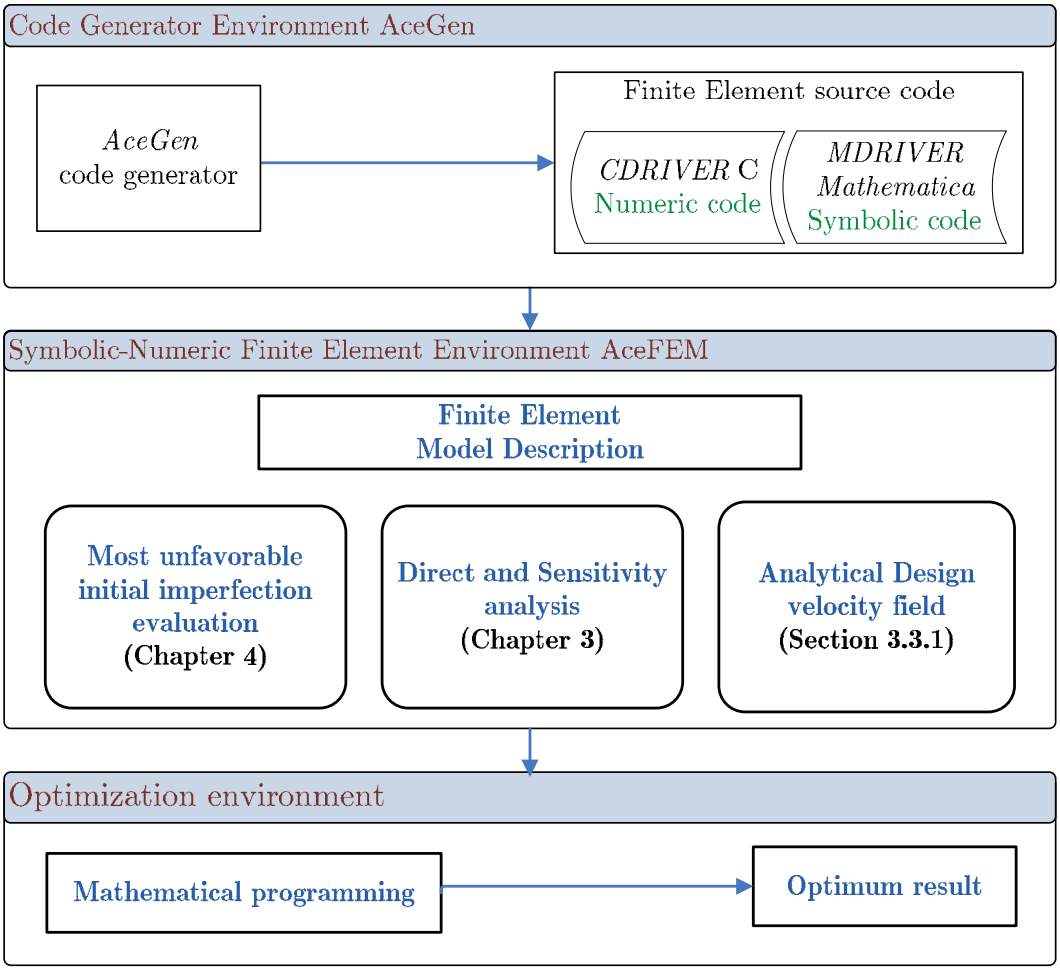

Fig. 43: Optimization using symbolic-numeric environment.
Slika 43: Optimizacija s pomočjo simbolno-numeričnega okolja.

The general flow of the method is shown in Fig. 43. In Fig. 44 the optimization loop is further explained in detail.

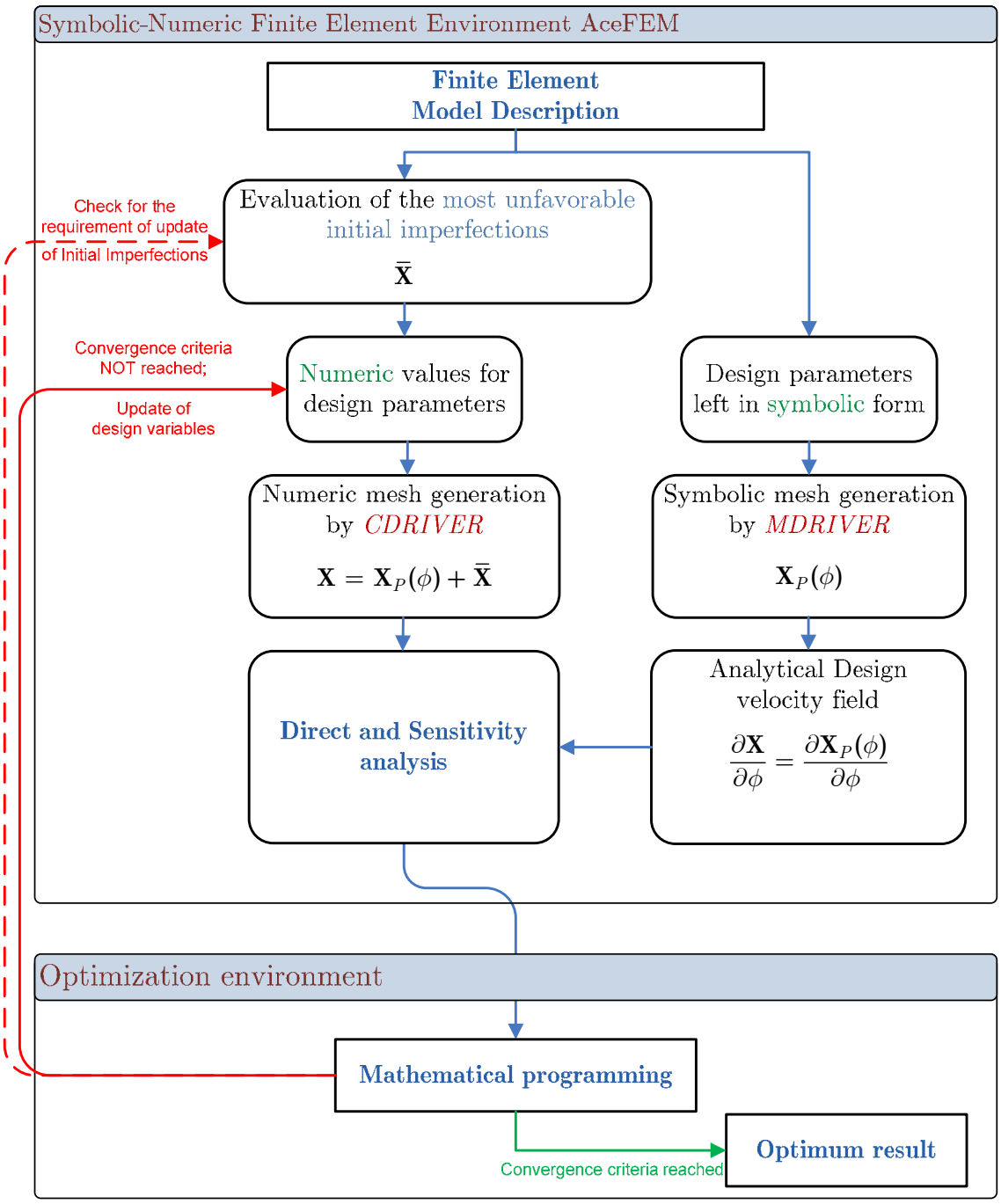

Fig. 44: Optimization loop using symbolic-numeric environment.
Slika 44: Optimizacijska zanka s pomočjo simbolno-numeričnega okolja.

Within the optimization process (see Fig. 44) the geometry of the structure is updated in two different loops. In the inner loop the geometry $\mathbf{X}(\phi)$ is changed due to the change of the design parameters done by the optimization algorithm. In the

outer loop the geometry is changed due to changed initial imperfections $\bar{\mathbf{X}}$. The method for evaluating the most unfavorable initial imperfections is presented in Fig. 24. The geometry can be written as:

$$\mathbf{X} = \mathbf{X}_P(\phi) + \bar{\mathbf{X}} \tag{24}$$

where $\mathbf{X}_P(\phi)$ is the perfect geometry ruled by the current design variables ϕ and $\bar{\mathbf{X}}$ the total imperfection vector described in Chapter 4. While the imperfections have to be considered in direct and sensitivity analysis, this is not true for the evaluation of the design velocity field:

$$\frac{\partial \mathbf{X}}{\partial \phi} = \frac{\partial \mathbf{X}_P(\phi_i) + \bar{\mathbf{X}}}{\partial \phi} = \frac{\partial \mathbf{X}_P(\phi)}{\partial \phi} \tag{25}$$

The design velocity field does not depend on the total imperfection vector nor does it change by varying the design parameters. Therefore, it has to be evaluated only once.

The most unfavorable imperfection is evaluated whenever the geometry changes to a certain extent. Together with the updated geometry the most unfavorable imperfection of the current geometry changes simultaneously. While the evaluation of the most unfavorable imperfections is a computationally demanding task, this is not done in every step of the optimization process. The initial imperfection is changed whenever the most unfavorable imperfection would cause a change in the limit load higher than a prescribed value λ_ε or would evolve in a change of the limit load state.

Conveniently, the basic shape of the most unfavorable imperfections generally does not change if minor updates of design variables are done by the optimization algorithm. Further on, the convergence of the optimization algorithm is better preserved when using the same initial imperfections and to update the initial imperfections sequentially on sets of optimal solution procedures.

The practical application of the developed algorithms is shown in numerical examples in the next chapter.

5.4 Numerical examples

5.4.1 2D cantilever shape optimization

To illustrate the limit load optimization procedure, a simple case of a 2D cantilever is studied first. The mathematical model consists of elastic-plastic finite strain, 2D, quadrilateral elements. An ideal elasto-plastic material is used. The geometry (see Fig. 45a) is parametrized with parameters ϕ which define the function of the height of the cross section along the x-axis $h(\phi)$. Constant continuous load q is applied at the top of the cantilever.

$$q = \lambda \cdot q_u \tag{26}$$

where λ is the load factor and q_u is the prescribed limit load of the structure. In order to evaluate the optimal structure shape for the limit state, the calculated limit load factor $\lambda_L(\phi)$ has to be exactly 1.

The goal is to minimize the volume of the structure:

$$\begin{gathered} \min f\,; \\ f = \mathbf{V}(\phi) \\ \lambda_L(\phi) - 1 = 0 \\ \Phi_P^k \leq 0 \end{gathered} \tag{27}$$

The constraints include a limit load factor equality constraint $\lambda_L = 1$ which forces the calculated limit load factor $\lambda_L(\phi)$ to take the prescribed value 1 at which the calculated limit load q matches the prescribed limit load of the structure q_u, and a set of inequality constraints $\Phi_P^k \leq 0$ which prescribe the minimum feasible values of parameters ϕ. The constrained problem is solved using an interior point method considering the merit function f_B:

$$f_B = w_1 \mathbf{V} + w_2 Log(\lambda_L - 1) + w_3 \sum_k \Phi_P^k \tag{28}$$

where w_i are the weights, $\mathbf{V}$ is the volume and Φ_P is barier function. The problem is solved with a standard quasi-newton algorithm using *Mathematica (Wolfram 2008)*. Fig. 45 shows the initial shape (a) and the optimal shape (b). Mises stresses are plotted. The structure with the optimal shape shows a smooth distribution of yield stress over the whole length of the structure.

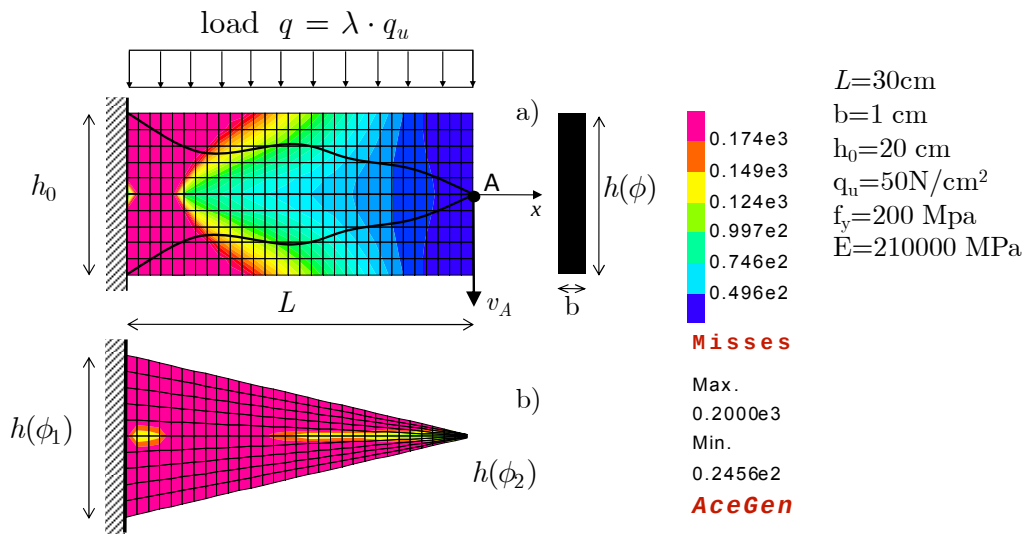

Fig. 45: Initial shape (a), Optimal shape (b).
Slika 45: Začetna oblika (a) in optimalna oblika (b).

The response load deformation curve of the structure with the optimal shape has to present a limit load curve with its maximum exactly at the given limit load $q = q_u$, where $\lambda_L = 1$. The parameters ϕ can describe an arbitrary function of the cross-section height. The simple example has been chosen as the optimum result according to the beam theory is a straight line which can be presented by only two parameters: ϕ_1 as the beginning height and ϕ_2 as the end height. The optimal shape remains the same, if the number of parameters ϕ is raised and different curves are presumed for the height function $h(\phi)$, such as splines or higher order polynomials.

The objective function f_B depending on two shape parameters can be graphically represented as a surface in three-dimensional space. Convergence of the optimization process considering shape parameters ϕ_1 and ϕ_2 is illustrated in Fig. 46. The objective function is plotted together with the points evaluated by the optimization algorithm to get to the optimum which is presented by the red point.

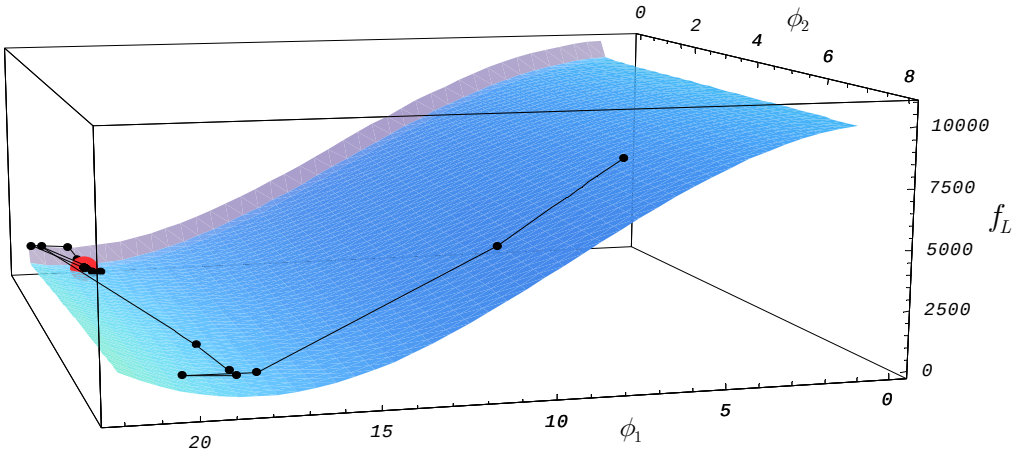

Fig. 46: Convergence of the optimization process for two shape parameters.
Slika 46: Konvergence optimizacijskega procesa za 2 parametra oblike.

In general, the responses of the structure with possible shapes tried by the optimization algorithm evolves in a different ultimate limit load factor λ_L and a different displacement v_A in every iteration as illustrated in Fig. 47. The ultimate limit load factor has to be exactly λ_L=1 at the optimum point, where the objective function has a minimum value.

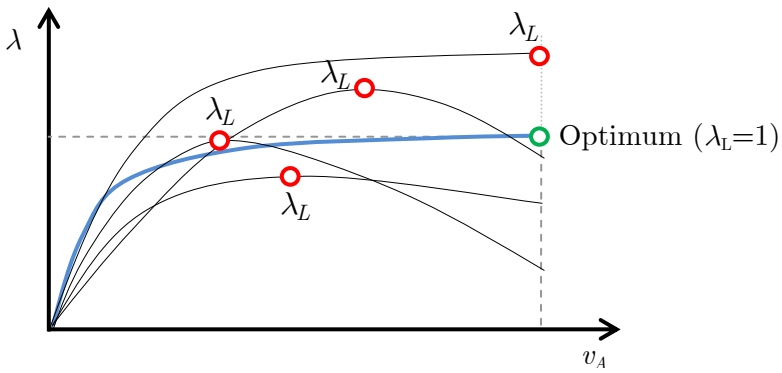

Fig. 47: Structural response of different shapes and the limit load optimal shape.
Slika 47: Odzivi konstrukcij z različnimi oblikami v primerjavi z optimalno obliko .

The optimal shape shown in Fig. 45b is expected, as it can be verified analytically. To evaluate the result analytically, it has to be assumed that the optimal shape is the one where every material point of the structure in its limit state reaches yield point. The result can be evaluated with the help of the standard beam theory:

$$\sigma_{PL}(x) = \frac{M(x)}{W_{pl}(x)} = \sigma_y \rightarrow h_{pl}(x) = \sqrt{\frac{2q}{b\sigma_y}}x \,, \tag{29}$$

where $M(x), W_{el}(x)$ in $W_{pl}(x)$ are the moment, elastic resistance moment and the plastic resistance moment at the length x measured from the free end of the cantilever, respectively. q is continuous load, b is the width and h the height of the cross section. A small difference in the numerical results $(h(\phi_1)_{num.} = 20.41$, $h(\phi_2)_{num.} = 0.29)$ with respect to the analytical results $(h(\phi_1)_{analyt.} = 21.21$, $h(\phi_2)_{analyt.} = 0)$ can be observed as the finite element mesh with the quad finite elements on the free end can not form an analytically sharp edge and there is no consideration of shear deformation in the analytical approach.

5.4.2 3D H cross-section thin-walled cantilever structure

In the present example a thin-walled cantilever structure is studied. Structures composed of thin–walled components in general prove a high degree of imperfection sensitivity. Therefore the use of imperfections in an analysis is mandatory for correct optimization results and the flow of the optimization process itself, as possible bifurcation points in the analysis are avoided and a realistic lowest limit load can be calculated.

The specific shape of the structure was chosen for representation purposes, as a variety of collapse mechanisms can be observed at the limit load. In conventional shape optimization dealing with bearing capacity of structures the shape is usually optimized for the state of the structure at the time when the first material point exceeds the elastic resistance or the first member buckles. No post-buckling or post-critical behavior is taken into account. In the present approach the collapse mechanism and the phenomena appearing at that time dictate the optimal shape of the structure. In this way, the shape of the structure is sought, which gives the maximal bearing resistance at the limit state, which is usually presented as a collapse of the structure.

Varying the thickness of shell components by excluding it from the design variables specific collapse mechanisms can be enforced. The limit state of the structure is characterized by pure plastic limit state when the sheet components are thick enough. Lowering the thickness of sheet components results in a plastic buckling limit state and further on in an elastic buckling limit state. It has to be mentioned that within conventional shape optimization only one collapse mechanism is considered at the

same time and therefore the optimal shape is not computed considering more possible collapse mechanisms.

The geometry of the studied cantilever structure is shown in Fig. 48. The thin-walled cantilever is modeled by elastic-plastic four-node shell elements based on finite rotations, 6 parameter shell theory combined with assumed natural strain formulation and two enhanced strain modes for improved performance (Wisniewski, Turska 2000, 2001). An ideal elasto-plastic material model has been used.

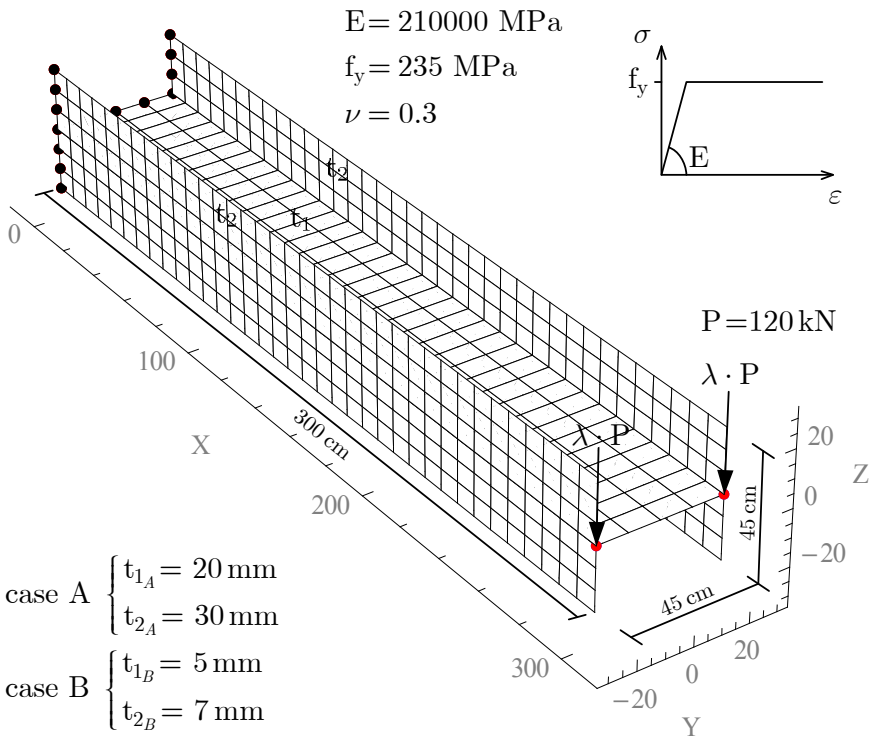

Fig. 48: Initial geometry of H cross-section cantilever.
Slika 48: Začetna geometrija H konzolnega nosilca.

Two fixed sets of wall thicknesses are considered:

- Case A: thick sheets, where plastic behavior dominates.
- Case B: thin sheets, where buckling behavior dominates.

The shape of the structure is parameterized with parameters ϕ as shown in Fig. 49. The geometry is symmetrical with respect to the XZ plane. The boundaries of the vertical sheets are varied in both Y and Z axes. The vertical sheets have to remain vertical and the horizontal sheet horizontal. The minimum dimension of both,

vertical and horizontal sheet is 10% of the initial dimension. Second order splines were chosen for interpolation of the boundary shape between the shape parameters.

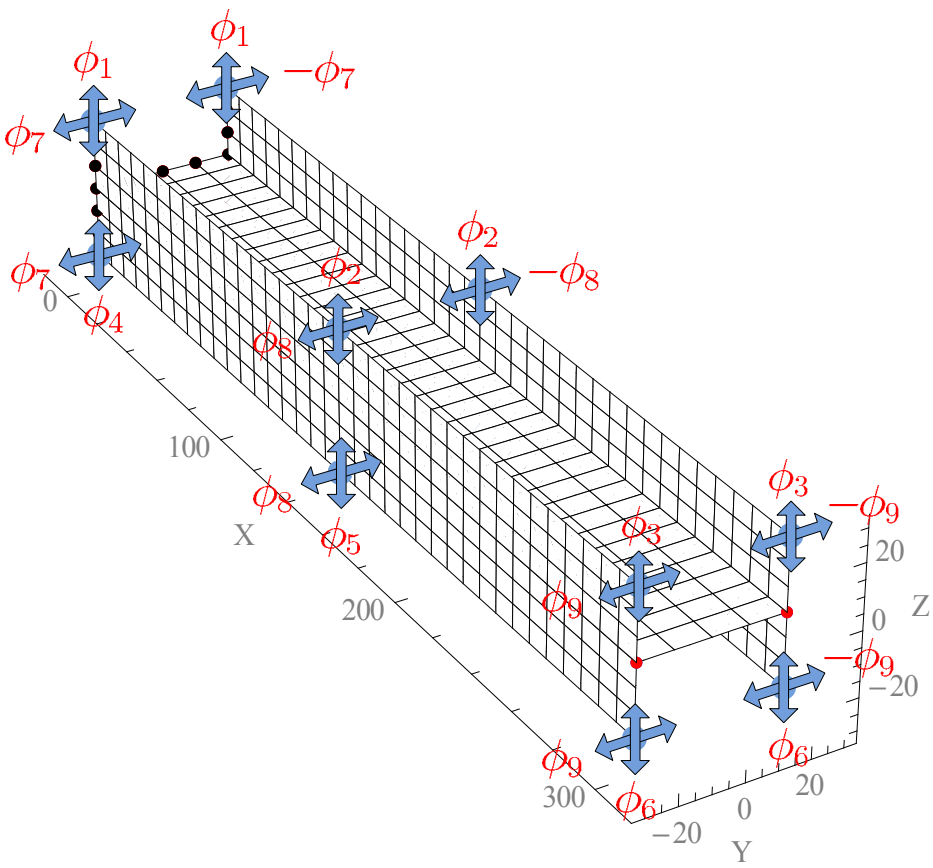

Fig. 49: H cross-section cantilever shape parameters.
Slika 49: Parametri oblike H konzolnega nosilca.

The goal is to minimize the volume of the structure:

$$\begin{aligned} &\min f\,; \\ &f = \mathbf{V}(\phi) \\ &\lambda_L(\phi) - 1 = 0 \\ &\Phi_P^k \leq 0 \end{aligned} \tag{30}$$

The constraints include a limit load factor equality constraint $\lambda_L = 1$ which forces the calculated limit load factor $\lambda_L(\phi)$ to take the prescribed value 1 at which the calculated limit load $\lambda \cdot \mathrm{P}$ matches the prescribed limit load of the structure P and a set of inequality constraints $\Phi_P^k \leq 0$ which prescribe the minimum feasible values of

parameters ϕ. The constrained problem is solved using an interior point method considering the merit function f_B :

$$f_B = w_1 \mathbf{V} + w_2 \, Log(\lambda_L - 1) + w_3 \sum_k Log(\phi^k - \phi_B^k) \tag{31}$$

where w_i are the weights, $\mathbf{V}$ is the volume, λ_L is the calculated limit load factor and ϕ_B^k the minimum value of the k-th shape parameter.

Within the optimization process the most unfavorable imperfection is evaluated according to the procedure described in Fig. 44. The shape optimization and the evaluation of the most unfavorable imperfection was done sequentially. The procedure stops when the evaluated most unfavorable imperfection does not evolve in a change of the calculated limit load factor λ_L of the optimal structure more than λ_ε, which was set to a value of 0.01. In Fig. 50 the most unfavorable imperfection shape is presented for the initial shape and the optimal shape considering case A shell thickness (thick sheets).

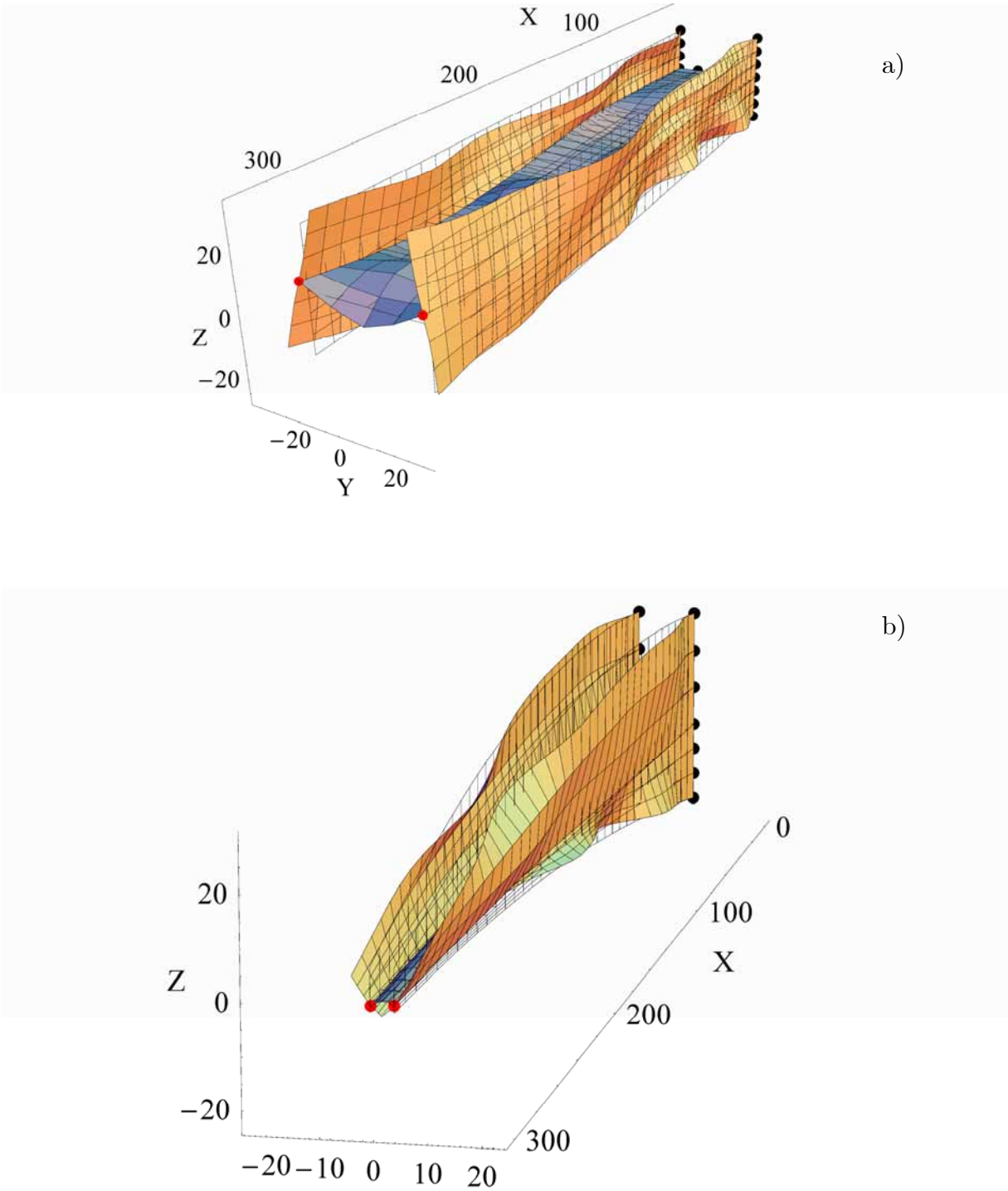

Fig. 50: The most unfavorable imperfection for the initial (a) and optimal shape (b) (Scale factor=30, Shell thickness A).

Slika 50: Najbolj neugodna začetna nepopolnost za začetno in optimalno obliko konstrukcije (Faktor povečave=30, Debelina pločevin A).

The limit load optimization iteration procedure can be observed in Fig. 51. The limit load curves are plotted for different iterates within optimization. The load-displacement curve considering the optimal shape is plotted in red. Mises stresses are plotted in the illustrations. Red color represents yield stress.

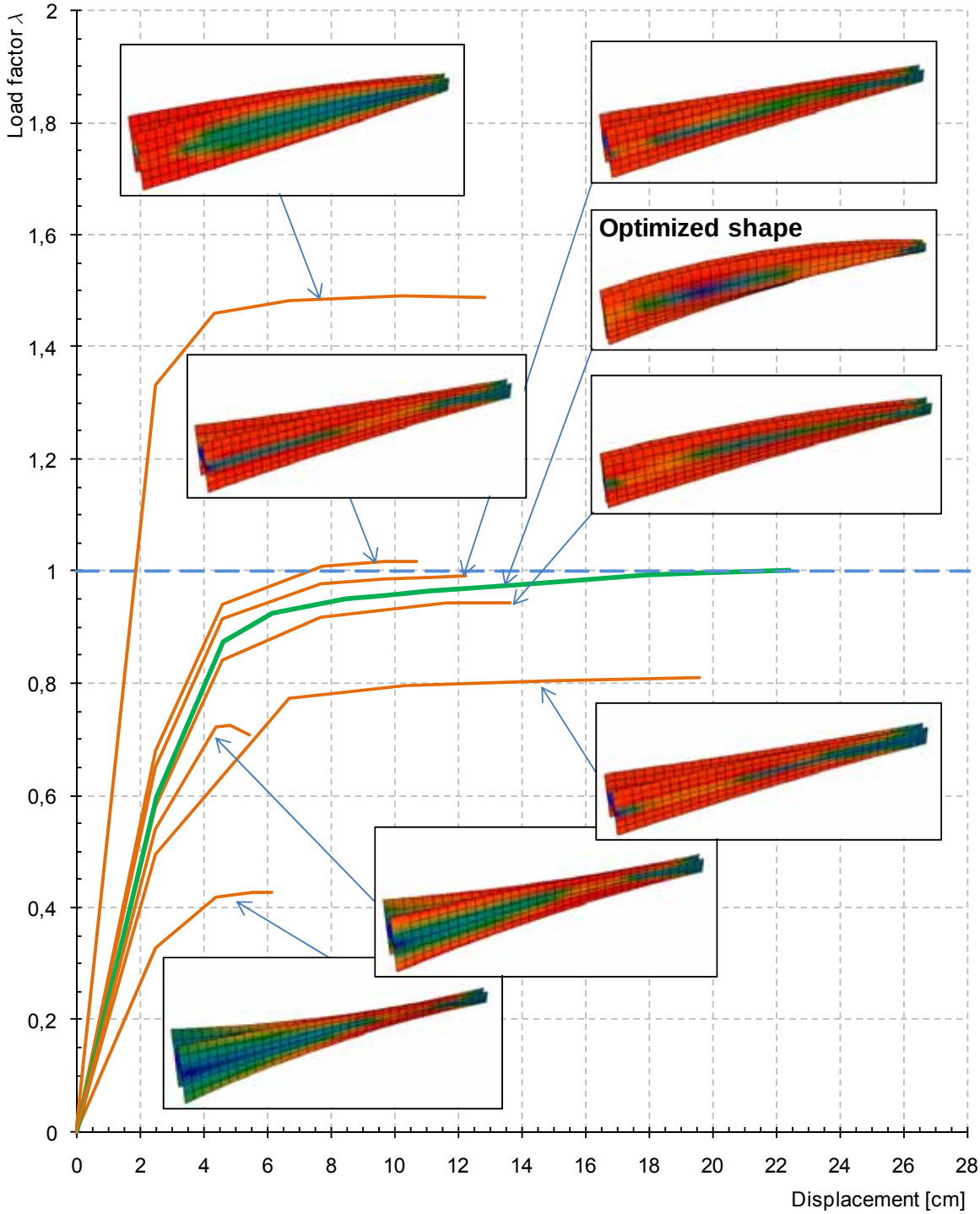

Fig. 51: Limit load shape optimization process.

Slika 51: Proces optimizacije oblike v mejnem stanju.

The evaluated optimal shape for case A shell thickness is illustrated in Fig. 52. The initial geometry at shape parameters being zero (transparent mesh) is sketched behind the optimal shape in order to illustrate the difference between the initial and optimal design.

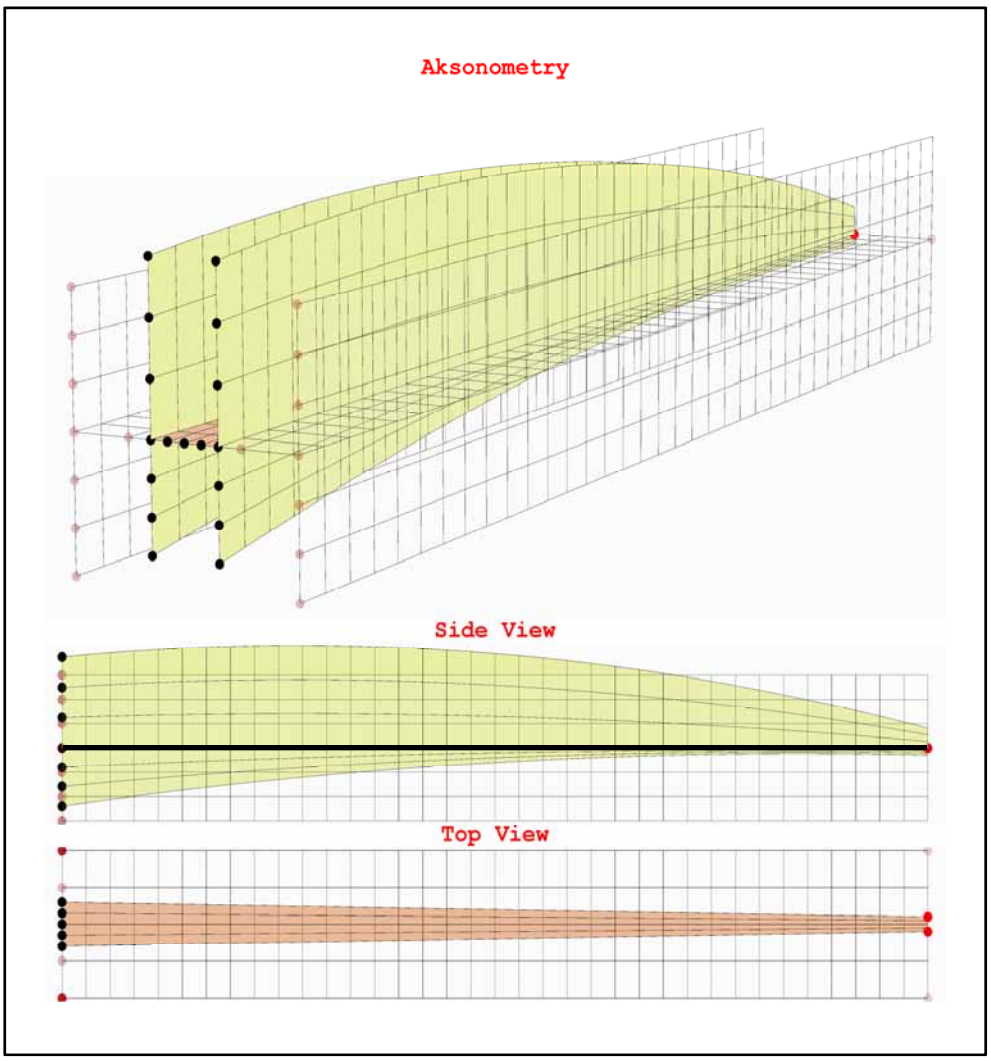

Fig. 52: Initial and optimum shape of H cross-section cantilever geometry for case A shell thickness.
Slika 52: Začetna in optimalna oblika H konzolnega nosilca za primer debeline pločevin A.

The material is not fully stressed to the yield point in the entire structure, as can be seen in Fig. 53, where Mises stresses are plotted for the optimal structure with a dense FE mesh. The explanation lies behind the way the constraints were chosen. The horizontal sheet has to remain horizontal and the vertical sheet under the horizontal sheet has a minimal height prescribed, which is at least 10% of the initial height of the vertical sheet. Using sheet thicknesses A, the sheets in compression stay compact throughout the optimization procedure and there is no risk of buckling.

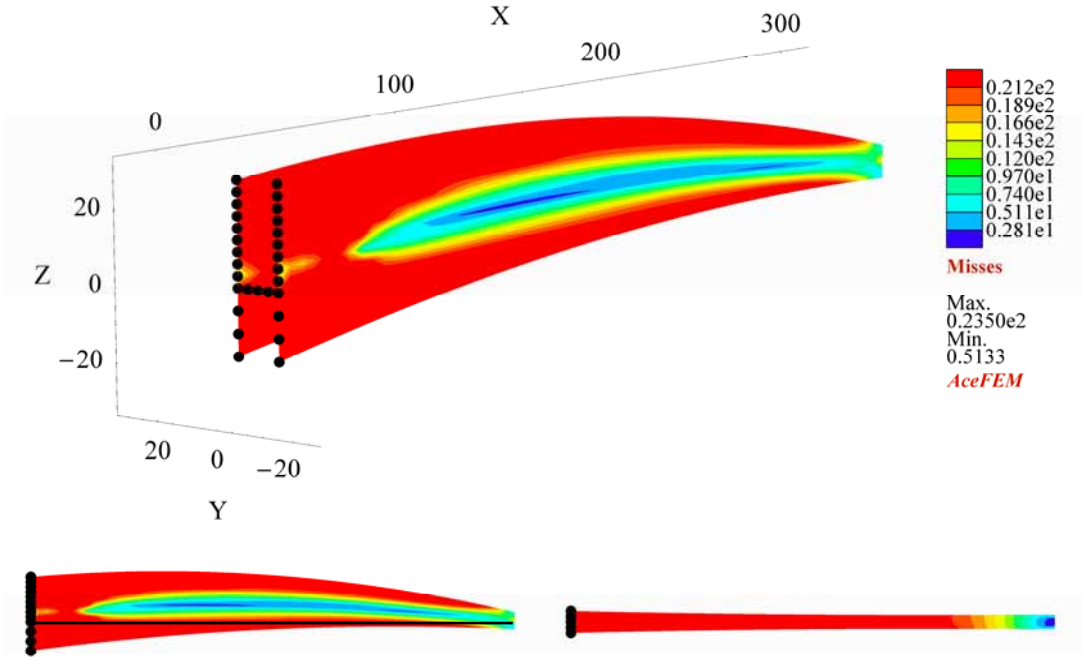

Fig. 53: Mises stress at limit state for optimal H cross-section cantilever shape (undeformed).

Slika 53: Misesove napetosti v mejnem stanju nosilnosti za H konzolnega nosilec z optimalno obliko (nedeformirana oblika).

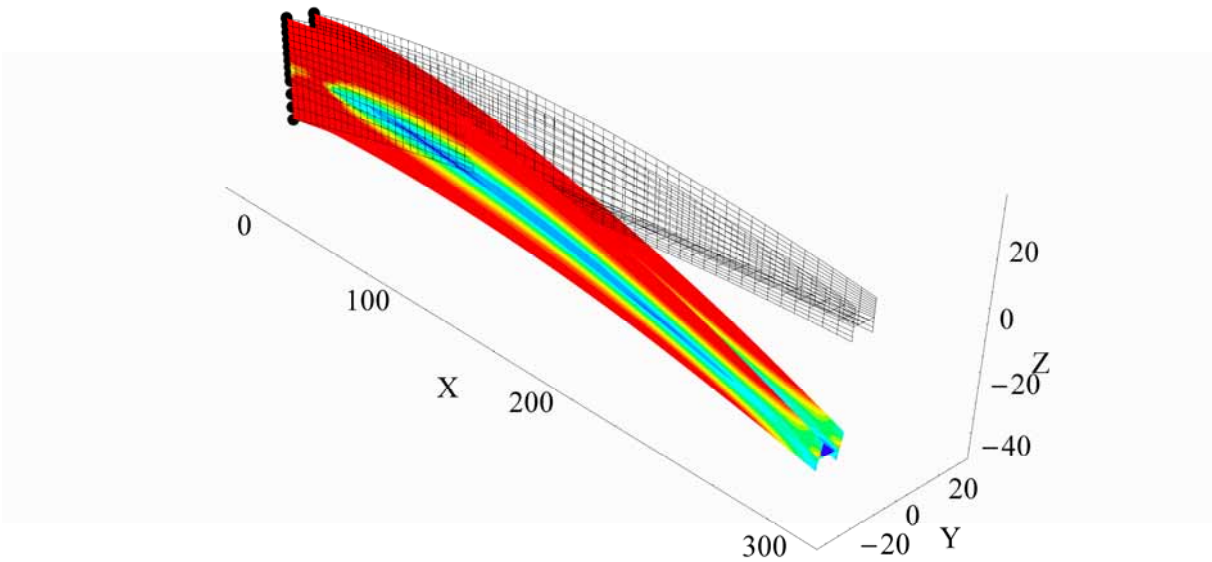

Fig. 54: Deformation of H cross-section cantilever at limit state (Scale Factor = 1) with Mises stress plotted.

Slika 54: Deformacije H konzolnega nosilca pri mejni obtežbi (Faktor povečave = 1) z vrisanimi Misesovimi napetostmi.

There is only a small amount of lateral displacements in the limit state where extensive rotation occurs. The collapse mechanism can therefore be considered as full plastification with only small amount of plastic buckling. The plastification of the material with increasing load up to the limit state is shown in Fig. 55.

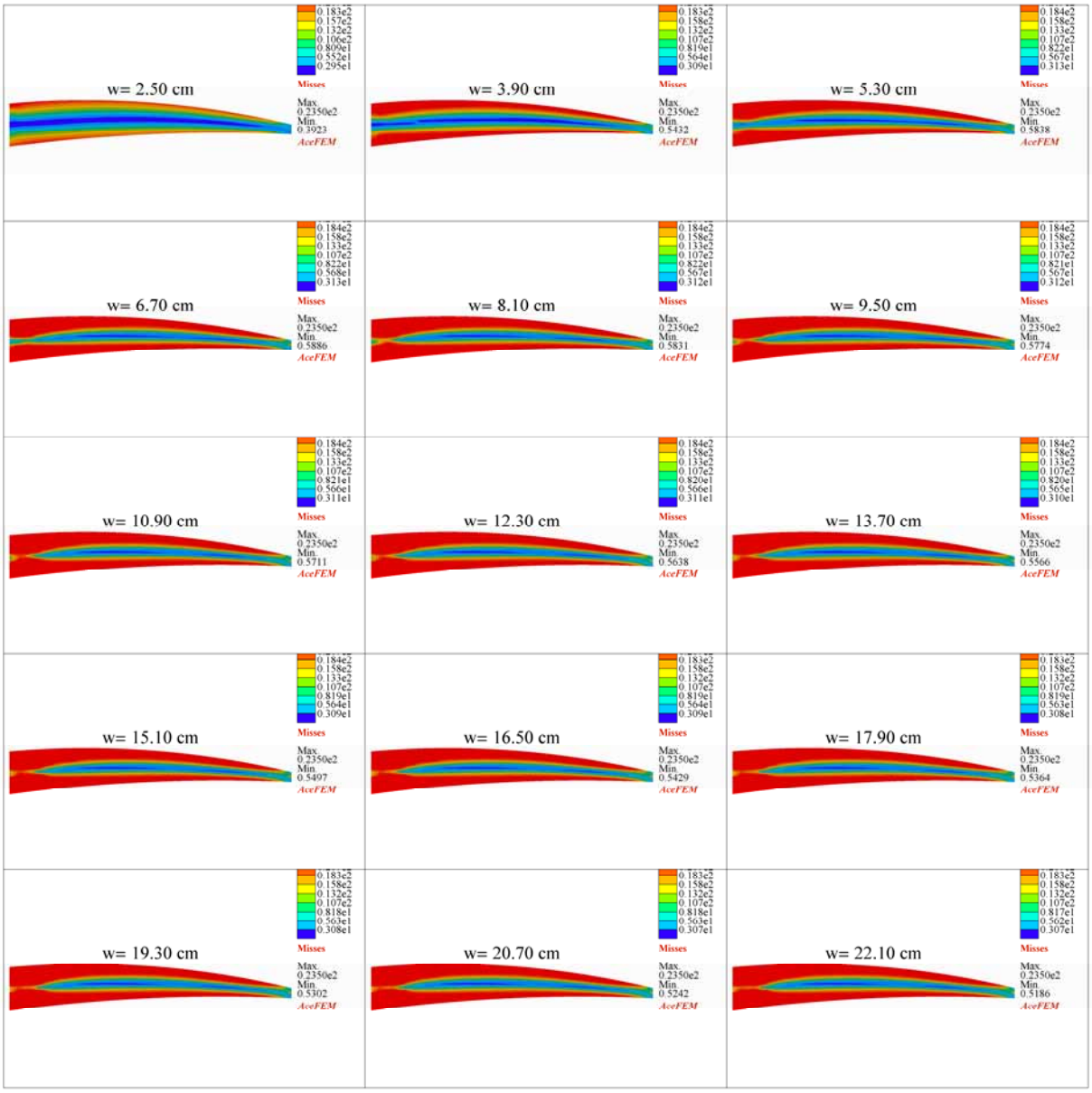

Fig. 55: Mises stress for the corresponding load-deformation curve plotted in Fig. 51.
Slika 55: Misesove napetosti za krivuljo sila-pomik prikazano na sliki 51.

Next, smaller shell thicknesses (case B) were chosen to stimulate the possibility of buckling behavior in order to additionally optimize the shape and to lower the volume of the structure. The initial imperfections calculated according to the method

explained in Chapter 4 used in the initial run and the final run of optimization are drawn in Fig. 56.

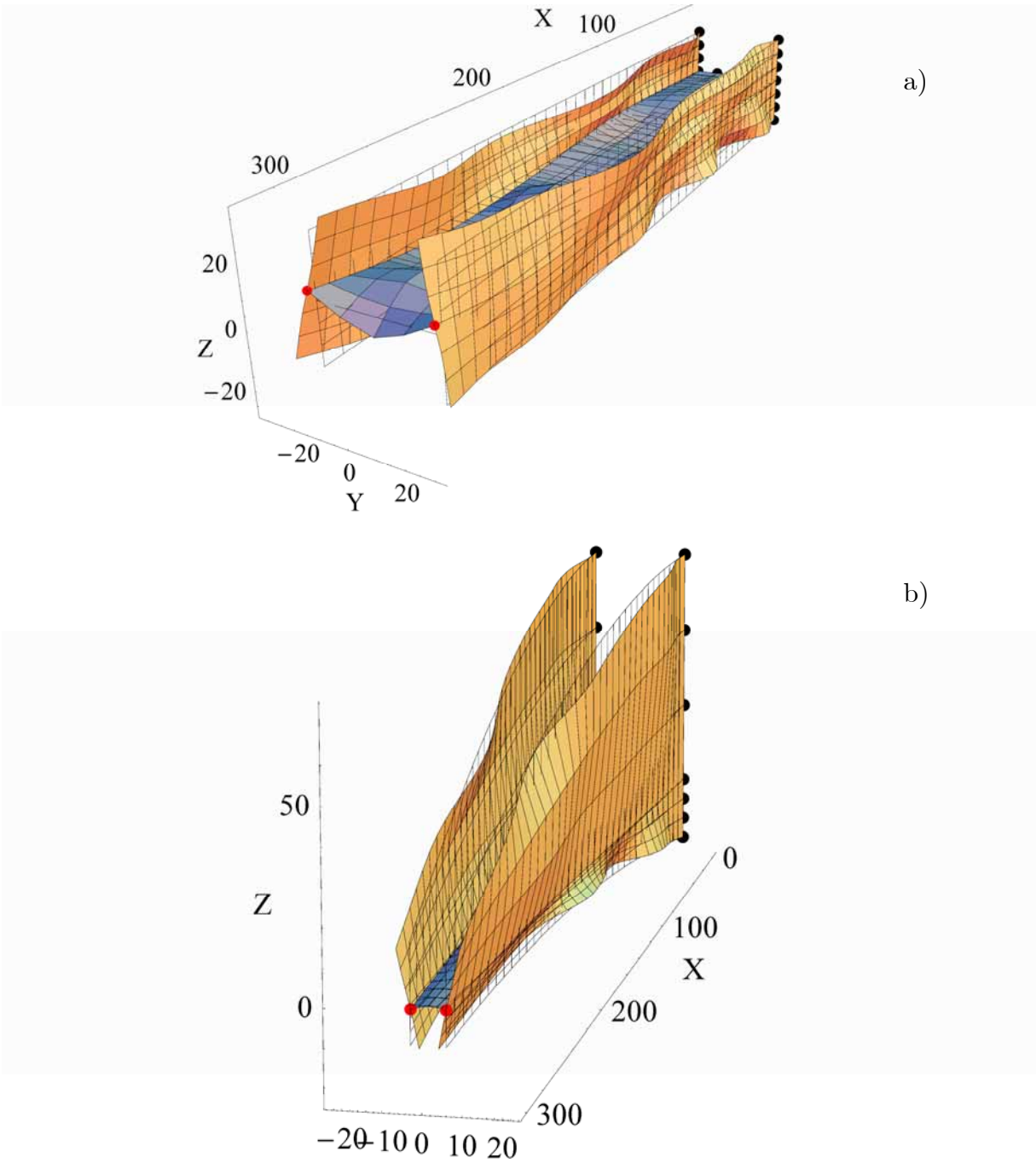

Fig. 56: The most unfavorable imperfection for the initial (a) and optimal shape (b) (Scale factor=30, Shell thickness B).

Slika 56: Najbolj neugodna začetna nepopolnost za začetno in optimalno obliko konstrukcije (Faktor povečave=30, Debelina pločevin B).

The evaluated optimal shape for shell thickness B is illustrated in Fig. 57 together with initial geometries. The limit load Mises stresses are plotted on the unreformed and deformed mesh in Fig. 58 and Fig. 59, respectively.

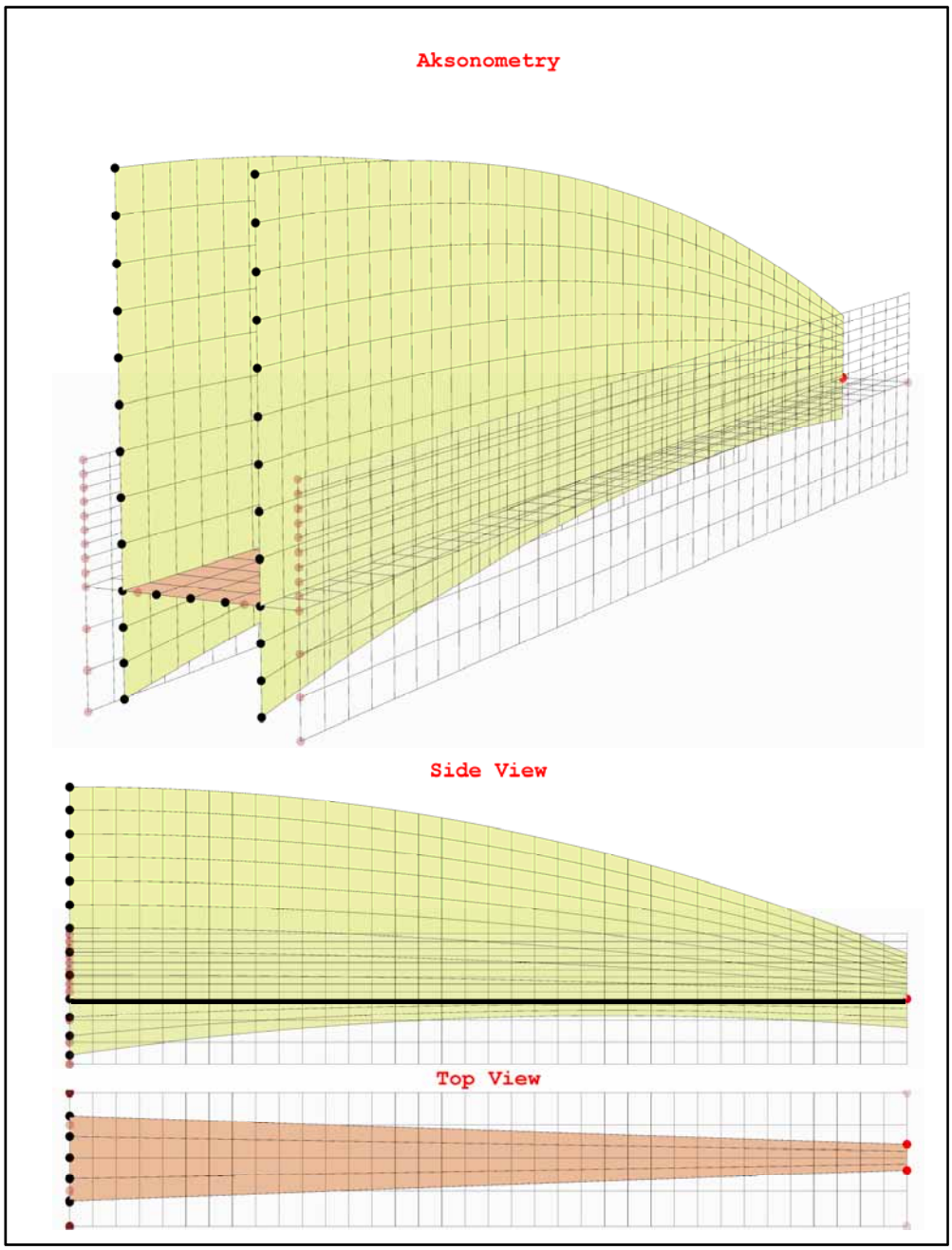

Fig. 57: Initial and optimum shape of H cross-section cantilever for case B shell thickness.
Slika 57: Začetna in optimalna oblika H konzolnega nosilca za primer debeline pločevin B.

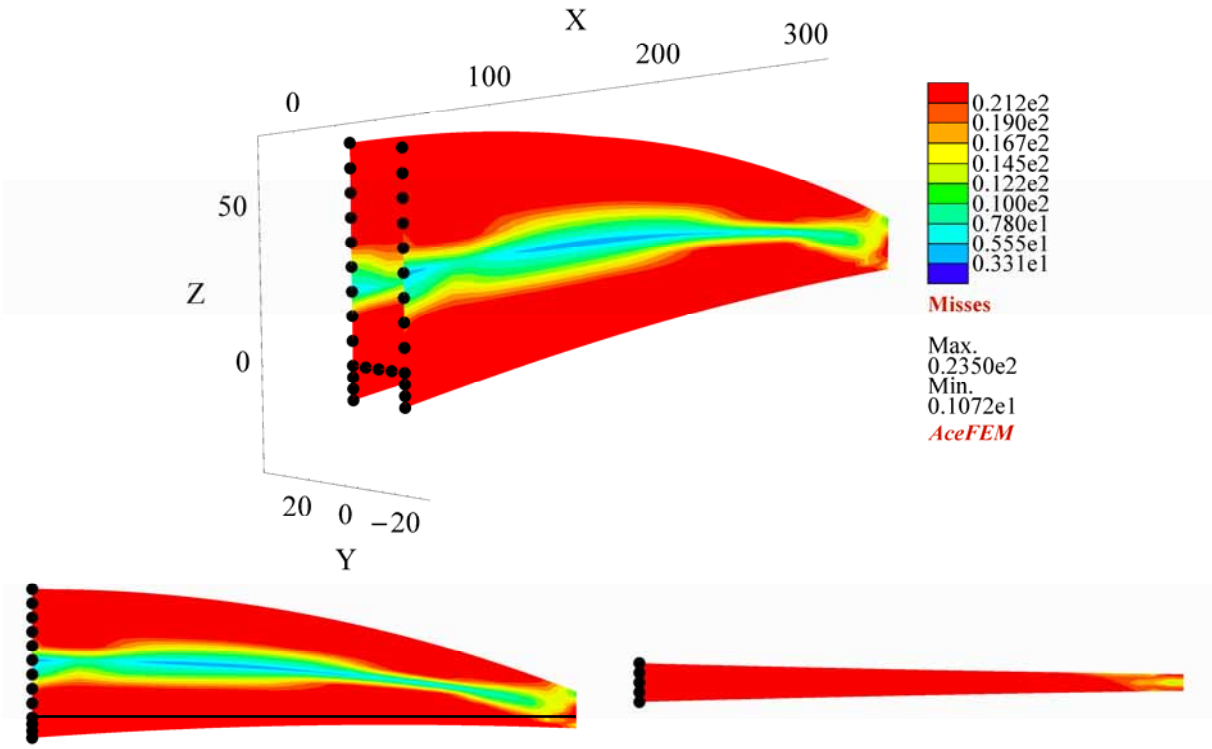

Fig. 58: Mises stress at limit state for optimal H cross-section cantilever shape (undeformed).

Slika 58: Misesove napetosti v mejnem stanju nosilnosti za H konzolnega nosilec z optimalno obliko (nedeformirana oblika).

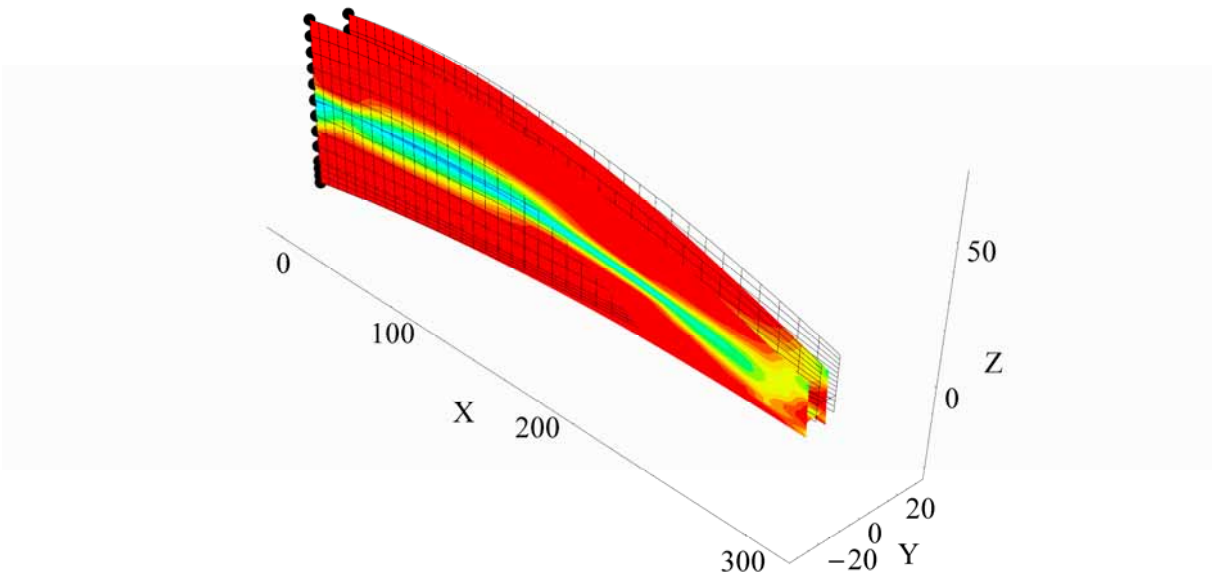

Fig. 59: Deformation of H cross-section cantilever at limit state (Scale Factor = 1) with Mises stress plotted.

Slika 59: Deformacije H konzolnega nosilca pri mejni obtežbi (Faktor povečave = 1) z izrisanimi Misesovimi napetostmi.

The plastification of the material with increasing load up to the limit state is shown in Fig. 60.

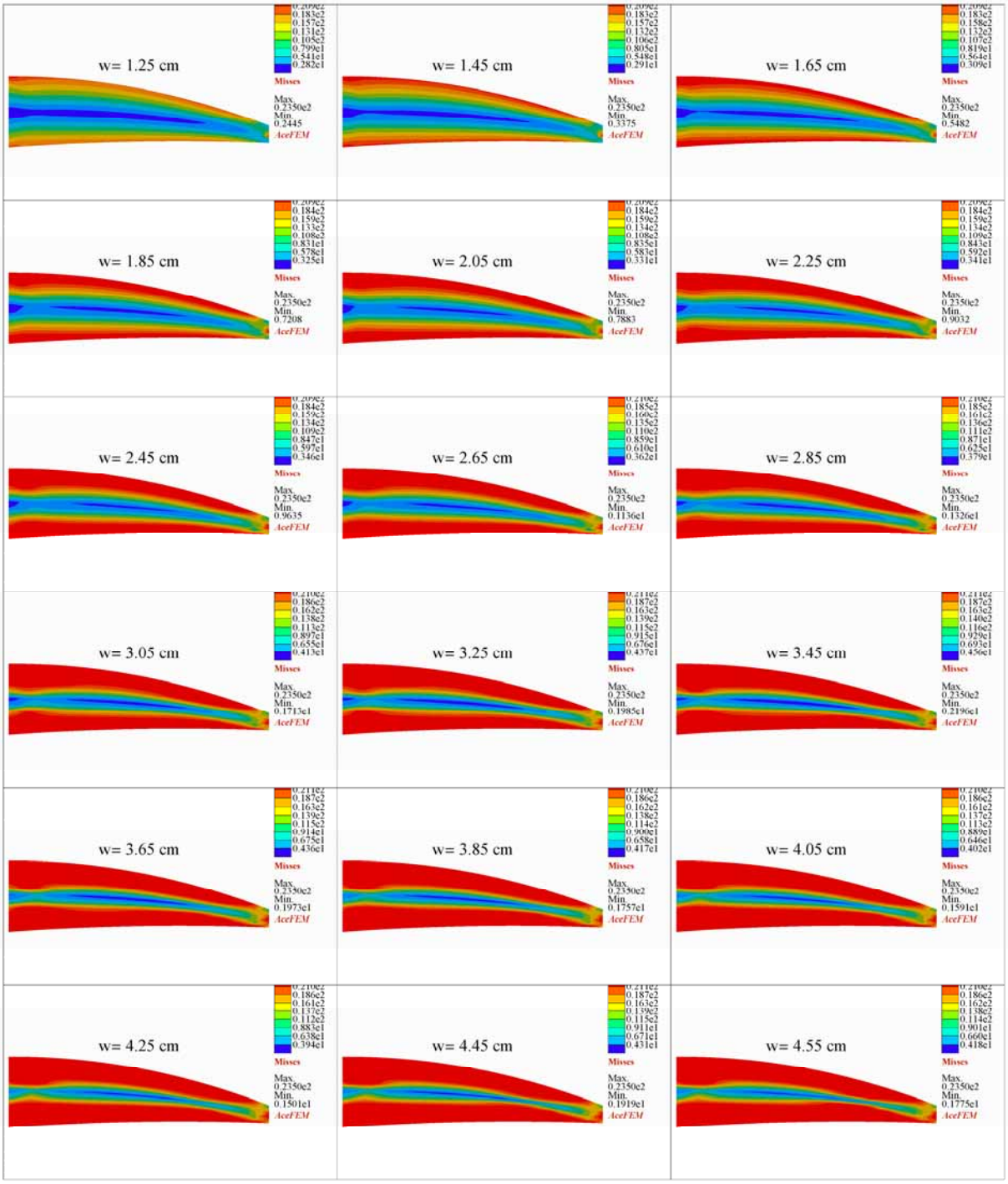

Fig. 60: Mises stress for the corresponding load-deformation curve plotted in Fig. 61.

Slika 60: Misesove napetosti za obtežno krivuljo prikazano na sliki 61.

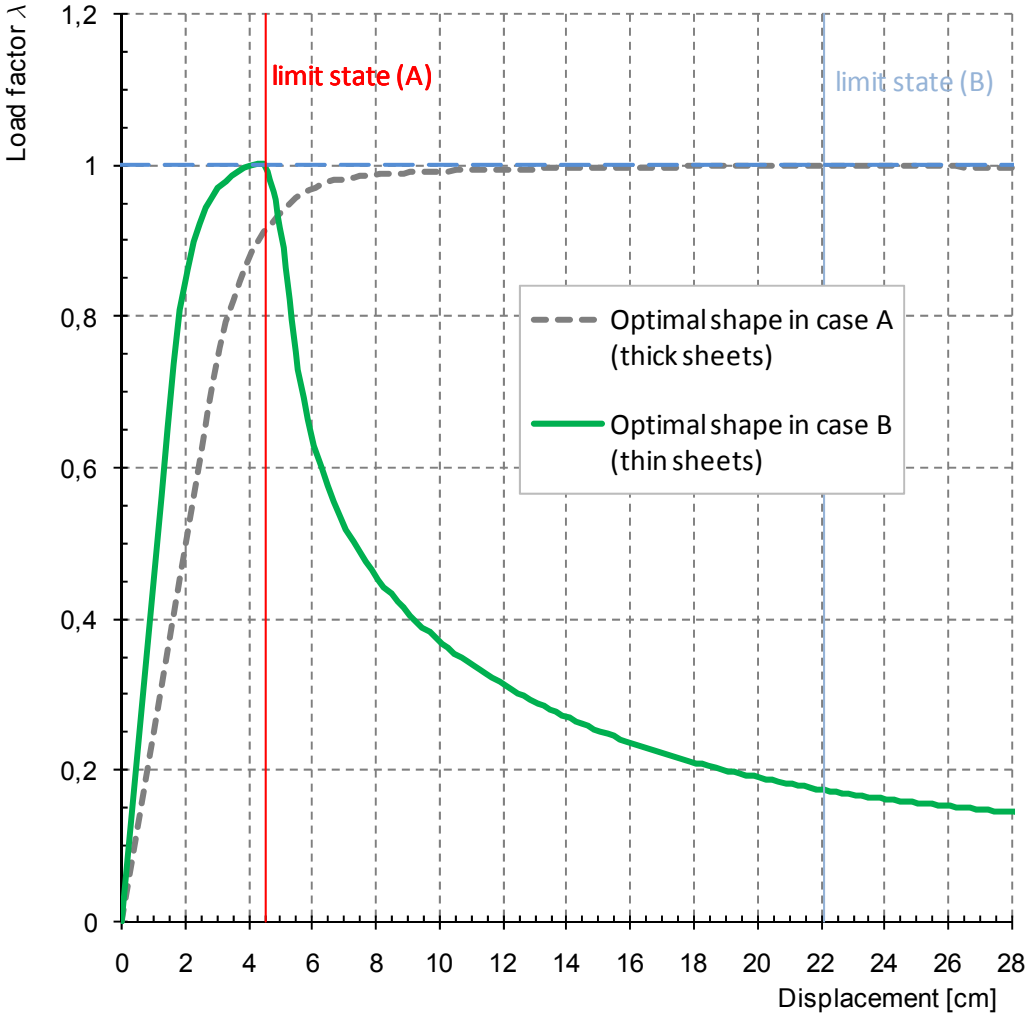

Fig. 61: Load-deformation curve for optimized shape in Case A and Case B.
Slika 61: Deformacijska krivulja za optimizirano obliko v primeru A in B.

In Fig. 61 the load-displacement curve is plotted for both studied optimal structures. In case A the limit load deformation behavior can be described as mostly plastification, while in case B plastic buckling is more pronounced during the optimization procedure. However the optimized structure has been considerably improved regarding buckling behavior of initial designs. The horizontal sheet of the optimal structure was positioned by the optimization algorithm in the most favorable way to support the vertical sheets in the compressed part which is prone to buckle.

The optimization algorithm searches for the minimum volume while the limit load must match the prescribed limit load. At the same time the most unfavorable initial imperfections are considered. This combination evolves in a search for a ductile, plastic structure behavior with a small sensitivity to buckling. The result is therefore

a robust structure with minimum weight and small sensitivity to buckling. The plastification zones are spread more widely through the structure which shows the full material usage. The whole optimization procedure can therefore be seen as an efficient tool for economical and safe design.

5.4.3 3D single storey steel building

In the present example a single storey steel building is being optimized according to the presented method. The initial shape is shown in Fig. 62. Loading conditions and the parameterization illustrated in Fig. 63 and Fig. 64 were used. The outer frames are loaded with the half load described in Fig. 63. Self weight is automatically added by the program. The structure's basic initial geometry is symmetrical according to the YZ plane. The shell parts of the structure are modeled by elastic-plastic four-node shell elements (Wisniewski, Turska 2000, 2001). The truss parts are modeled by truss elements and have the function of lateral load transmission only. The entire load is added on the frames only. The distance between frames is $e = 10$m.

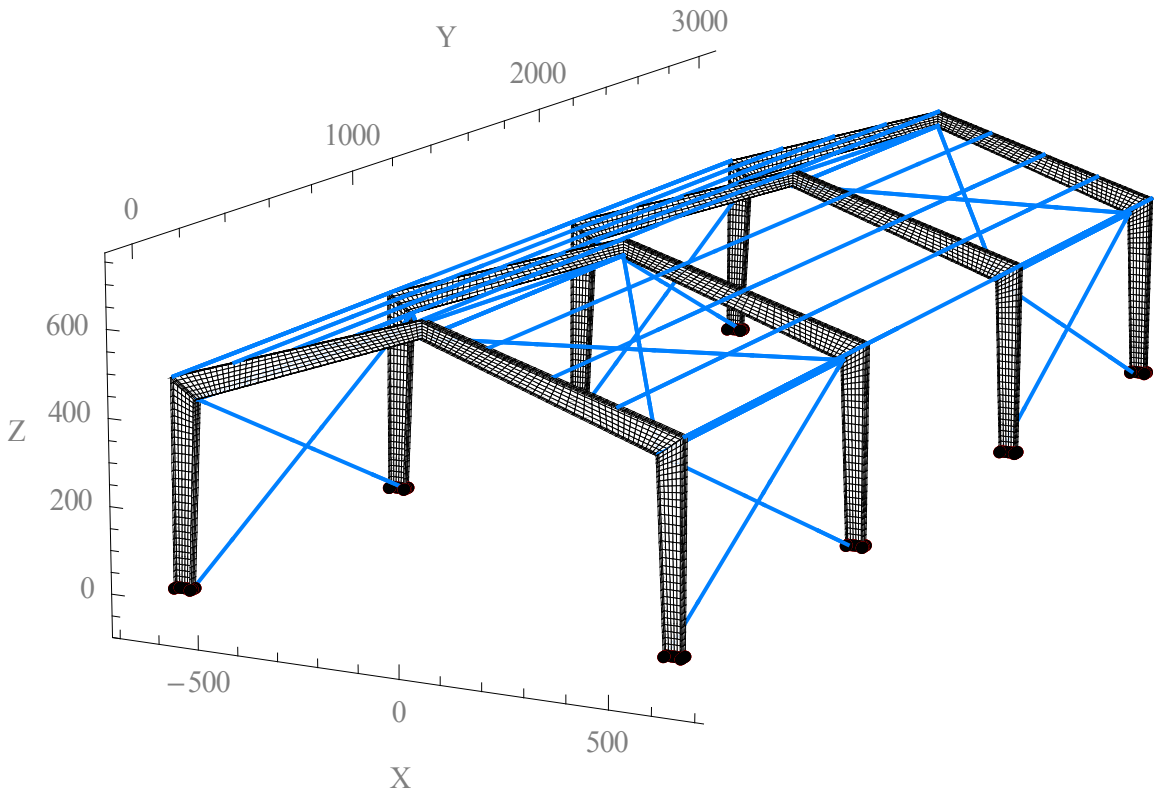

Fig. 62: Initial geometry of single storey steel building.
Slika 62: Začetna geometrija enoetažne jeklene hale.

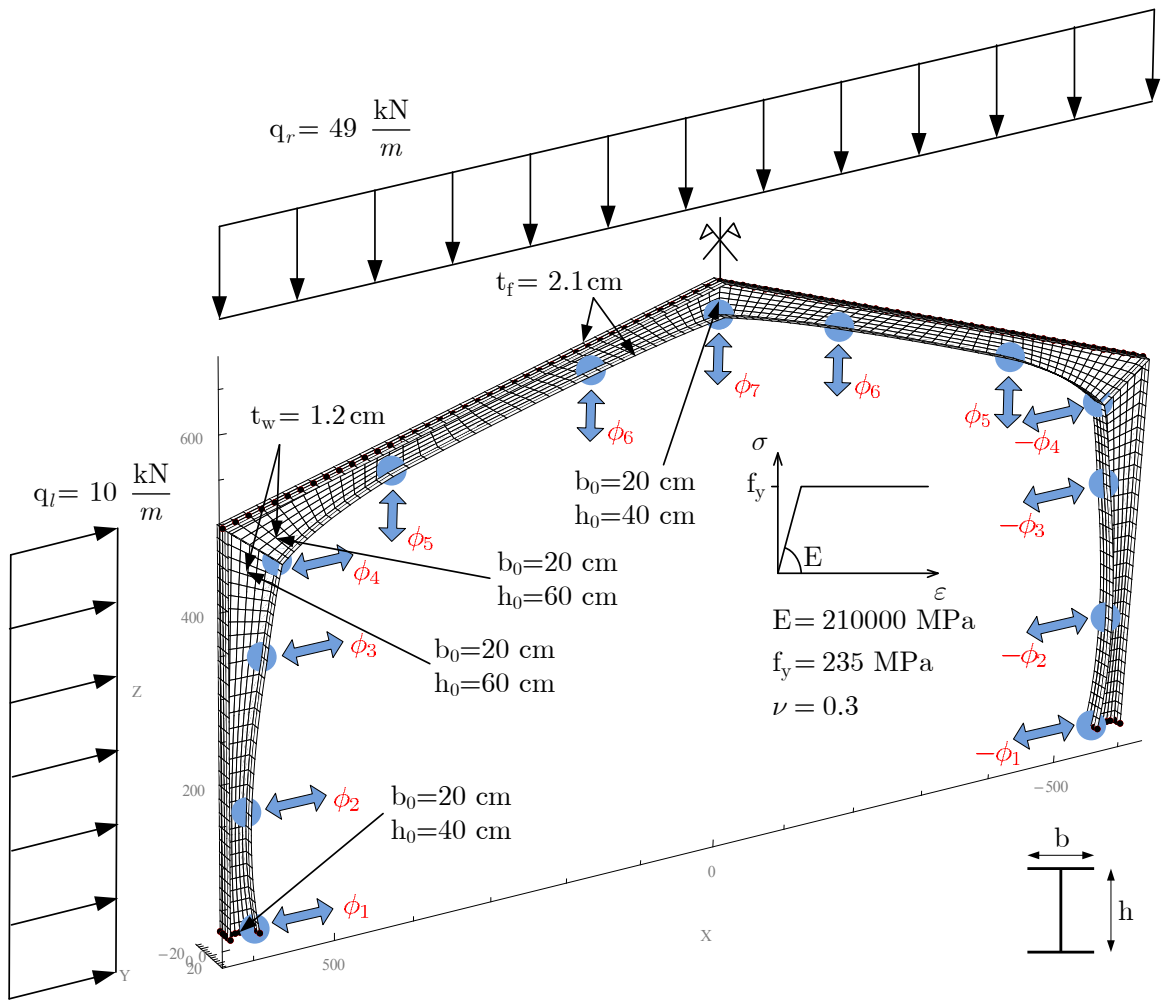

Fig. 63: Loading conditions and shape parameterization for the inner frame.
Slika 63: Obtežbe in prametrizacija oblike za notranji okvir.

The shape parameters ϕ are used to change the height of the cross-section h in the way:

$$h = h_0 + \phi \cdot h_0 = h_0(1 + \phi) \tag{32}$$

Second order splines were chosen for interpolation of the boundary shape between the shape parameters.

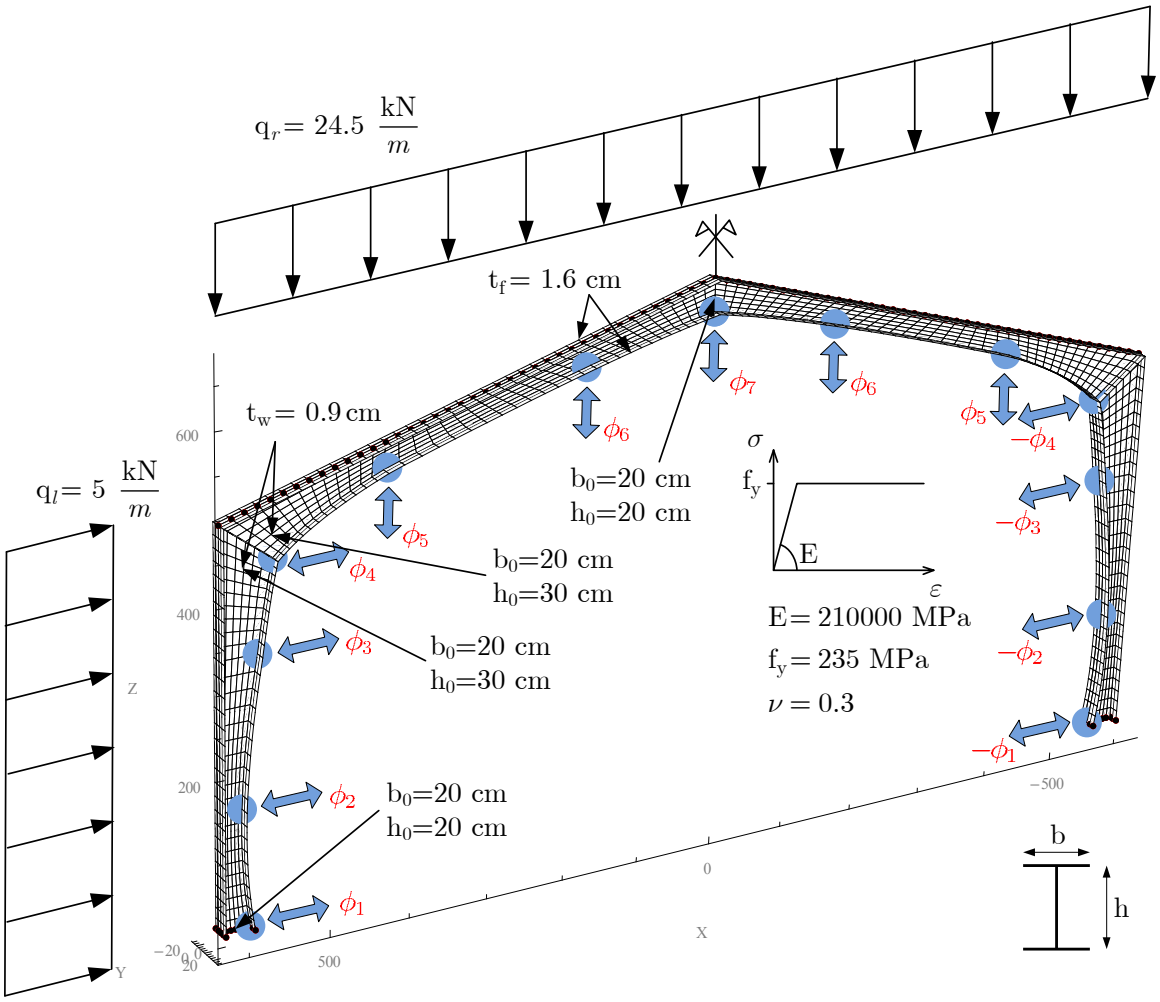

Fig. 64: Loading conditions and shape parameterization for the outer frame.
Slika 64: Obtežbe in prametrizacija oblike za zunanji okvir.

The procedure described in Fig. 44 is applied to find the optimum shape of the structure. Optimization of the entire structure is computationally demanding. Further on, only the frames are subjected to shape optimization. Therefore the two characteristic frames were chosen for investigation: the outer frame with only half external load applied and the inner frame fully loaded by external forces. The initial and the optimal shape are illustrated for the final run of the optimization algorithm for the inner frame and the outer frame in Fig. 65 and Fig. 66, respectively. Mises stresses are plotted at the limit load deformation state in Fig. 67 and Fig. 68.

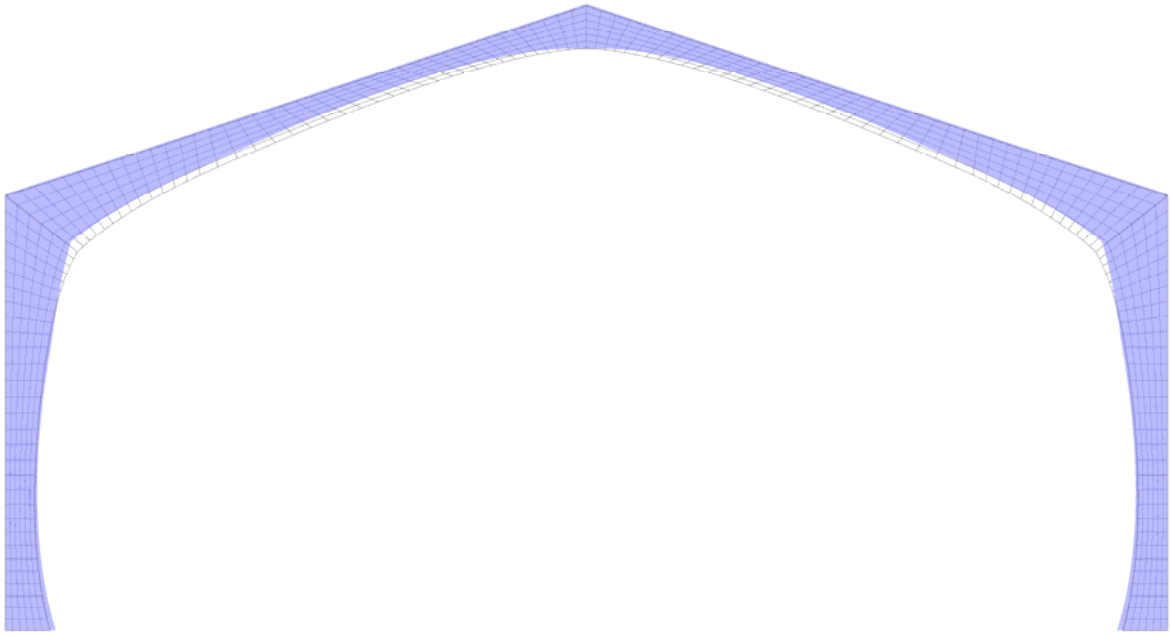

Fig. 65: Optimum shape of the inner frame of the steel structure with the initial geometry in the final optimization run.

Slika 65: Optimalna oblika notranjega okvira jeklene konstrukcije v zadnjem krogu optimizacijskega procesa.

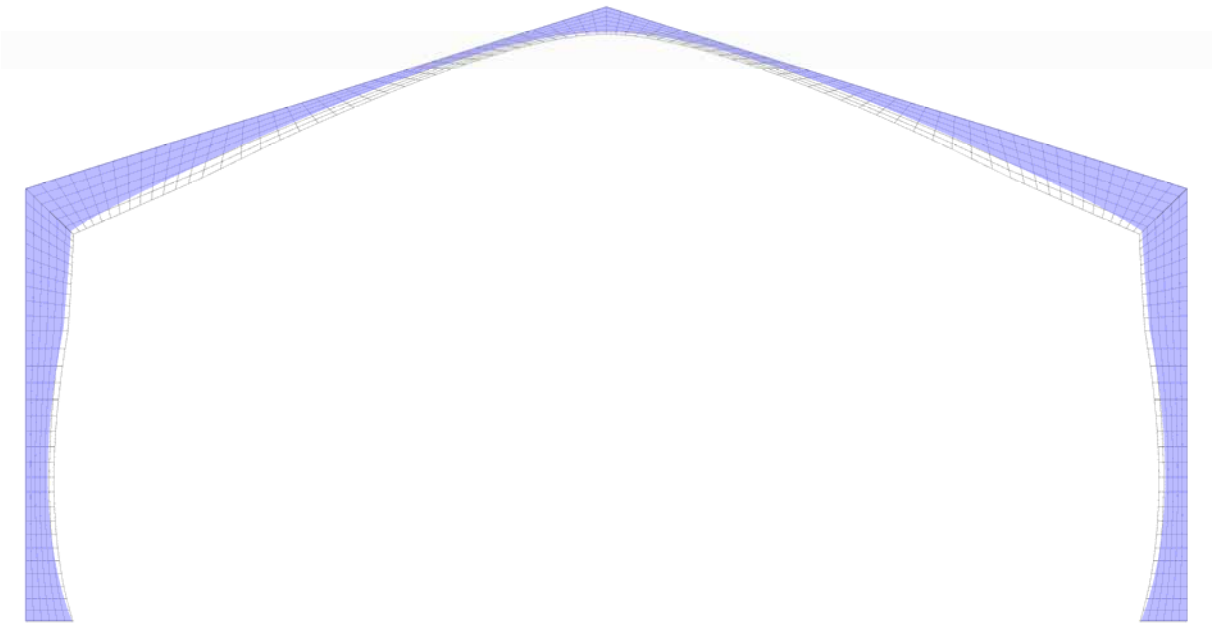

Fig. 66: Optimum shape of the outer frame of the steel structure with the initial geometry in the final optimization run.

Slika 66: Optimalna oblika zunanjega okvira jeklene konstrukcije v zadnjem krogu optimizacijskega procesa.

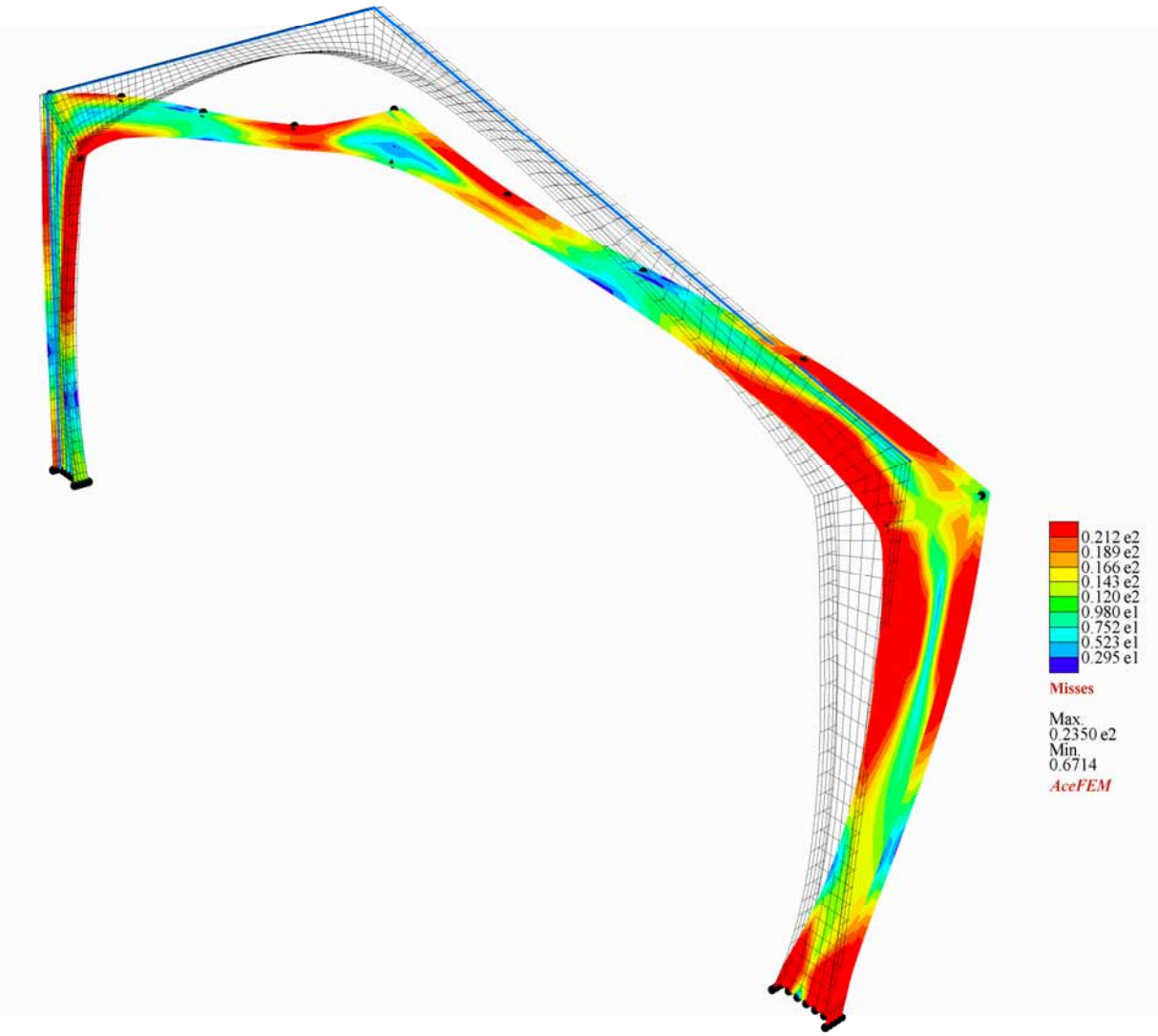

Fig. 67: Deformation of the inner frame at limit state (Scale Factor = 10).

Slika 67: Deformacije notranjega okvira pri mejni obtežbi (Faktor povečave = 10).

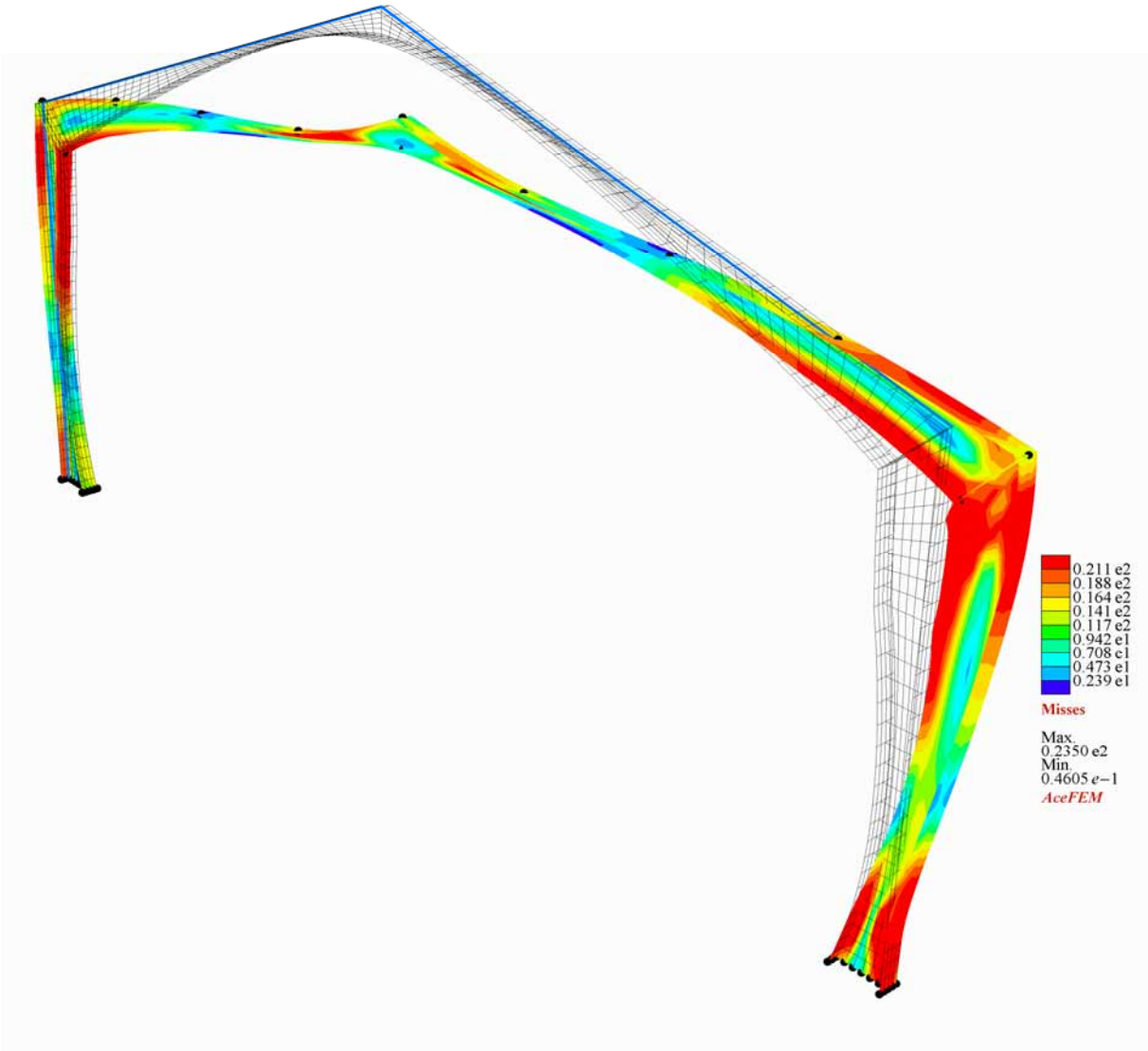

Fig. 68: Deformation of the outer frame at limit state (Scale Factor = 10).

Slika 68: Deformacije zunanjega okvira pri mejni obtežbi (Faktor povečave = 10).

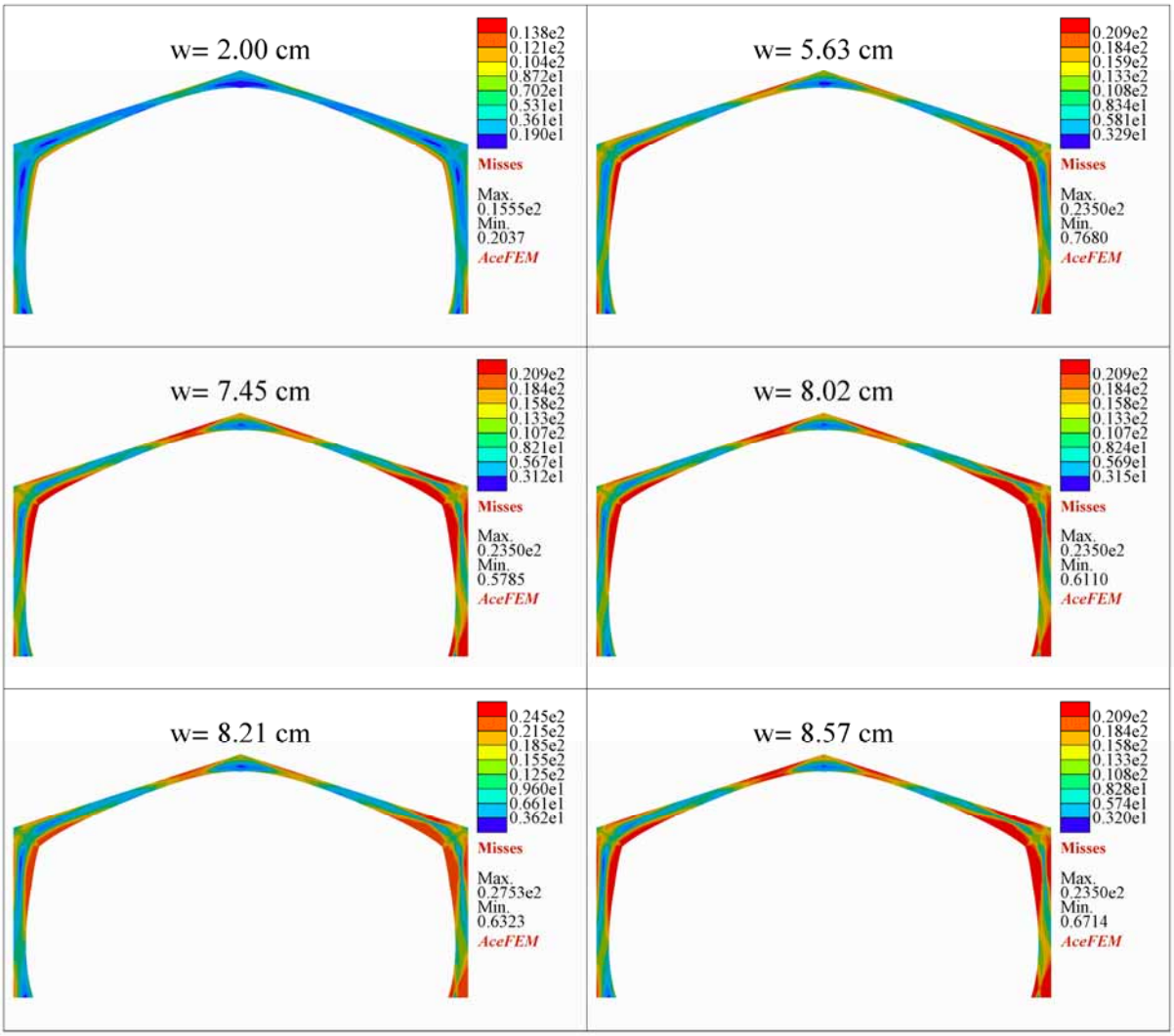

Fig. 69: Mises stress for inner frame for the corresponding load-deformation curve plotted in Fig. 71.

Slika 69: Misesove napetosti za notranji okvir za obtežno krivuljo prikazano na sliki 71.

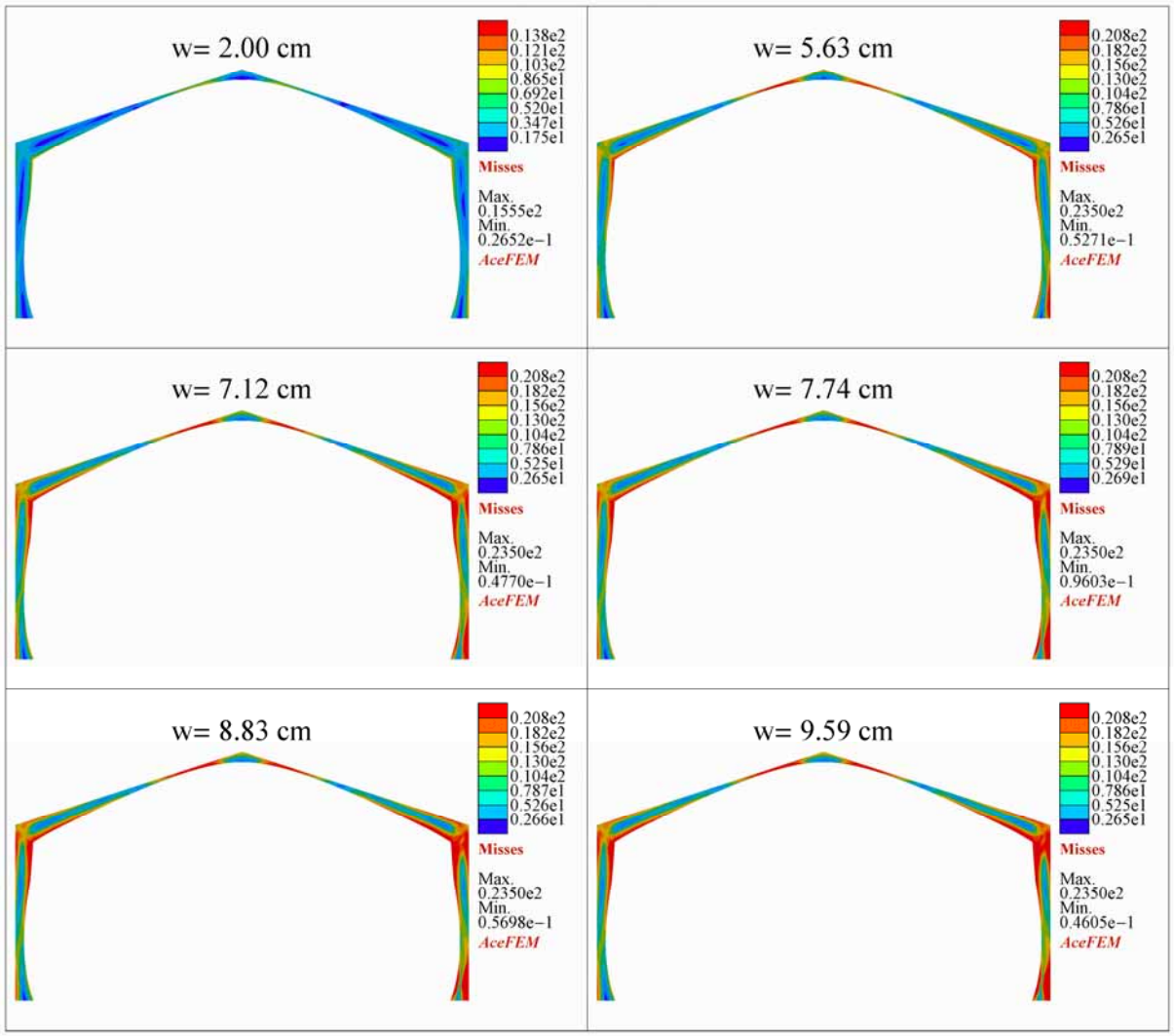

Fig. 70: Mises stress for outer frame for the corresponding load-deformation curve plotted in Fig. 71.

Slika 70: Misesove napetosti za zunanji okvir za obtežno krivuljo prikazano na sliki 71.

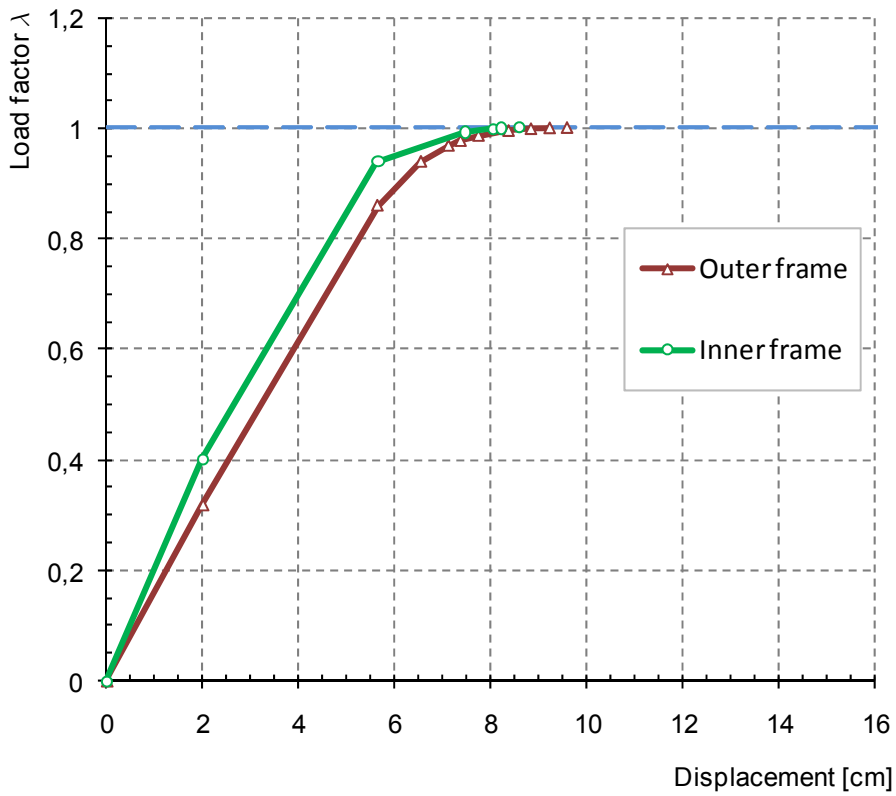

Fig. 71: Load-deformation curves for the inner and the outer frame with the optimized shape.
Slika 71: Deformacijski krivulji za notranji in zunanji okvir z optimalno obliko.

In Fig. 69 and Fig. 70 the Mises stress development with increasing the load up to the limit state is plotted. The corresponding load-displacement curves are plotted in Fig. 71. Because of the symmetrical shape parametrization and unsymmetrical loading conditions it is impossible for the entire structure to be in plastic state. The optimized structure has a shape which is optimal for the loading conditions considered in the example. Because of the symmetric parametrization the structure is optimized for opposite direction of loads in X direction also. If different ratios of horizontal and vertical loads had to be considered, this could be done with multi objective optimization procedures. Another way is to evaluate an optimum shape for every loading condition and then combine them in a way in which all constraints are still satisfied.

The optimized structure is shown in Fig. 72. The optimization parameters for the optimized structure are shown in Table 5.

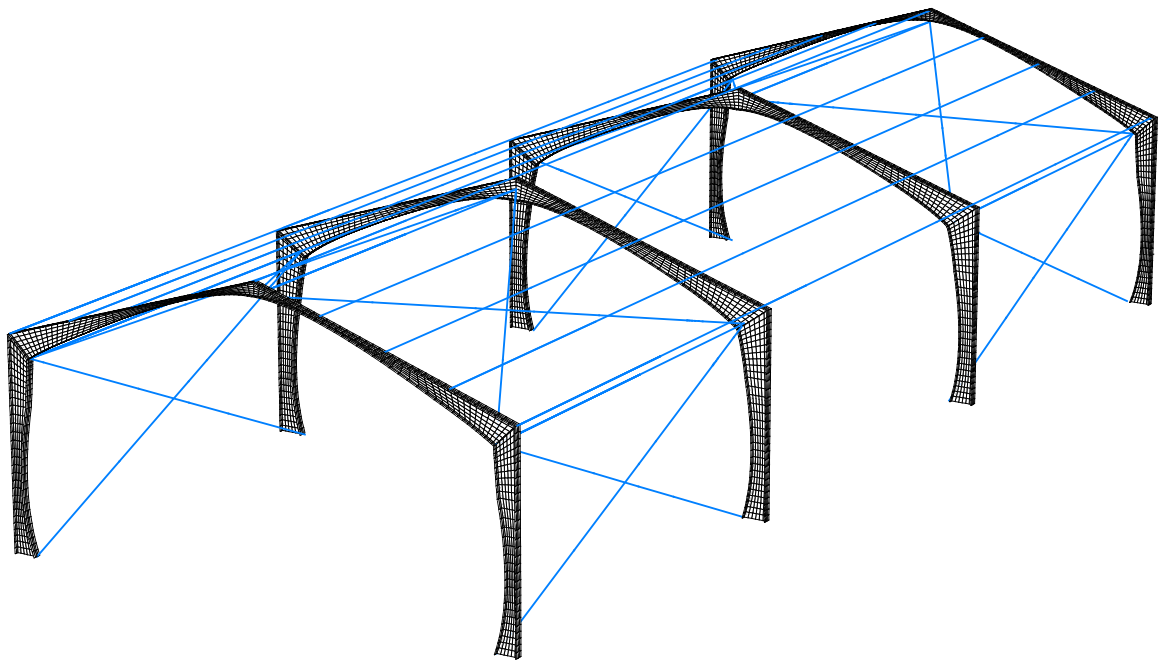

Fig. 72: Optimized shape of single story steel building.
Slika 72: Optimizirana oblika enonadstropne jeklene hale.

Table 5: Optimization parameter values for the optimized structure.
Tabela 5: Vrednosti projektnih parametrov pri optimalni obliki konstrukcije.

Frame	ϕ_1	ϕ_2	ϕ_3	ϕ_4	ϕ_5	ϕ_6	ϕ_7
inner	0,39	-0,42	-0,24	0,21	0,42	-0,61	0,23
outer	1,52	-0,51	-0,17	0,64	-0,40	-0,79	0,46

6 Final Conclusions

The objective of this thesis was to develop a shape optimization method which is capable to be used in practical design. According to the majority of technical standards a structure has to be designed with regard to all possible influences with a certain probability to occur in its lifetime. Modern technical standards prescribe ultimate limit state design for structures where the structure is designed for a variety of ultimate states in order not to collapse or to exceed limit states in the foreseen lifetime. Standard known shape optimization approaches do not consider ultimate states for arbitrary structures. Usually the structures are subjected to volume, cost or other behavior related (e.g. eigen frequency, stiffness, etc.) optimization criteria. As the evaluation of a realistic limit load is a demanding task, conventional shape optimization techniques use stress criteria, simple buckling or bifurcation criteria rather than a real limit load. These approaches are not capable of providing an optimal shape for the ultimate state of an arbitrary structure.

In the presented approach a limit load optimization is introduced, capable of evaluating the limit load of a structure by simultaneously considering the effects of imperfections, geometrical nonlinearities and material nonlinearity. The limit load is then used in the optimization algorithm as a constraint. Residual stresses in form of initial stresses have not yet been included explicitly into the analysis, but were considered by the equivalent geometrical imperfections approach. According to the technical standards, with all relevant phenomena considered, the optimized structure therefore presents the final design with no checks further necessary.

A numeric-symbolic approach to limit load shape optimization was studied. The numeric-symbolic system enables the use of arbitrary symbolical shape parameterization which is not possible within conventional approaches. The design velocity field can be analytically computed and therefore an exact sensitivity analysis can be carried out. Accurate sensitivity information is of crucial importance for proper gradient shape optimization used in the approach.

Limit load evaluation and limit load shape optimization of imperfection sensitive structures demands a proper consideration of initial imperfections. The shape and size of initial imperfections have a major influence on the response of the structure and its ultimate state. Further on, shape optimization applied on the perfect geometry of structures can lead to non-optimal results, e.g. very light structures but very sensitive

to buckling. Despite intensive research of theoretical, experimental and numerical aspects of stability limit of imperfection-sensible structures, there is still no consensus on how the ultimate state should be evaluated, owing to numerous difficulties which arise.

While imperfections are not known in advance, a method for direct determination of the most unfavorable imperfection of structures by means of ultimate limit states was developed. The method has been implemented as an internal and separate optimization algorithm within the global shape optimization process. Within the presented approach it has been shown that with the use of geometrical and material nonlinear direct and sensitivity analysis of imperfect structure combined with optimization it is possible to directly evaluate the imperfection shape of a structure, at which the ultimate load of the structure is the smallest. Additionally, the method is not limited to the linear natural equilibrium path and small imperfections, and allows introduction of various constraints on the shape of the initial imperfection.

Usually imperfection analyses with a great number of repetitions are done to determine which combinations are unfavorable. Despite the effort, it is still very hard to determine how the limit load is lowered by the gathered imperfection shapes in comparison with the most unfavorable ones. According to the results of the presented approach, it is difficult to characterize certain structures with certain types of imperfections. Every change in thickness, geometry or loading conditions can lead to a drastic change of the worst imperfection shape.

In complex imperfection sensible structures, where intuitive determination of initial most unfavorable imperfections is not possible or where there is lack of known empirically obtained worst imperfections, the use of a method for determining the worst initial shape is essential.

Because of the high unpredictability of the imperfection forms, the technical standards for designing thin-walled structures recommend to use empirical methods to define initial imperfections used for nonlinear analyses. The ultimate loads of structures evaluated in accordance with the method presented turned out to be smaller than the ultimate loads considering various combinations of imperfections prescribed by the technical standards or calculated with approaches based on Koiters asymptotic theory or parametric studies. It can be concluded that these methods may lead to too optimistic results. On the other hand, the probability of the real structure's imperfections to take the exactly most unfavorable form is very low. However, the information about the structures lowest limit load due to initial imperfections is of high importance when analyzing structures. In this sense it is

possible to establish that the consideration of imperfections in a geometrically and materially nonlinear analysis is a task where a holistic method for finding the worst imperfection is indispensable.

The importance of the ability to evaluate the most unfavorable initial geometrical imperfections as presented in the thesis is further stressed out within the limit load optimization procedure. Full geometrical and material nonlinearity is considered throughout the global optimization process consistently, resulting in efficient and robust, ultimate limit load structure design. The limit load approach used within the shape optimization algorithm and the optimization algorithm for finding the most unfavorable initial imperfection induces a search for a shape of the structure at which the structure develops plastic, ductile behavior, less sensitive to buckling and, on the other hand, with the minimum volume possible. The result is a robust structure with minimum weight and small sensitivity to buckling.

The design of structures with the limit load optimization approach using the developed method for the determination of the most unfavorable imperfections presents a novel approach to economical engineering structure design. The use of a symbolic-numeric system offers a successful combination of limit load structural analysis and optimization methods. Considering all the relevant phenomena the presented approach can represent a design of economical and safe structures and therefore a superior alternative to conventional ultimate limit state design.

The most important original contributions can be stressed out:

- The development of the method for evaluation of the most unfavorable initial geometric imperfections.
- The development of limit load shape optimization algorithms considering full nonlinearity and most unfavorable initial imperfections.
- The evaluation of the analytical design velocity and the exact sensitivity analysis using symbolic-numeric environment.

7 Povzetek

7.1 Uvod

Integracija optimizacijskih metod v procese projektiranja konstrukcij je kompleksna naloga, ki zahteva povezavo znanja iz več znanstvenih področij. Da bi sintezo konstrukcij lahko uporabili kot zamenjavo klasičnemu pristopu k projektiranju konstrukcij, je potrebno razviti učinkovito optimizacijsko metodo z upoštevanjem vseh bistvenih fenomenov, ki vplivajo na obnašanje konstrukcij.

Splošen cilj dela v okviru disertacije je razviti metodo za optimizacijo oblike konstrukcij z upoštevanjem mejnega stanja, ki bi jo bilo možno uporabiti za projektiranje konstrukcij. Predstavljen je simbolno numerični pristop k optimizaciji oblike za mejno stanje konstrukcij. V sklopu določitve mejne obtežbe je bila razvita metoda za določitev najbolj neugodnih začetnih nepopolnosti, ki lahko bistveno vplivajo na nosilnost konstrukcij. Podrobno obravnavana področja so bila:

- Uporaba simbolno numeričnega sistema za določitev mejne obtežbe konstrukcij ter optimizacijo oblike. Simbolni razvoj in avtomatska generacija končnih elementov za direktno in občutljivostno analizo.
- Izračun najbolj neugodnih začetnih nepopolnosti konstrukcij, v smislu mejnih stanj konstrukcije.
- Uporaba poljubne simbolne parametrizacije oblike in analitičen izračun polja začetnih občutljivosti ter točna občutljivostna analiza.
- Razvoj učinkovitega optimizacijskega algoritma za optimizacijo oblike s pomočjo vseh zgoraj omenjenih prijemov.

7.2 Direktna in občutljivostna analiza

V okviru disertacije je bila uporabljena direktna in občutljivostna analiza s sočasno določitvijo mejnega stanja konstrukcije. Splošni izrazi, ki so prikazani v nadaljevanju, so uporabljeni tako pri določitvi najbolj neugodne začetne nepopolnosti kot tudi pri optimizaciji oblike konstrukcij. V vseh postopkih so uporabljeni rezultati direktne in občutljivostne analize v mejnem stanju konstrukcije.

Mejno stanje nosilnosti konstrukcij je v splošnem definirano z limitno točko ravnotežne poti. Takšna definicija se izkaže nezanesljiva v primeru realnih, nepopolnih konstrukcij. Limitno stanje lahko nastopi šele pri nerealno velikih pomikih ali deformacijah konstrukcije, zato je potrebno mejno stanje dodatno omejiti. Mejno stanje smo določili s pomočjo najmanjšega obtežnega faktorja, dobljenega po naslednjih kriterijih: maksimalni obtežni faktor (v limitni točki) (a), obtežni faktor pri bifurkaciji pred dosego limitne točke (b), obtežni faktor pri največji dovoljeni deformaciji, kadar pride do tega pred limitno ali bifurkacijsko točko (c).

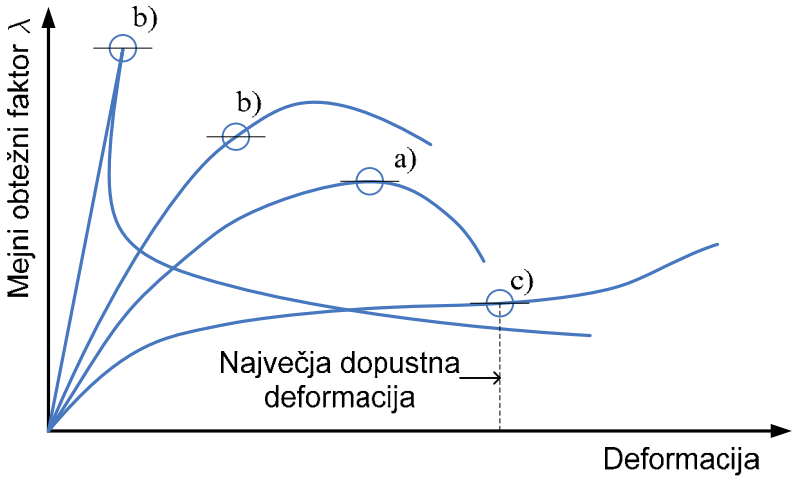

Slika 1: Definicija računskih mejnih stanj (EN 1993 1-5 2004).

7.2.1 Direktna analiza

Za določitev mejnega stanja konstrukcije je potrebna geometrijsko in materialno nelinearna analiza. Problem, ki ga je potrebno rešiti, po terminologiji predstavljeni v (Michaleris, et al. 1994), predstavlja nelinearen, tranzienten, povezan sistem. Uporabljena je standardna metoda predpisanih pomikov (glej e.g. Crisfield 1996, 1997), kjer je sistem enačb razširjen z dodatno spremenljivko λ in dodatnim pogojem g_c, ki predstavlja dodatno enačbo za prirastke posplošenih pomikov. Enačbe, ki jih je potrebno rešiti v vsaki integracijski točki, lahko zapišemo:

$$\bar{\boldsymbol{\Psi}} = \begin{Bmatrix} \boldsymbol{\Psi}\left(\bar{\mathbf{a}}, \bar{\mathbf{a}}^p, \mathbf{b}, \mathbf{b}^p\right) \\ g_c\left(\bar{\mathbf{a}}, \bar{\mathbf{a}}^p\right) \end{Bmatrix} = 0$$

$$\boldsymbol{\Phi}\left(\mathbf{a}, \mathbf{a}^p, \mathbf{b}, \mathbf{b}^p\right) = 0 \tag{1}$$

$$\bar{\mathbf{a}} = \{\mathbf{a}, \lambda\}$$
$$\bar{\mathbf{a}}^p = \left\{\mathbf{a}^p, \lambda^p\right\}$$

$$g_c = u_m - \gamma\, \bar{u}_m \tag{2}$$

Splošna formulacija polno implicitne, kvadratno konvergentne, direktne analize je predstavljena na sliki 2.

Globalni nivo
$\bar{\boldsymbol{\Psi}}(\bar{\mathbf{a}},\ \mathbf{b}(\mathbf{a})) = 0$ ${}_{\boldsymbol{\Phi}}\mathbf{K} \cdot \dfrac{\partial \mathbf{b}}{\partial \mathbf{a}} = -\dfrac{\partial \boldsymbol{\Phi}}{\partial \mathbf{a}} \Rightarrow \dfrac{\partial \mathbf{b}}{\partial \mathbf{a}}$ ${}_{\boldsymbol{\Psi}}\mathbf{K} = \dfrac{\partial \bar{\boldsymbol{\Psi}}}{\partial \mathbf{a}}$ ${}_{\boldsymbol{\Psi}}\mathbf{K}\Delta\bar{\mathbf{a}} + \bar{\boldsymbol{\Psi}} = 0$ $\bar{\mathbf{a}} := \bar{\mathbf{a}} + \Delta\bar{\mathbf{a}}$
Lokalni nivo
$\boldsymbol{\Phi}(\mathbf{b}) = 0$ ${}_{\boldsymbol{\Phi}}\mathbf{K} = \dfrac{\partial \boldsymbol{\Phi}}{\partial \mathbf{b}}$ ${}_{\boldsymbol{\Phi}}\mathbf{K}\Delta\mathbf{b} + \boldsymbol{\Phi} = 0$ $\mathbf{b} := \mathbf{b} + \Delta\mathbf{b}$

Slika 2: Splošna formulacija za direktno analizo tranzientnih, povezanih, nelinearnih problemov.

V uporabljenem zapisu $\mathbf{a}$ predstavlja vektor globalnih parametrov elementa, $\mathbf{b}$ je vektor neznanih lokalnih parametrov, definiranih za vsako integracijsko točko (plastične deformacije, spremenljivke utrjevanja, itd.), $\mathbf{a}^p$ je vektor globalnih parametrov v prejšnjem koraku, $\mathbf{b}^p$ je neznanih lokalnih parametrov v prejšnjem koraku, $\mathbf{\Psi}$ vektor globalnih enačb in $\mathbf{\Phi}$ vektor lokalnih enačb.

7.2.2 Analitična občutljivostna analiza in polje začetnih občutljivosti

Občutljivostna analiza se uporablja za izračun spremembe odziva konstrukcije z ozirom na variacijo projektnih parametrov ϕ in predstavlja ključen del gradientnih metod optimizacije. Uporaba občutljivostne analize v optimizaciji oblike za mejno stanje konstrukcije zahteva rešitev tranzientnega, povezanega sistema enačb, z upoštevanjem geometrijske in materialne nelinearnosti. Zahtevnost izpeljave izrazov za občutljivostno analizo je bil ključen razlog za uporabo simbolno numeričnega sistema (Korelc 2007a, b). Uporabljena je metoda neposrednega odvajanja (Michaleris, et al. 1994). Zaradi tranzientne narave problema je potrebno občutljivosti izračunati na koncu vsakega obtežnega koraka skozi vso analizo. Ustrezne enačbe so predstavljene na sliki 3.

Eden od ključnih problemov uporabe občutljivostne analize v gradientnih metodah optimizacije oblike, je izračun polja začetnih občutljivosti (Korelc, Kristanič 2005). Polje začetnih občutljivosti $(\partial\mathbf{X} / \partial\phi)$ opiše spremembo koordinat vozlišč končnih elementov ($\mathbf{X}$) glede na poljubno izbran projektni parameter ϕ.

Medtem ko lahko odvode karakterističnih količin končnega elementa (reziduum, tangentne matrike, itd.) po projektnih parametrih izrazimo s pomočjo avtomatiziranih postopkov (Korelc 2007b), to ne velja za polje začetnih občutljivosti. Glavna ovira se pojavi pri povezavi projektnih parametrov s pozicijo vozlišč. Te povezave ni možno povsem splošno izraziti s standardnimi pristopi generacije mreže končnih elementov, niti s specializiranimi pred-procesorji ali CAD orodji, saj je izbira projektnih parametrov stvar svobodne izbire projektanta.

Globalni nivo

$$\bar{\mathbf{\Psi}}\left(\bar{\mathbf{a}}, \bar{\mathbf{a}}^p, \mathbf{b}, \mathbf{b}^p, \phi\right) = 0$$

$$_{\mathbf{\Psi}}\mathbf{K}\frac{D\mathbf{a}}{D\phi} = \frac{\tilde{D}\bar{\mathbf{\Psi}}}{\tilde{D}\phi}$$

$$\frac{\tilde{D}\bar{\mathbf{\Psi}}}{\tilde{D}\phi} = \left(\begin{array}{l} \frac{D\bar{\mathbf{\Psi}}}{D\,\mathbf{a}^p}\frac{D\,\mathbf{a}^p}{D\phi} + \frac{D\bar{\mathbf{\Psi}}}{D\,\mathbf{b}^p}\frac{D\,\mathbf{b}^p}{D\phi} + \underline{\underline{\frac{D\bar{\mathbf{\Psi}}}{D\phi}}} - \\ -\frac{D\bar{\mathbf{\Psi}}}{D\,\mathbf{b}}\left(_{\mathbf{\Phi}}\mathbf{K}\right)^{-1} \\ \left(\frac{D\mathbf{\Phi}}{D\phi} + \frac{D\mathbf{\Phi}}{D\,\mathbf{a}^p}\frac{D\,\mathbf{a}^p}{D\phi} + \frac{D\mathbf{\Psi}}{D\,\mathbf{a}^p}\frac{D\,\mathbf{a}^p}{D\phi}\right) \end{array}\right)$$

Lokalni nivo

$$\mathbf{\Phi}\left(\mathbf{a}, \mathbf{a}^p, \mathbf{b}, \mathbf{b}^p\right) = 0$$

$$_{\mathbf{\Phi}}\mathbf{K}\frac{D\mathbf{b}}{D\phi} = \frac{\tilde{D}\mathbf{\Phi}}{\tilde{D}\phi}$$

$$\frac{\tilde{D}\mathbf{\Phi}}{\tilde{D}\phi} = \left(\begin{array}{l} \frac{D\mathbf{\Phi}}{D\,\mathbf{a}}\frac{D\,\mathbf{a}}{D\phi} + \\ + \frac{D\mathbf{\Phi}}{D\,\mathbf{a}^p}\frac{D\,\mathbf{a}^p}{D\phi} + \frac{D\mathbf{\Phi}}{D\,\mathbf{b}^p}\frac{D\,\mathbf{b}^p}{D\phi} \end{array}\right)$$

Slika 3: Splošna formulacija za občutljivostno analizo tranzientnih povezanih nelinearnih problemov.

Uporabljen je simbolno-numerični pristop izračuna polja začetnih občutljivosti, s pomočjo simbolno-algebraičnega sistema *Mathematica* (Wolfram 2008) in simbolno-numeričnega okolja za končne elemente *AceFEM* (Korelc 2007a). Prednost simbolnih sistemov je ta, da operirajo s poljubnimi izrazi. Zato lahko projektni parametri v fazi opisa modela in generacije mreže končnih elementov ostanejo v simbolni obliki. Koordinate vozlišč končnih elementov tako predstavljajo formule, ki so eksplicitno izražene s projektnimi parametri. Polje začetnih občutljivosti lahko nato izračunamo naenkrat z enostavnim ukazom za odvajanje (npr. $D[SMSNodes,\phi]$), kjer *SMSNodes* vsebuje koordinate vozlišč v simbolni obliki, ϕ pa predstavlja projektne parametre.

Problem, ki se pri tem pojavi, je numerična neučinkovitost simbolnih sistemov v primerjavi z okolji za končne elemente, programiranimi v C-ju ali Fortran-u. Rešitev je v uporabi okolja za končne elemente, ki lahko deluje na simbolni ravni in je hkrati numerično učinkovito. Uporabljeno okolje *AceFEM* sestoji iz dveh funkcionalno identičnih modulov. Prvi je napisan v simbolnem jeziku programa *Mathematica* (*MDriver*) in omogoča izračun polja začetnih občutljivosti s simbolno podano mrežo KE. Drugi modul je napisan v jeziku C (*CDriver*) in je s programom *Mathematica* povezano s protokolom *MathLink*. Oba modula delujeta iz *Mathematice* in imata enako strukturo podatkov, funkcije, ukazni jezik in vhodne podatke (podrobno v Korelc 2007a, Korelc 2007b). Postopek analitične določitve polja začetnih občutljivosti z uporabo simbolno numeričnega sistema je shematsko prikazan na sliki 4. Z uporabo analitično izračunanega polja začetnih občutljivosti je mogoče izvesti natančno občutljivostno analizo, ki je ključnega pomena za natančnost in učinkovit potek gradientnih metod optimizacije.

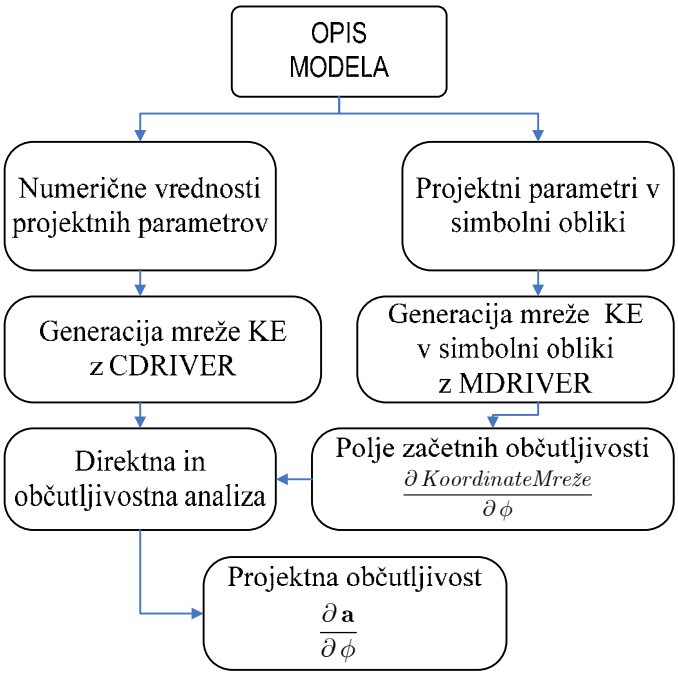

Slika 4: Potek občutljivostne analize s pomočjo simbolno numeričnega MKE okolja.

Opisane postopke je možno uporabiti na problemih poljubne kompleksnosti. Predstavljeni direktna in občutljivostna analiza, sta uporabljeni v določitvi najbolj neugodne začetne nepopolnosti kot tudi v optimizaciji oblike konstrukcij.

7.3 Določitev najbolj neugodnih začetnih nepopolnosti

Začetna nepopolnost konstrukcij je posledica napak pri izdelavi, ki se jim praktično ni mogoče izogniti. Rezultati nelinearnih numeričnih analiz konstrukcijskih elementov in konstrukcij so lahko v veliki meri odvisni od izbire oblike začetnih nepopolnosti, kar je še posebej izraženo pri obravnavi tankostenskih konstrukcij, občutljivih na spremembo začetne geometrije. Dobro znane razlike med mejno nosilnostjo konstrukcij, izračunane z računalniškimi analizami, ter izmerjene s preizkusi v laboratoriju, je možno zmanjšati z ustreznim upoštevanjem začetnih nepopolnosti.

Pri določitvi mejnega stanja konstrukcij v okviru optimizacije oblike, je upoštevanje začetnih nepopolnosti zelo ugodno, saj pripomore k natančnejši določitvi mejne obtežbe in hkrati ugodno vpliva na proces optimizacije, saj se je na tak način mogoče izogniti bifurkacijskim točkam v ravnotežni poti idealnih modelov konstrukcij.

Določitev najbolj neugodne začetne nepopolnosti predstavlja zahteven nelinearen optimizacijski problem, ki je v splošnem v vsakdanji inženirski praksi, praktično nerešljiv v danem časovnem okviru. Z uporabo direktne in občutljivostne analize ter optimizacijskih algoritmov je možno neposredno določiti najbolj neugodno obliko geometrijske nepopolnosti, pri kateri konstrukcija izkaže najnižjo možno nosilnost v okviru obravnavanega problema (Kristanič, Korelc 2008). Pri tem so upoštevane geometrijske, konstrukcijske in materialne nepopolnosti, ki so zajete v obliki ekvivalentnih geometrijskih nepopolnostih ter predpisanih lastnostih materiala.

Osnovna ideja predlaganega pristopa je zamenjava nelinearnega optimizacijskega problema z iteracijskim postopkom, v katerem je potrebno reševati le linearne optimizacijske probleme. V okviru metode je možno uporabiti tehnološke pogoje, katerih uporaba je ključnega pomena, saj se je izkazalo, da pri neupoštevanju pravilnih geometrijskih pogojev lahko privede do izračuna nerealistično majhnih mejnih obtežb.

Oblika iskane najbolj neugodne začetne nepopolnosti je določena z linearno kombinacijo izbranih baznih oblik:

$$\mathbf{X} = \mathbf{X}_p + \sum_{j=1}^{N} \alpha_j \mathbf{\Gamma}_j \ , \tag{3}$$

kjer je $\mathbf{X}_p$ začetna, popolna geometrija, N je število izbranih oblik v bazi, α_j so neznani parametri oblike in $\mathbf{\Gamma}_j$ j-ta oblika iz baze oblik. Baza oblik $\mathbf{\Gamma}$ je lahko izbrana poljubno, vendar mora biti linearno neodvisna. Vsebuje lahko različne nabore

oblik. To so uklonske oblike ($\mathbf{\Gamma}^A$), lastni vektorji ($\mathbf{\Gamma}^B$) začetne togostne matrike $\mathbf{K}_0$, lastni vektorji ($\mathbf{\Gamma}^C$) togostne matrike $\overline{\mathbf{K}}_0$ konstrukcije s spremenjenimi robnimi pogoji, deformacijske oblike ($\mathbf{\Gamma}^D$) in empirično znane neugodne oblike ($\mathbf{\Gamma}^E$). Končna baza oblik $\mathbf{\Gamma}$ je tako:

$$\mathbf{\Gamma} = \mathbf{\Gamma}^A \cup \mathbf{\Gamma}^B \cup \mathbf{\Gamma}^C \cup \mathbf{\Gamma}^D \cup \mathbf{\Gamma}^E \tag{4}$$

V okviru metode je iskana tista nepopolna oblika $\mathbf{X}$, pri kateri je mejna nosilnost konstrukcije najnižja. Potek metode je prikazan na sliki 5. Neznani parametri $\boldsymbol{\alpha}$, pri katerih bo mejna nosilnost najnižja, so računani iterativno v okviru optimizacijskega procesa. V k-ti iteraciji lahko zapišemo:

$$\begin{aligned}
\mathbf{X}_k &= \mathbf{X}_{k-1} + \Delta\mathbf{X}_k \\
\Delta\mathbf{X}_k &= \sum_{i=1}^{N} \Delta\alpha_i^k \, \mathbf{\Gamma}_i \\
\alpha_i^k &= \alpha_i^{k-1} + \Delta\alpha_i^k \\
\overline{\mathbf{X}}_k &= \sum_{i=1}^{N} \alpha_i^k \, \mathbf{\Gamma}_i
\end{aligned}, \tag{5}$$

kjer je $\mathbf{X}_k$ nepopolna oblika, $\Delta\alpha_i^k$ prirastek parametrov, $\Delta\mathbf{X}_k$ prirastek nepopolnosti in $\overline{\mathbf{X}}_k$ skupna nepopolnost. Prirastek parametrov $\Delta\alpha_i^k$ v k-ti iteraciji je dobljen z rešitvijo optimizacijskega problema. Za začetni približek je lahko izbrana kar prva bazna oblika Γ_1:

$$\begin{aligned}
\alpha_i^0 &= 0; \; \Delta\alpha_i^0 = \begin{cases} \dfrac{e_0}{\max \Gamma_i} & i = 1 \\ 0 & i \neq 1 \end{cases} \\
\mathbf{X}_0 &= \mathbf{X}_p + \Delta\alpha_1^0 \, \Gamma_1
\end{aligned} \tag{6}$$

Postopek je zaključen, ko je dosežen pogoj $\left\| \Delta\alpha_i^k \right\| < toleranca$.

V vsaki iteraciji je izvedena nelinearna direktna in občutljivostna analiza konstrukcije z geometrijo $\mathbf{X}_k$. Parametri oblike α_i^k najbolj neugodne oblike $\mathbf{X}_k$ v trenutnem koraku, so izračunani s pomočjo optimizacijskega postopka, ki je popolnoma ločen od direktne in občutljivostne analize. Takšen pristop nam omogoča uporabo poljubnega naprednega optimizacijskega algoritma.

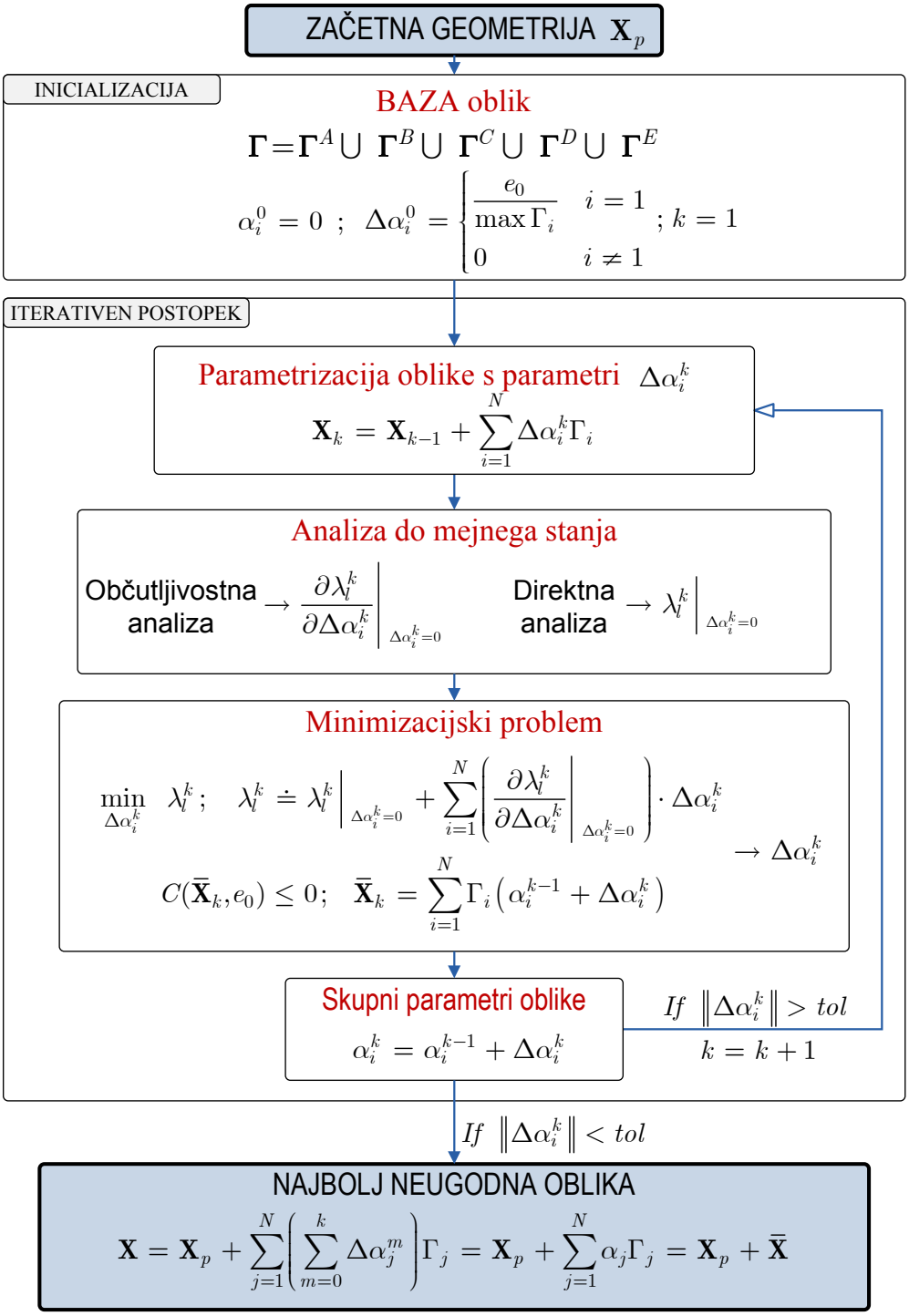

Slika 5: Potek metode določitve najbolj neugodne začetne nepopolnosti.

Alternativen in bolj točen pristop bi lahko predstavljalo reševanje polno povezanega problema, vendar zaradi numerične prezahtevnosti trenutno za večje sisteme, še ni mogoč. Polno povezan problem je bil poenostavljen na ta način, da je bil z uporabo

občutljivosti mejni obtežni faktor nepopolne konstrukcije razvit v Taylorjevo vrsto okoli mejnega obtežnega faktorja nepopolne konstrukcije. Enačbo mejnega obtežnega faktorja lahko zapišemo na sledeči način:

$$\lambda_l^k \doteq \lambda_l^k \Big|_{\Delta\alpha_i^k=0} + \sum_{i=1}^{N} \left(\frac{\partial \lambda_l^k}{\partial \Delta\alpha_i^k} \Big|_{\Delta\alpha_i^k=0} \right) \cdot \Delta\alpha_i^k \,, \tag{7}$$

kjer je $\lambda_l^k \Big|_{\Delta\alpha_i^k=0}$ izračunani mejni obtežni faktor v k-ti iteraciji in $\frac{\partial \lambda_l^k}{\partial \Delta\alpha_i^k} \Big|_{\Delta\alpha_i^k=0}$ občutljivost mejnega obtežnega faktorja na optimizacijske parametre v trenutnem koraku. Uporabljen iterativni pristop nam omogoča, da najbolj neugodno nepopolno obliko konstrukcije iščemo na nepopolni konstrukciji. Pri tem se najbolj neugodna oblika iz prejšnje iteracije uporabi za začetno nepopolnost v trenutni iteraciji. S tem je zagotovljena natančnost tudi v primerih velikih nepopolnosti. V vsaki iteraciji je potrebno rešiti minimizacijski problem (8), kjer iščemo takšne $\Delta\alpha_i^k$, pri katerih bo λ_l^k minimalen, pod pogojem, da je amplituda oblike, ki jo določajo parametri α_i^k, v predpisanih mejah. Mejne amplitude e_0 so določene s principom ekvivalentnih geometrijskih nepopolnosti, ki jih določajo tehnični predpisi (EN 1993 1-5 2004, EN 1993 1-6 2006). Optimizacijski problem lahko zapišemo:

$$\begin{array}{c} \min\limits_{\Delta\alpha_i^k} \lambda_l^k \\ C(\overline{\mathbf{X}}_k, e_0) \leq 0 \end{array} \,, \tag{8}$$

kjer $C(\overline{\mathbf{X}}_k, e_0)$ predstavlja omejitveno funkcijo. Funkcija λ_l je linearna, medtem ko je omejitvena funkcija $C(\overline{\mathbf{X}}_k, e_0)$ v odvisnosti od zasnove lahko samo ena, izrazito nelinearna funkcija, ali skupek več linearnih funkcij. V prvem primeru je potrebno problem reševati z razširjeno Lagrangevo metodo, v drugem primeru in predvsem pri obravnavi večjih problemov, pa lahko uporabimo metode linearnega programiranja.

Z večanjem števila upoštevanih oblik v bazi oblik se napaka diskretizacije najbolj neugodne oblike približuje napaki diskretizacije mreže končnih elementov, kar zagotavlja konvergenco metode z gostenjem mreže končnih elementov in večanjem števila upoštevanih oblik.

7.4 Optimizacija oblike konstrukcij

V okviru disertacije je bil razvit algoritem za gradientno optimizacijo oblike konstrukcij za mejno stanje konstrukcije. Za izračun gradientov je bila uporabljena analitična občutljivostna analiza. V direktni in občutljivostni analizi so bile upoštevane začetne nepopolnosti, določene z metodo za določitev najbolj neugodne začetne nepopolnosti.

Uporabljeno simbolno numerično okolje pri reševanju problemov z gradientnimi metodami optimizacije, omogoča uporabo kombinacije naprednih simbolnih zmožnosti ter hkratne numerične učinkovitosti okolja (Korelc 2002, Korelc 2007a, b).

Postopek optimizacije v simbolno numeričnem okolju je prikazan na sliki 6. Z uporabo avtomatskega odvajanja, simultane optimizacije in preverjanja izrazov z uporabo *AceGen*–a (Korelc 2007b), je pridobljena učinkovita koda končnega elementa. Za simbolno obravnavo v okviru metode končnih elementov je uporabljeno okolje *AceFEM* (Korelc 2007a). V skladu s postopki, opisanimi v 7.2.2, je izračunano analitično polje začetnih občutljivosti z delom *AceFEM*-a, z zmožnostjo simbolnega obravnavanja problemov *MDriver.* Analitično polje začetnih občutljivosti je nato uporabljeno v izračunu občutljivosti z numeričnim delom *AceFEM*-a (*CDriver).* Odvodi namenske funkcije in pogojev po projektnih spremenljivkah so nato posredovani optimizacijskemu algoritmu v okviru okolja *Mathematica* (Wolfram 2008). Kot je bilo že poudarjeno, so natančne gradientne informacije, izračunane na podlagi analitičnega polja začetnih občutljivosti, odločilnega pomena za konvergenco optimizacijskega algoritma, še posebej, kadar obravnavamo probleme z upoštevanjem geometrijske in materialne nelinearnosti.

AceGen in *AceFEM* delujeta znotraj okolja *Mathematica*, kar je zelo priročno, saj ni potrebno uporabljati vmesnikov za povezavo z drugimi okolji za optimizacijo. Poleg tega *Mathematica* nudi paleto modernih optimizacijskih algoritmov, ki se neprestano nadgrajujejo in jih je možno uporabiti direktno z *AceFEM-ovo direktno in občutljivostno analizo.*

Splošen potek optimizacijske metode je predstavljen na sliki 6, splošna optimizacijska zanka na sliki 7.

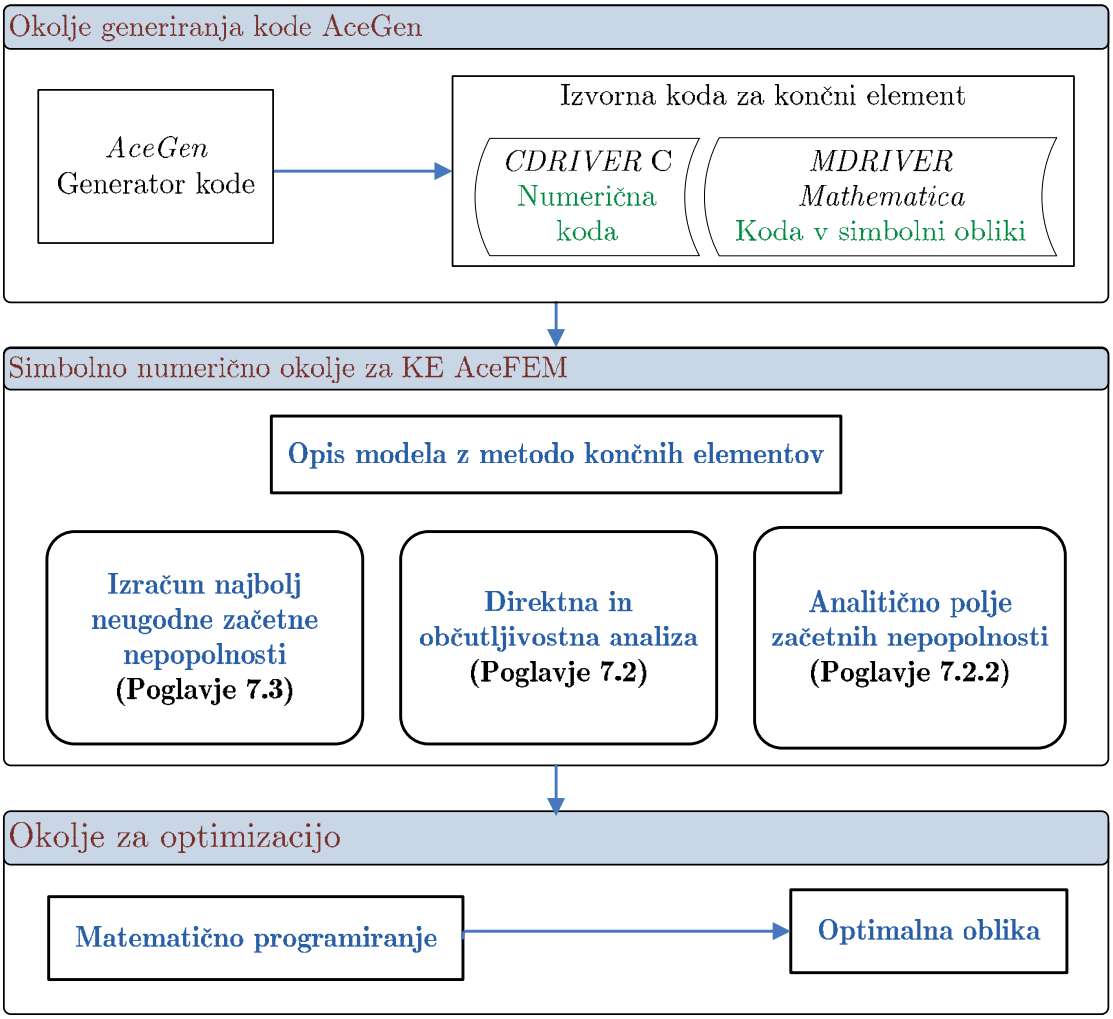

Slika 6: Optimizacija s pomočjo simbolno-numeričnega okolja.

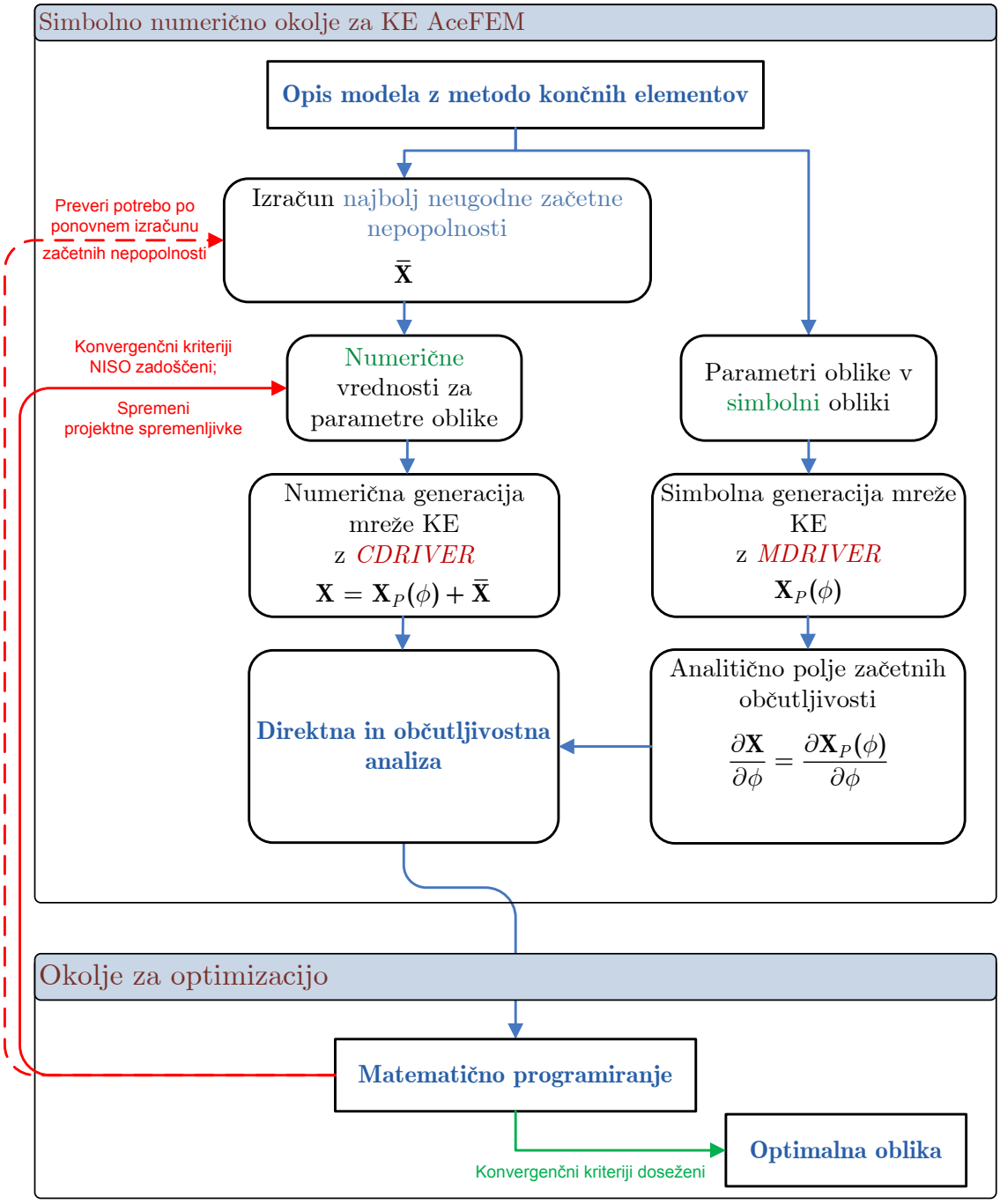

Slika 7: Optimizacijska zanka s pomočjo simbolno-numeričnega okolja.

Znotraj optimizacijskega procesa (slika 7) je geometrija konstrukcije posodobljena zaporedoma v dveh iteracijskih zankah. V notranji zanki se v skladu z optimizacijskim algoritmom spreminjajo projektne spremenljivke ϕ, ki določajo geometrijo $\mathbf{X}(\phi)$. V zunanji iteracijski zanki se geometrija konstrukcije spremeni zaradi spremenjenih najbolj neugodnih začetnih nepopolnosti $\overline{\mathbf{X}}$. Metoda za določitev najbolj neugodne nepopolnosti je predstavljena na sliki 5. Geometrijo konstrukcije lahko zapišemo kot:

$$\mathbf{X} = \mathbf{X}_P(\phi) + \overline{\mathbf{X}} \tag{9}$$

kjer je $\mathbf{X}_P(\phi)$ idealna geometrija konstrukcije in $\overline{\mathbf{X}}$ celoten vektor nepopolnosti kot opisano v poglavju 7.3. Nepopolna oblika mora biti upoštevana v direktni in občutljivostni analizi, medtem ko se za izračun polja začetnih občutljivosti lahko uporabi idealna geometrija konstrukcije, saj velja:

$$\frac{\partial \mathbf{X}}{\partial \phi} = \frac{\partial \mathbf{X}_P(\phi_i) + \overline{\mathbf{X}}}{\partial \phi} = \frac{\partial \mathbf{X}_P(\phi)}{\partial \phi} \tag{10}$$

Polje začetnih občutljivosti ni odvisno od celotnega vektorja začetnih nepopolnosti $\overline{\mathbf{X}}$ in se ne spreminja pri spremembi projektnih spremenljivk ϕ. Zaradi tega ga je potrebno izračunati le enkrat.

Najbolj neugodno začetno nepopolnost je potrebno izračunati vsakič, ko se geometrija konstrukcije v okviru optimizacije oblike spremeni do določene mere. Skupaj s spremenjeno geometrijo se spreminja tudi oblika najbolj neugodne nepopolnosti. Izračun najbolj neugodne nepopolnosti je računsko zahteven, zato je ugodno, če izračuna ni potrebno izvajati v vsaki iteraciji optimizacije oblike. Izračun je izveden samo takrat, ko bi spremenjena oblika začetnih nepopolnosti spremenila mejni obtežni faktor za več kot λ_ε, ali bi se spremenilo mejno stanje. Ugotovljeno je bilo, da se oblika neugodnih začetnih nepopolnosti ne spreminja bistveno pri majhnih spremembah projektnih spremenljivk. Poleg tega je konvergenca optimizacijskega algoritma bolje ohranjena, če se oblika začetnih nepopolnosti ne spreminja. V predlaganem pristopu se izračun najbolj neugodnih nepopolnosti izvrši izmenoma z optimizacijo oblike, kar se je izkazalo kot uspešen pristop pri iskanju optimalne končne oblike konstrukcije.

7.5 Zaključek

Cilj disertacije je bil razviti optimizacijsko metodo, katero bi bilo možno uporabiti v projektiranju konstrukcij. Večina modernih tehničnih standardov pri projektiranju konstrukcij zahteva, da je nosilnost konstrukcije takšna, da bo v svoji življenjski dobi z dano verjetnostjo prenesla vse predvidene obtežbe in da ne bo presegla projektiranih mejnih stanj. Standardni postopki optimizacije oblike konstrukcij v splošnem ne upoštevajo mejnih stanj konstrukcij. Običajno se konstrukcije optimizira z ozirom na njihov volumen, ceno, ali kakšno drugo lastnost, kot recimo lastna frekvenca ali togost. Izračun pravilne mejne obtežbe konstrukcije je zahtevna naloga, zato se pri klasični optimizaciji oblike konstrukcij uporabljajo kriteriji napetosti, prvega nastopa elastičnega uklona ali nastop bifurkacijske točke. Ti pristopi v splošnem ne omogočajo izračuna optimalne oblike za dejansko mejno stanje konstrukcije.

V predstavljenem pristopu je prikazana optimizacija oblike za mejno stanje, v okviru katere je možno natančno določiti mejno obtežbo konstrukcije, s hkratnim upoštevanjem začetnih nepopolnosti ter materialnih in geometrijskih nelinearnosti ter jo uporabiti kot pogoj v procesu optimizacije. V metodo še ni implementirana možnost eksplicitnega upoštevanja zaostalih napetosti. Upoštevati jih je možno implicitno s pomočjo metode nadomestnih geometrijskih nepopolnosti. V skladu s tehničnimi standardi je na tak način ob predpostavki, da so zajeti vsi relevantni fenomeni, s pomočjo optimizacijskih algoritmov možno projektirati konstrukcije.

V okviru disertacije je bil uporabljen simbolno numerični pristop k optimizaciji oblike. Ta omogoča poljubno simbolno parametrizacijo konstrukcije, kar ni mogoče pri klasičnih pristopih k optimizaciji oblike. Simbolna oblika omogoča analitičen izračun polja začetnih občutljivosti, s čimer je možno izvesti natančno občutljivostno analizo, ki je temeljnega pomena za uspeh uporabljenih gradientnih metod optimizacije.

V primeru konstrukcij, ki so občutljive na spremembo začetne geometrije, določitev mejne obtežbe ter optimizacija oblike v mejnem stanju, zahtevata pravilno upoštevanje začetnih nepopolnosti. Velikost in oblika začetnih nepopolnosti lahko ima velik vpliv na odziv konstrukcije ter njeno mejno stanje. Nadalje je možno, da je ob neupoštevanju začetnih nepopolnosti rezultat optimizacije napačen, saj se kot rezultati lahko pojavijo zelo lahke konstrukcije, ki so zelo občutljive na pojav uklona. Kljub številnim raziskavam, eksperimentalnemu delu ter numeričnim analizam konstrukcij, občutljivih na spremembo geometrije, med strokovnjaki še vedno ni

enotnega mnenja, na kakšen način izračunati mejno stanje, kar je možno pripisati številnim težavam, ki se pojavijo.

Nepopolnosti konstrukcije niso znane v naprej, zato je bila razvita metoda za določitev najbolj neugodne nepopolnosti nanašajoč se na mejno stanje konstrukcije. Metoda je implementirana kot interni ločen optimizacijski algoritem znotraj globalne optimizacije oblike konstrukcije. Prikazano je, da je s pomočjo geometrijsko in materialno nelinearne analize nepopolnih konstrukcij kombinirane z optimizacijo, možno direktno določiti začetno nepopolno obliko, pri kateri konstrukcija izkaže najmanjšo možno mejno nosilnost. Metoda ni omejena na linearno obtežno pot in ne na majhne nepopolnosti ter omogoča vpeljavo različnih tehnoloških pogojev glede same oblike.

Običajno je potrebno za določitev neugodne kombinacije začetnih nepopolnosti opraviti številne analize. Kljub naporu je težko določiti stopnjo, do katere se zmanjša mejna obtežba konstrukcije z upoštevanjem tako dobljenih začetnih nepopolnosti in z izračunano najbolj neugodno nepopolnostjo. Na podlagi rezultatov predstavljenega pristopa je težko okarakterizirati določene konstrukcije z določenimi tipi nepopolnosti. Vsaka sprememba v debelini, obliki ali obtežbi lahko povzroči drastično spremembo najbolj neugodne oblike.

Pri kompleksnih konstrukcijah, občutljivih na spremembo oblike, kjer je težko intuitivno določiti neugodne nepopolnosti in kjer empirično pridobljenih neugodnih oblik ni na voljo, je uporaba metode za določitev najbolj neugodnih nepopolnosti nujna.

Zaradi nepredvidljivosti oblik nepopolnosti, tehnični standardi predlagajo uporabo empiričnih metod določanja začetnih nepopolnosti v numeričnih analizah. Mejne obtežbe konstrukcij, izračunane s pomočjo predstavljene metode, so se izkazale za manjše, kot bi jih dobili s pomočjo kombiniranja različnih oblik po priporočilih standardov ali s pristopi, ki temeljijo na Koiterjevi asimptotični teoriji ali parametričnimi študijami. Te metode lahko pripeljejo do preveč optimističnih rezultatov. Po drugi strani je verjetnost, da bi realna konstrukcija imela najbolj neugodno začetno obliko, zelo majhna. Kljub temu je informacija, katera nepopolnost je najbolj neugodna, zelo pomembna, kadar numerično simuliramo obnašanje konstrukcij. V tem smislu je mogoče povzeti, da je uporaba celostne metode določitve najbolj neugodnih nepopolnosti pri geometrijsko in materialno nelinearni analizi, nepogrešljiva.

Pomembnost možnosti izračuna najbolj neugodnih začetnih nepopolnosti se nadalje izkaže pri uporabi le teh v optimizaciji oblike v mejnem stanju nosilnosti. Skozi celoten proces optimizacije je konsistentno upoštevana polna geometrijska in materialna nelinearnost, kar omogoča efektiven in robusten način projektiranja konstrukcij. Pristop, ki upošteva dejansko mejno obtežbo ter uporabo najbolj neugodnih nepopolnosti, povzroči, da je v okviru optimizacije oblike iskana takšna konstrukcija, ki izkazuje plastično in duktilno obnašanje z zmanjšano nevarnostjo nastanka nestabilnosti ter po drugi strani minimalnim volumnom konstrukcije. Na tak način je rezultat predlagane metode optimizacije robustna konstrukcija z minimalno težo ter minimalno možnostjo uklona pri danih pogojih.

Projektiranje konstrukcij z integracijo metod optimizacije oblike za mejno stanje ter določitve najbolj neugodne začetne nepopolnosti, predstavlja nov in napreden pristop k projektiranju konstrukcij. Uspešno kombinacijo analize mejne obtežbe in optimizacijskih metod omogoča uporaba simbolno numeričnega okolja za analizo konstrukcij. Z upoštevanjem vseh pomembnih fenomenov, lahko predlagan pristop predstavlja način projektiranja varnih in ekonomičnih konstrukcij, ter s tem boljšo alternativo klasičnemu projektiranju konstrukcij na mejna stanja.

Pomembnejše izvirne prispevke k tehničnim znanostim predstavljajo naslednji razviti postopki:

- Razvoj metode za določitev najbolj neugodne začetne geometrijske nepopolnosti.
- Razvoj algoritmov za optimizacijo oblike konstrukcij v mejnem stanju z upoštevanjem najbolj neugodnih nepopolnosti.
- Izračun analitičnega polja začetnih nepopolnosti in točna občutljivostna analiza s pomočjo simbolno-numeričnega okolja.

References

Arora, J. S. 2004. Introduction to Optimum Design. San Diego, Academic Press: 728 p.

Arora, J. S., Lee, T. H., Cardoso, J. B. 1992. Structural Shape Sensitivity Analysis - Relationship between Material Derivative and Control Volume Approaches. Aiaa Journal, 30, 6: 1638-1648.

Bažant, Z. P., Cedolin, L. 2003. Stability of structures : elastic, inelastic, fracture, and damage theories. Mineola, N.Y., Dover Publications: 1011 p.

Bletzinger, K. U., Ramm, E. 2001. Structural optimization and form finding of light weight structures. Computers & Structures, 79, 22-25: 2053-2062.

Bonnans, J. F., Gilbert, J. C., Lemaréchal, C., Sagastizábal, C. A. 2006. Numerical Optimization Theoretical and Practical Aspects. New York, Springer: 490 p.

Camprubi, N., Bischoff, M., Bletzinger, K. U. 2004. Shape optimization of shells and locking. Computers & Structures, 82, 29-30: 2551-2561.

Cappello, F., Mancuso, A. 2003. A genetic algorithm for combined topology and shape optimisations. Computer-Aided Design, 35, 8: 761-769.

Chang, K. H., Choi, K. K., Tsai, C. S., Chen, C. J., Choi, B. S., Yu, X. M. 1995. Design Sensitivity Analysis and Optimization Tool (Dso) for Shape Design Applications. Computing Systems in Engineering, 6, 2: 151-175.

Chang, K. H., Tang, P. S. 2001. Integration of design and manufacturing for structural shape optimization. Advances in Engineering Software, 32, 7: 555-567.

Che, J., Tang, S. 2008. Research on integrated optimization design of hypersonic cruise vehicle. Aerospace Science and Technology, In Press, Corrected Proof.

Choi, K. K., Chang, K.-H. 1994. A study of design velocity field computation for shape optimal design. Finite Elements in Analysis and Design, 15, 4: 317-341.

Choi, K. K., Kim, N. H. 2005a. Structural sensitivity analysis and optimization 1, Linear systems. New York, Springer Science+Business Media: 446 p.

Choi, K. K., Kim, N. H. 2005b. Structural sensitivity analysis and optimization 2, Nonlinear systems and applications. New York, Springer Science+Business Media: 447-772 p.

Crisfield, M. A. 1996. Non-Linear Finite Element Analysis of Solids and Structures. New York, Wiley: 362 p.

Crisfield, M. A. 1997. Non-Linear Finite Element Analysis of Solids and Structures, Volume 2, Advanced Topics. New York, Wiley: 508 p.

Deml, M., Wunderlich, W. 1997. Direct evaluation of the 'worst' imperfection shape in shell buckling. Comput Method Appl M, 149, 1-4: 201-222.

Dinkler, D., Pontow, J. 2006. A model to evaluate dynamic stability of imperfection sensitive shells. Comput Mech, 37, 6: 523-529.

El Damatty, A. A., Nassef, A. O. 2001. A finite element optimization technique to determine critical imperfections of shell structures. Struct Multidiscip O, 23, 1: 75-87.

Elishakoff, I. 2000. Uncertain buckling: its past, present and future. Int J Solids Struct, 37, 46-47: 6869-6889.

EN 1090/2. 2007. Execution of steel structures and aluminium structures – Part 2: Technical requirements for steel structures. Brussels, European Committee for Standardization

EN 1993 1-5. 2004. Eurocode 3: Design of steel structures, Part 1.5: Plated structural elements., Brussels, European Committee for Standardization

EN 1993 1-6. 2006. Eurocode 3: Design of steel structures, Part 1.6: Strength and stability of Shell Structures., Brussels, European Committee for Standardization

Ewert, E., Schweizerhof, K., Vielsack, P. 2006. Measures to judge the sensitivity of thin-walled shells concerning stability under different loading conditions. Comput Mech, 37, 6: 507-522.

Garcia, M. J., Gonzalez, C. A. 2004. Shape optimisation of continuum structures via evolution strategies and fixed grid finite element analysis. Struct Multidiscip O, 26, 1: 92-98.

Godoy, L. A. 2000. Theory of Elastic Stability: Analysis and Sensitivity. Philadelphia., Taylor and Francis.

Haftka, R. T., Grandhi, R. V. 1986. Structural Shape Optimization - a Survey. Comput Method Appl M, 57, 1: 91-106.

Hansen, J. S., Liu, Z. S., Olhoff, N. 2001. Shape sensitivity analysis using a fixed basis function finite element approach. Struct Multidiscip O, 21, 3: 177-195.

Hardee, E., Chang, K.-H., Tu, J., Choi, K. K., Grindeanu, I., Yu, X. 1999. A CAD-based design parameterization for shape optimization of elastic solids. Advances in Engineering Software, 30, 3: 185-199.

Ho, D. 1974. Buckling load of non-linear systems with multiple eigenvalues. International Journal of Non-Linear Mechanics, 6, 5: 649-662.

Hörnlein H.R.E.M. 2000. Effiziente semi–analytische gradienten-berechnung in der strukturoptimierung. Z. Angew. Math. Mech., 81: 669-670.

Hughes, T. J. R. 2000. Finite Element Method - Linear Static and Dynamic Finite Element Analysis Mineola, NY, Dover.

Jang, G. W., Kim, Y. Y. 2005. Sensitivity analysis for fixed-grid shape optimization by using oblique boundary curve approximation. Int J Solids Struct, 42, 11-12: 3591-3609.

Johansson, B., Maquoi, R., Sedlacek, G., Muller, C., Beg, D. 2007. Commentary and worked examples to EN 1993-1-5 "Plated structural elements". Luxembourg, Office for Official Publications of the European Communities: 226 p.

Kegl, M. 2000. Shape optimal design of structures: an efficient shape representation concept. Int J Numer Meth Eng, 49, 12: 1571-1588.

Koiter, W. T. 1945. Over de stabiliteit van het elastisch evenwicht. doctor, Techische Hooge School, Delft. English translation : Edward Riks (1969), The stability of elastic equilibrium. Stanford University.

Korelc, J. 1997. Automatic generation of finite-element code by simultaneous optimization of expressions. Theoretical Computer Science, 187: 231-248.

Korelc, J. 2002. Multi-language and multi-environment generation of nonlinear finite element codes. Eng Comput-Germany, 18, 4: 312-327.

Korelc, J. 2007a. AceFEM, Mathematica finite element environment. Ljubljana, University of Ljubljana, Faculty of Civil and Geodetic Engineering. http://www.fgg.uni-lj.si/Symech/.

Korelc, J. 2007b. AceGEN, Multi-Language, Multi-Environment numerical code generation. Ljubljana, University of Ljubljana, Faculty of Civil and Geodetic Engineering. http://www.fgg.uni-lj.si/Symech/.

Korelc, J., Kristanič, N. 2005. Evaluation of Design Velocity Field by Direct Differentiation of Symbolically Parameterized Mesh. In: Plasticity: fundamentals and applications: proceedings of the eighth international conference on computational plasticity, E. Onate, (ed.), CIMNE, Barcelona, Spain, 380-383.

Kristanič, N., Korelc, J. 2008. Optimization method for the determination of the most unfavorable imperfection of structures. Comput. Mech., DOI:10.1007/s00466-008-0288-9.

Lanzo, A. D. 2000. A Koiter's perturbation strategy for the imperfection sensitivity analysis of thin-walled structures with residual stresses. Thin Wall Struct, 37, 1: 77-95.

Lanzo, A. D., Garcea, G. 1996. Koiter's analysis of thin-walled structures by a finite element approach. Int J Numer Meth Eng, 39, 17: 3007-3031.

Lemaitre, J., Chaboche, J.-L. 1990. Mechanics of Solid Materials. Cambridge, Cambridge University Press: 556 p.

Li, Q., Steven, G. P., Querin, O. M., Xie, Y. M. 1999. Evolutionary shape optimization for stress minimization. Mechanics Research Communications, 26, 6: 657-664.

Li, W., Li, Q., Steven, G. P., Xie, Y. M. 2005. An evolutionary shape optimization for elastic contact problems subject to multiple load cases. Comput Method Appl M, 194, 30-33: 3394-3415.

Marsden, J. E., Hughes, T. R. J. 1994. Mathematical foundations of elasticity. New York, Dover Publications.

Maute, K., Nikbay, M., Farhat, C. 2000. Analytically based sensitivity analysis and optimization of nonlinear aeroelastic systems. 8th AIAA/USAF/NASA/ISSMO Symposium on Multidisciplinary Analysis and Optimization, AIAA, Long Beach, CA, 2000–4825.

Maute, K., Schwarz, S., Ramm, E. 1999. Structural optimization - The interaction between form and mechanics. Zeitschrift Fur Angewandte Mathematik Und Mechanik, 79, 10: 651-673.

Meske, R., Lauber, B., Schnack, E. 2006. A new optimality criteria method for shape optimization of natural frequency problems. Struct Multidiscip O, 31, 4: 295-310.

Michaleris, P., Tortorelli, D. A., Vidal, C. A. 1994. Tangent Operators and Design Sensitivity Formulations for Transient Nonlinear Coupled Problems with Applications to Elastoplasticity. Int J Numer Meth Eng, 37, 14: 2471-2499.

Nocedal, J., Wright, S. 2006. Numerical Optimization. New York, Springer: 664 p.

O.C. Zienkiewicz, J.S. Campbell. 1973. Shape optimization and sequential linear programming. In: R.H. Gallagher, O. C. Zienkiewicz, (eds.). Optimum Structural Design. New York, Wiley: 109-126.

OptiStruct. 2008. OptiStruct manual. Altair Engineering Inc. www.altair.com.

Oral, S. 1996. An improved semianalytical method for sensitivity analysis. Structural Optimization, 11, 1: 67-69.

Papadopoulos, V., Papadrakakis, M. 2005. The effect of material and thickness variability on the buckling load of shells with random initial imperfections. Comput Method Appl M, 194, 12-16: 1405-1426.

Ramm, E., Mehlhorn, G. 1991. On shape finding methods and ultimate load analyses of reinforced concrete shells. Engineering Structures, 13, 2: 178-198.

Rong, J. H., Jiang, J. S., Xie, Y. M. 2007. Evolutionary structural topology optimization for continuum structures with structural size and topology variables. Advances in Structural Engineering, 10, 6: 681-695.

Ryu, C. H., Lee, Y. S. 2007. A study on Ranked Bidirectional Evolutionary Structural Optimization (R-BESO) method for fully stressed structure design based on displacement sensitivity. Journal of Mechanical Science and Technology, 21, 12: 1994-2004.

Saliba, R., Padra, C., Venere, M. J., Taroco, E., Feijoo, R. A. 2005. Adaptivity in linear elastic fracture mechanics based on shape sensitivity analysis. Comput Method Appl M, 194, 34-35: 3582-3606.

Samareh, J. A. 1999. A novel shape parametrization approach. In: NASA/TM-1999-209116. Hampton, Virginia.

Schenk, C. A., Schueller, G. I. 2003. Buckling analysis of cylindrical shells with random geometric imperfections. International Journal of Non-Linear Mechanics, 38, 7: 1119-1132.

Schmidt, H. 2000. Stability of steel shell structures - General Report. J Constr Steel Res, 55, 1-3: 159-181.

Schmit, L. A. 1960. Structural Design by Systematic Synthesis. In. Proc. 2nd Conference on Electronic Computation. New York, American Society of Civil Engineers: 105-132.

Schneider, W. 2006. Stimulating equivalent geometric imperfections for the numerical buckling strength verification of axially compressed cylindrical steel shells. Comput Mech, 37, 6: 530-536.

Schneider, W., Brede, A. 2005. Consistent equivalent geometric imperfections for the numerical buckling strength verification of cylindrical shells under uniform external pressure. Thin Wall Struct, 43, 2: 175-188.

Schneider, W., Tirnmel, I., Hohn, K. 2005. The conception of quasi-collapse-affine imperfections: A new approach to unfavourable imperfections of thin-walled shell structures. Thin Wall Struct, 43, 8: 1202-1224.

Schranz, C., Krenn, B., Mang, H. A. 2006. Conversion from imperfection-sensitive into imperfection-insensitive elastic structures. II: Numerical investigation. Comput Method Appl M, 195, 13-16: 1458-1479.

Schwarz, S., Maute, K., Ramm, E. 2001. Topology and shape optimization for elastoplastic structural response. Comput Method Appl M, 190, 15-17: 2135-2155.

Song, C. Y., Teng, J. G., Rotter, J. M. 2004. Imperfection sensitivity of thin elastic cylindrical shells subject to partial axial compression. Int J Solids Struct, 41, 24-25: 7155-7180.

Steven, G. P., Li, Q., Xie, Y. M. 2002. Multicriteria optimization that minimizes maximum stress and maximizes stiffness. Computers & Structures, 80, 27-30: 2433-2448.

Tang, P. S., Chang, K. H. 2001. Integration of topology and shape optimization for design of structural components. Struct Multidiscip O, 22, 1: 65-82.

Uysal, H., Gul, R., Uzman, U. 2007. Optimum shape design of shell structures. Engineering Structures, 29, 1: 80-87.

van Keulen, F., Haftka, R. T., Kim, N. H. 2005. Review of options for structural design sensitivity analysis. Part 1: Linear systems. Comput Method Appl M, 194, 30-33: 3213-3243.

Wisniewski, K., Turska, E. 2000. Kinematics of finite rotation shells with in-plane twist parameter. Comput Method Appl M, 190, 8-10: 1117-1135.

Wisniewski, K., Turska, E. 2001. Warping and in-plane twist parameters in kinematics of finite rotation shells. Comput Method Appl M, 190, 43-44: 5739-5758.

Wolfram. 2008. Mathematica 6.0, The user guide. Wolfram Research, Inc.

Wriggers, P., Simo, J. C. 1990. A General Procedure for the Direct Computation of Turning and Bifurcation Points. Int J Numer Meth Eng, 30, 1: 155-176.

Wunderlich, W., Albertin, U. 2000. Analysis and load carrying behaviour of imperfection sensitive shells. Int J Numer Meth Eng, 47, 1-3: 255-273.

Wunderlich, W., Albertin, U. 2002. Buckling behaviour of imperfect spherical shells. International Journal of Non-Linear Mechanics, 37, 4-5: 589-604.

Zienkiewicz, O. C., Taylor, R. L. 2000a. The finite element method. Vol. 2, Solid mechanics. Oxford Butterworth-Heinemann: 459 p.

Zienkiewicz, O. C., Taylor, R. L. 2000b. The fnite element method. Volume 1. The Basis. Oxford Butterworth-Heinemann: 689 p.